LBL-7381
UC-25
TID-4500-R66

WEAR RESISTANT ALLOYS FOR COAL HANDLING EQUIPMENT

M. S. Bhat, Victor F. Zackay, and
Earl R. Parker

January 1 - September 30, 1977

Prepared for the U. S. Department of Energy
under Contract W-7405-ENG-48

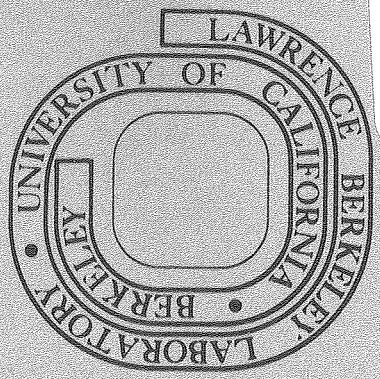

LBL-7381

Lawrence Berkeley Laboratory
Materials and Molecular Research Division
University of California
Berkeley, California 94720

WEAR RESISTANT ALLOYS FOR COAL HANDLING EQUIPMENT

Progress Report
for the Period

January 1 - September 30, 1977

M. S. Bhat
Victor F. Zackay
Earl R. Parker

Prepared for
The United States Department of Energy

TABLE OF CONTENTS

TABLE OF CONTENTS (Cont.)

FOREWORD

This report describes the progress made during the period January 1 through September 30, 1977 on the project "Wear Resistant Alloys for Coal Handling Equipment". The project was administered by the Division of Materials and Exploratory Research of ERDA (now the Department of Energy) with Dr. Thomas Cox as the Contract Monitor and Mr. Water Bakker as the Contract Manager. This report was prepared by Dr. M. S. Bhat, Project Leader for the program at the Lawrence Berkeley Laboratory, University of California, Berkeley, California.

The research was performed under the direction of Professors Victor F. Zackay and Earl R. Parker of the Materials Science and Mineral Engineering Department of the University of California, Berkeley. The program was initially managed by Dr. M. Dilip Bhandarkar (during the first two months) and since then by Dr. M. S. Bhat. The sub-contract for designing and building the dry abrasive and slurry erosion tester was directed by Mr. Alan V. Levy of the Lawrence Berkeley Laboratory, and Dr. S. Jahanmir of the Mechanical Engineering Department, University of California, Berkeley. The details of the work performed on the slurry erosion tester will be presented in a separate report by Mr. Alan V. Levy. Other research personnel of the Lawrence Berkeley Laboratory who were involved were the following:

Graduate Students:	R. Garriga
	W. Garrison
	H. Hirano
	N. Kar
	T. Lechtenberg
Research Helpers	S. Bandel
	M. Carlson
	D. Leong
	G. Lesh

ABSTRACT

The in-service operating conditions of coal transport and fragmentation equipment involve various combinations of dry or liquid slurry abrasion, impact loading, and temperatures that may vary from ambient to elevated (500 ^{o}F - 1000 ^{o}F). Both 2-body and 3-body abrasive wear can be encountered. The published literature contains little information on testing materials under the various abrasive conditions that are of concern, especially 3-body wear. However, a number of tests were identified which may serve to provide wear data under different service conditions. A dry abrasive wear tester, to be used for screening alloys, was constructed. A review of the alloy steel literature was completed and was used to select low-alloy and secondary hardening steel compositions for screening. Initial screening criteria included the stipulation of a hardness of R_c55 with an impact toughness of around 15 ft lbs or a fracture toughness of 80 KSI$\sqrt{in.}$, depending on the application being considered. Several of the steels that were evaluated to date appeared to meet these criteria. A systematic development of secondary hardening steels has been evolved and it has been shown that good combinations of strength and toughness were achieved through proper composition and microstructural control. These higher alloyed steels appear to be suited for long-term, elevated-temperature service. The lower alloy Cr-Ni-Mo and Cr-Si-Mo steels investigated also exhibited good combinations of strength and toughness and may be suitable for ambient temperature use.

1. OBJECTIVE AND SCOPE

The goal of the program is to develop wear resistant alloys for coal transportation and fragmentation equipment. The program will utilize the advancements in low alloy steel technology of high strengh (hardness), high toughness alloys to develop wrought and cast steels that will meet targets for improved performance of coal transportation and fragmentation equipment. A three-year program will be conducted involving the following three tasks:

Task I - Establish alloy design criteria through studies of the relationships between mechanisms and alloy microstructure for the principal wear components of coal handling and processing equipment. Develop evaluation tests that will simulate, in the laboratory, the service operation of the components.

Task II - Develop steels with increased hardness and sufficient toughness that will have acceptable costs in mill/foundry production, and characterize their microstructure, mechanical properties, and wear resistance.

Task III - Produce and evaluate experimental quantities of components from the developed alloys through laboratory and in-service tests.

A basic study of wear mechanisms will be conducted concurrently and will contribute to Task I of the present program.

Four component areas are within the scope of the program. These are: (1) feeder components for reaction vessels (coal feeders), (2) coal moving equipment such as chutes and coal loader shovels, (3) coal crushing and milling equipment, and (4) mining equipment such as drag line bucket points and continuous miner picks. (Materials useful for bucket points and miner picks may evolve from research on alloys for the first three items, but item 4 is considered to be of incidental, rather than primary, concern in the project.)

The program scope and alloy design criteria for each of the component areas mentioned above will vary according to the known and expected in-service operating conditions of the components. Dry coal feeder components such as the screw, containment vessel, and nozzle are expected to experience in-service operation at both room and elevated (500 ^{o}F - 1000 ^{o}F) temperatures. Therefore, the alloy design criteria would consider these in-service conditions and the program scope will include component testing under these conditions.

Alloys for components of coal fragmentation equipment (coal crushers) will be designed to resist concurrent impact and abrasion at ambient temperatures. Coal transport equipment such as loading shovels and chutes do not have as severe wear requirements as do feeder and crusher components. A principal design objective in this case will be a reduction in alloying element content, without loss of hardness and impact toughness, to reduce cost.

2. PROGRESS SUMMARY

In evaluating the program progress, it is pointed out that although the final research proposal was not approved by ERDA (now DOE), until mid-January, a program start date of January 1, 1977 was mutually agreed to by ERDA and Lawrence Berkeley Laboratory. The program progress is compared against program schedule with this agreed-upon start date. The comparison is shown in Figure 1.

2.1 TASK I - ALLOY PERFORMANCE CRITERIA

As shown in the Figure, Task I is on schedule. Discussions with coal equipment producers, designers, and contractors were helpful in defining the expected operating conditions in coal transportation and fragmentation equipment. An extensive literature survey was conducted in the general area of abrasion mechanisms, wear testing, and relevant metallurgical factors. An alloy screening device which would test for abrasion resistance was designed, constructed, and calibrated with standard materials. Abrasive wear factors under high stress conditions were determined for a low alloy ultra-high strength steel in various heat treated conditions, using a laboratory jaw crusher. The wear factors compared favorably with data available in the literature for similar steels of the same carbon content.

2.2 TASK II - ALLOY DESIGN

Task II activities are on schedule. Over fifty different compositions have been cast and quite a few of them have been evaluated for their mechanical properties and microstructure. Valuable information on alloy design has been accumulated. Fifty-pound ingots of 4340 + 1.5Al + 1.5Si steel were cast at ESCO Corporation and the wear resistance in jaw crusher tests was determined for three different heat-treated conditions.

2.3 TASK III - COMPONENT EVALUATION

Although the evaluation of 4340 + 1.5Al + 1.5Si steel components was scheduled, only laboratory-size jaw crusher plates have been evaluated.

3. TECHNICAL PROGRESS

During the period January 1 through September 30, technical progress was made in program tasks I and II, as described below.

3.1 TASK I - ALLOY PERFORMANCE CRITERIA

3.1.1 Identification of In-Service Operating Conditions of Components

Several discussions were carried out with personnel from Ingersoll-Rand Research, Inc., Ralph M. Parsons Company, Foster-Miller Associates, Inc., ESCO Corporation, and Albany Metallurgy Research Center - Bureau of Mines. A study was also conducted of some preliminary reports on the coal equipment development contracts (as a part of the demonstration plant program[1,2]) sponsored by Fossil Energy - ERDA. Based on these discussions and studies, the following operating conditions were identified for the component areas that are under the scope of this program.

3.1.1.1 Dry Coal Feeders

A number of different kinds of dry coal feeders are being considered, and the results of the preliminary studies were presented at a recent conference on coal feeding systems held at Pasadena[3]. Based on the work done by different laboratories and companies, an evaluation was made by the Jet Propulsion Laboratory[4], and the extension of work on a number of feeders was recommended, to assure probabilities of successful development for specific applications. The particular feeder to be used would depend on the process used, which would control parameters such as pressure, coal size, lifetime of feeder, etc. Upon considering all these factors, one of the types of feeders which was estimated to have a large probability of successful commercialization was the screw feeder. From an examination of the experiences presented with screw-type feeders, it was clear that wear occurred (during fairly short-term

tests) on the terminating flight of the screw[5]. During this time period, no wear was observed in the barrel liner. Screw wear was also observed by other investigators[6], who also obtained wear on the front part of the screw. The wear could have been due to the wedging of the coal particles against the barrel liner and the screw wall. Three-body abrasion should be high at the outer end of screw tips where the velocity of the feed material is high and at the exit end due to high pressure and velocity. Thus, the wear in such feeder systems can be due to relatively high stress dry abrasion of a three-body type, involving coal particles (sizes of ¼ in. and smaller) under pressure or wedged between two metal surfaces having relative motion. The coal particles can fracture during this process. In order to anticipate any other types of wear situations which might occur in screw feeders, some papers on experiences in injection molding machines were referred to[7,8]. It was found that, in addition to the high stress 3-body wear, some adhesive wear might also occur. This is because there could be contact between barrel and screw due to factors such as misalignment, uneven feeding, and non-uniform heating, although under normal operating conditions, the screw is expected to "float" in the center of the barrel. Temperatures of 500 ^{o}F - 1000 ^{o}F may be encountered depending upon whether the whole barrel assembly is heated, or because some heating occurs in those parts in close proximity to the gasification vessels. Presently, the exact nature of the interface between the feeder and the gasification vessel is not clear.

3.1.1.2 Slurry Coal Feeder

Liquid slurry erosion at ambient to elevated (500 ^{o}F - 1000 ^{o}F) temperatures can be expected. Details regarding slurry feeders will be reported by Alan V. Levy in a separate report.

3.1.1.3 Coal Loader Shovels and Chutes

Ambient temperatures; relatively low stress dry abrasion of a two-body type (contact between two surfaces having relative motion) involving coal and rock in forms ranging from small particles to large chunks can be encountered. Light impact may be encountered in some cases.

3.1.1.4 Coal Crushing and Milling Equipment

Dry abrasion involving both high contact pressure and impact. Surface temperatures may go up as high as 1000 ^{o}F in certain applications.

3.1.1.5 Mining Equipment

Mining equipment such as drag line bucket points and continuous miner picks. Dry abrasion at ambient temperatures involving impact which may be severe at times when rock seams are encountered. High strain rate fatigue and elevated surface temperatures are of concern. Again, it is emphasized that these findings were of an incidental nature, evolved during the general discussions that were held. No attempts will be made as a part of the present contract to pursue this item further. On the other hand, the findings listed under the above items will be considered in designing alloys and in developing laboratory simulation tests for alloy screening and component evaluation.

3.1.2 Results of a Literature Survey on Wear Testing Devices

A literature survey was conducted to evaluate critically past work on abrasive wear tests for high hardness steels. It was discovered that while several investigations had been carried out on two-body abrasion[9], only a limited amount of work had been done on testing steels under three-body abrasive conditions[10,11]. Some of the principal test devices discussed in the literature are described here.

3.1.2.1 Two-Body Abrasion

Richardson[12] used a pin-on-disk device. A pin-type wear specimen was mounted in a weighted arm which caused the pin to bear down on a revolving turntable which was covered with an adhesive-backed abrasive cloth. The arm was hinged on a tracking mechanism which allowed the wear specimen to follow a spiral path on the abrasive cloth so that the specimen did not wear in the same track during each revolution of the disk. Only a schematic sketch of the device was presented by Richardson, and no details were given of the actual test set-up procedure.

The American Society of Lubrication Engineers Catalog of Friction and Wear Devices[13] has compiled a comprehensive list of several wear testing devices with short descriptions of each device. Unfortunately, most of the devices were developed for lubricant testing and it is not known whether the operating parameters of the machines are compatible with abrasive wear studies of the type that are within the scope of the present contract. However, useful information regarding temperature and atmospheric controls for testing can be obtained from the references that are cited in the catalog.

A paper describing details of a two-body abrasion testing machine construction, performance, and test procedures was published by Muscara and Sinnot[14]. They developed a wear testing machine based on a Bridgeport vertical milling machine that allowed accurate control of parameters that were believed to be important, namely, type of abrasive, load, abrasive particle size, length of abrasive path, specimen diameter, speed of abrasive surface and specimen, and lubrication. Pin-type wear specimens were used in contact with bonded-abrasive cloth surfaces. Three different abrasives were used, namely alumina, silicon carbide, and garnet. The test was used for relative ranking of materials based on their abrasive wear resistance.

Bayer et al[15] developed a testing machine for determining the wear of a material under repeated impacts. The device hurls bullet-shaped projectiles against a rotating or stationary semi-infinite metal surface. Either the bullet or the metal surface, or both, can be examined for wear effects.

3.1.2.2 Three-Body Abrasion

Borik[16] described some of the current testing methods in both two- and three-body wear situations. He also tested steels and cast irons in three-body abrasion. Two types of wear testing machines were used. The first was a ball mill where the test material was shaped into grinding balls for the mill. The test can take two weeks to run, and, due to the large number of grinding balls that must be used in each test, the test requires a considerable amount of test material.

The second and more economical type of test proposed by Borik used a laboratory-size, single-toggle jaw crusher. With this test it was also possible to include a reference material on each test run so that the wear results for different materials could be related to a common reference. The use of a reference material also made it possible to eliminate the effects of test condition variability between successive runs. Rectangular plates 8x5-1-inches in size were used as test specimens. Crushed rock, 1-1/2 to 2 inches in size, was used as abrasive. It was reported that the test could detect small differences between the abrasion resistance of test materials. A detailed test description has been presented by Borik and Sponseller[11], and the test results including the effects of metallurgical variables on wear have been discussed by Borik and Schalz[17].

Another tester which has been receiving attention as a standardized abrasive wear tester is the rubber wheel abrasive tester which was originally

conceived by Haworth[18]. This tester can be used either with dry sand or with a sand slurry. The tester has been described in detail by Borik[19]. The test essentially consists of pressing a specimen of known weight with a known pressure against a rotating rubber-rimmed steel wheel. Either dry sand can be poured from the top or a sand slurry can be used as the abrasive medium. Other kinds of slurries such as industrial waste slurries[10] can also be used. A number of laboratories use this tester to simulate low stress abrasion[20,21,22]. This tester is supposed to produce abrasive wear results which correlate well with mining field equipment data[22].

Other kinds of laboratory abrasive wear testers in current use are an impact abrasion, incendivity tester[23], which simulates impact wear in flammable gas mixtures; a modified commercial Falex No. 6 friction and wear tester[24], which can simulate ambient and elevated temperature (approximately 500 ^{o}F maximum) abrasive testing, and a grinding wheel tester developed by ABEX Corporation Research Center which simulates gouging wear[25]. In addition to these laboratory tests, field tests are also conducted, e.g., in ball mills[16].

The literature survey clearly indicated the wide variety of testers available which simulate, in the laboratory, different service conditions, and rank materials differently. Based on this survey, it was concluded that the ESCO laboratory jaw crusher test, which is a modified version of the one proposed by Borik and Sponseller[11], would be suitable for screening and simulation testing of alloys that would be used in components (such as those in coal crushers) experiencing dry high stress, impact abrasion in service. It is also anticipated that the impact incendivity tester at the Albany, Bureau of Mines Metallurgy Research Center would be used for alloy evaluation. However, these tests would not simulate the in-service conditions expected

in coal-feeders, coal loader shovels, or chutes. For the coal feeder application, abrasion of a three-body type is anticipated. A tester to simulate this kind of abrasion has been designed presently for ambient temperature use. The tester will eventually be modified for high temperature use. The dry sand rubber wheel tester might be used for the low stress applications.

During the past year, a two-body, abrasive, pin-on-disk type, wear tester has been designed and constructed for alloy screening purposes. The details of the tester are given below.

3.1.3 Design and Construction of a Wear Screening Device for Dry Abrasion

The following report was submitted by Dr. S. Jahanmir through Mr. Alan V. Levy.

3.1.3.1 Description of Wear Tester

For evaluation and selection of alloys for coal handling equipment, it was required to simulate the operating conditions as closely as possible and at the same time have a simple test to avoid a long and complicated test program. For this purpose, an abrasive wear tester was designed and constructed at LBL. The current design does not include capabilities for elevated-temperature tests. However, modifications may be made at a later date for high temperature tests.

The overall view of the abrasive wear tester is shown in Figure 2. The side view of the pin-on-disk test configuration is observed in Figure 3. The specimen is a 1/4-in.-diameter pin with an 1/8-in. radius of curvature at the contact end. The disk which has a diameter of 4 in. is given a rotary motion and the pin can be kept stationary or moved radially on the disk. When the pin is stationary, the same track will be traversed on the disk; however, for the radial motion of the pin, the contact path on the disk is a spiral and a fresh area of the disk will be in contact with the pin after each revolution.

A close-up of the pin-holding section of the abrasive wear tester is shown in Figure 4. This assembly is also used to apply the normal contact load and to measure the frictional force. The normal load on the specimen is applied by attaching weights to the weight pan and will be varied to simulate in-service loads. The frictional force is measured by means of a strain ring arrangement. The strain ring is designed to be flexible and deform elastically under the action of the frictional force. This deformation is measured by strain gauges attached to the ring and is monitored through the recorder to indicate the frictional force. The pin holder and strain ring assembly are connected to a pair of pillow blocks. The weight of the assembly is balanced by the counterweight. This assembly is attached to a tracking mechanism to provide the radial motion of the pin on the rotating disk.

The abrasive wear tester can be used for both two-body and three-body wear. Two-body abrasive wear is achieved by constructing an abrasive disk from the type of abrasive powder to be used for testing. The abrasive is bonded to the disk face. For three-body abrasive wear, a cup is constructed around the contacting surfaces to hold the abrasive powder. The abrasive particles are carried to the contact by the rotating action of the disk.

The maximum normal load is 20 lbs which is great enough to simulate in-service loads. The speed range of the turntable is between 25 to 200 rpm which gives a maximum speed of 2,500 in./min at the contact with a 4-in. disk. In order to achieve higher speeds, the turntable can be made larger. The maximum allowable diameter of the turntable is 8 in.

3.1.4 Experiments with the Pin-on-Disk Tester

The following information was provided by Howard H. Hirano, a graduate student in mechanical engineering, working under the guidance of Professor Iain Finnie, for Mr. Alan V. Levy.

The abrasive used for most of the testing consisted of Carbimet silicon abrasive papers with pressure-sensitive adhesive backing. Unless otherwise noted, the specimens were dead weight loaded with 1.1 lbs against 120 grit silicon carbide abrasive paper. All of the tests were performed at the same constant speed of rotation of 20 rpm for 45 seconds. The mechanism which controlled the radial traversing of the specimen was adjusted so that all of the specimens travelled from 1.8-in. radius to 0.54-in. radius in the 45 seconds. Thus, all the specimens were abraded for the same distance which was determined to be 110.24 ins. The average velocity of the abrasive, relative to the specimen, was 146.5 in./min. The abrasive paper was changed before each test and examination of the wear track on the paper indicated that the radial traversing speed was adequate to ensure that the specimen was continually exposed to fresh abrasive. The specimen dimensions were 0.25-in. diameter and 0.7-in. length. One end of each specimen was machined hemispherical to discourage any initial effects due to misorientation. Following machining, the specimens were lightly buffed with 600 grit silicon carbide abrasive paper.

The materials initially used for standardization and calibration were 7075 aluminum and AISI 4340 steel. Both these materials were heat treated to various levels of hardness. The hardnesses used are given in Table I. Tests were run to study load and particle size effects. The wear volume (which was defined as the volume removed per unit distance travelled) was directly proportional to the load applied on the specimen as shown in Figure 5 for the 7075 aluminum specimens. The graph connecting the data points does not pass through the origin. This behavior was attributed to the fact that the specimen support arm of the wear tester was not perfectly balanced. Such a behavior has also been observed in a similar kind of test as reported

by Muscara and Sinnot[14]. In their particular study, the abrasive used was alumina of various particle sizes.

The effect of the abrasive particle size was interesting. For particle sizes larger than approximately 100 μm, there was no effect of size on wear as shown in Figure 6. A similar behavior has been reported by Date and Malkin[26] for two-body abrasion, and by Finnie for erosive wear[27]. Other investigators have also observed a similar effect of grit size on abrasion rate[14,28]. As pointed out by Muscara and Sinnot[14] the critical grit size beyond which wear rate is independent of grit size has been reported to vary between 45μ and 150μ. Although the exact reasons for the existence of a critical grit size are not known, it has been suggested that the reason could be because particles, only in elastic contact with the metal, carry load without causing abrasion[29]. Obviously, further study is needed for clarification of this behavior. For the purpose of investigating the effect of the mechanical properties, it was decided to use a fixed abrasive size (approximately 115μm) for all the tests.

The wear rate (which is defined as the volume removed per unit distance travelled per unit load) is shown as a function of hardness for 7075 aluminum and AISI 4340 in Figures 7 and 8. In these steels, it appeared that, in general, abrasive wear decreased with increase in hardness as has been reported by Khruschov and Babishev[30].

Further tests are necessary to study the effect of abrasive hardness on wear rates, and critical grit sizes. The reproducibility of wear rates with 4340 steel and other materials such as 1020 steel in such a type of test has to be determined, before standards for obtaining abrasion factors can be arrived at. As pointed out by work done at the University of Notre Dame[31], 1020 steel exhibited less variability as compared to 4340 steel in the dry sand rubber wheel test, and consequently the 1020 steel is being used as the standard.

3.1.5 Results of Jaw Crusher Tests

High stress abrasion tests on modified 4340 steel were conducted with a laboratory jaw crusher at ESCO Corporation. The details of the ESCO jaw crusher test have already been given elsewhere[32]. The steel studied was 4340 + 1.5Al + 1.5Si, and three different heat treated conditions were used. The steel was obtained as 50-lb ingots by air induction melting. The ingots were forged at 1200 ^{o}C and homogenized at 1200 ^{o}C. The heat treatments consisted of austenitizing at 1000 ^{o}C for one hour, Aqua-quenching* and tempering at 300 ^{o}C (one hour), 300 ^{o}C (two hours), and at 350 ^{o}C (one hour), and air cooling to room temperature. The chemical compositions provided by ESCO are shown in Table II for the three different heats. The hardness of the wear plates before the test, and the wear factors determined are shown in Table III. The standard used was steel T1 at a hardness of 270 BHN. Also shown in the Table are results of similar steels tested at ESCO[33] and at Climax Molybdenum Company[20]. The wear ratios obtained on the experimental steels are as good as, or better than, the results reported for the ESCO steels and AISI 4340 steel. A detailed analysis of these results will be presented in the next quarterly report when data on microstructure and toughness will be available.

Although the pin-on-disk tester showed that the wear rate is directly proportional to hardness, the results of the jaw crusher tests do not show this correlation. More detailed work needs to be done before some of the results discussed above can be analyzed.

* Aqua-quenching refers to quenching in a solution of a commercial additive in water which reportedly results in cooling rates closer to oil quenching.

3.2 TASK II - ALLOY DESIGN

It has been clearly established that metallurgical variables such as microstructure and composition, and mechanical properties play a key role in controlling wear behavior[14,17,20,22,35-41]. Hurricks[35] has written an excellent review paper on the subject. However, the exact correlation between metallurgical variables, mechanical properties and abrasive wear is, at the present time, not very clear. For example, some of the correlations which have been observed are:

i. In steels the abrasive wear resistance appeared to increase with carbon content[20]

ii. Martensitic matrices appeared to exhibit better abrasion resistance as compared to ferrite, pearlite, bainite, or austenite[20]

iii. The relationship between abrasive wear and fracture toughness is complex[42]. For wrought and cast, low-alloy steels, it appeared that steels which exhibited a low impact toughness possessed better abrasion resistance at least in gouging wear tests[20]. However, this correlation is not simple and one has to be careful in alloy selection. For example, others have pointed out that lower fracture toughness can lead to increased wear[34].

iv. In general, steels with higher hardness possess better wear resistance[30,43,44]. However, it has been shown that such a correlation is not necessarily true in every case[25]. In addition, the work hardening characteristic of the steel is very important[30,35,45].

v. Other microstructural factors which control wear are: type of dispersed phase, its size, distribution, hardness, and coherency with matrix, and retained austenite and its stability[35].

It is obvious that the observed wear rates will not only be controlled by metallurgical factors, but also by the service conditions. Keeping all these factors in mind, alloy design during the first year of the program was based mainly on metallurgical factors. (As Task I progresses, it is anticipated that design parameters based on wear studies will be available for the alloy design phase.) The initial two design criteria used in developing new alloy compositions were hardness and toughness. A review of the information available in the literature and past research work conducted at LBL was utilized in establishing the allow design criteria discussed below.

3.2.1 Alloy Design Criteria

The initial alloy design criteria were based on the following considerations:

(1) Improvement of hardness and toughness through microstructural control,

(2) Attainment of different microstructures that would lead to the same hardness, and possibly the same toughness, so that the role of properties (other than hardness and toughness) in wear resistance can be established,

(3) Achieving elevated temperature capability through alloy selections, including secondary hardening steels, which are known to maintain high hardness levels, even on long-time exposures, at temperatures up to 1000 ^{o}F,

(4) Selection of alloys with the minimum possible carbon content consistent with good welding practice. Also lower carbon contents minimize the internal stresses and, therefore, lower the tendency for quench cracking. In addition, the propensity for the formation of internally twinned martensite is considerably reduced, thus avoiding a consequent loss in toughness.

It was believed that low alloy steels would meet the requirements of the ambient temperature applications that are within the scope of the current program. Higher alloy content steels would be needed to provide elevated temperature capability. Four families of steels were selected for initial screening:

Series A - Martensitic and bainitic secondary hardening steels

Series B - Secondary hardening matrix steels

Series C - Cr-Ni-Mo steels (modified AISI 4340 steel)

Series D - Cr-Si-Mo steels (modified ESCO steels)

The design of Series A steels involved a consideration of many factors which are summarized below.

Carbon Content

(1) The data in the literature shows that a minimum of 0.35% is needed to attain significant hardness levels (in the neighborhood of R_C55) at the secondary hardening peak[46].

(2) Only a marginal improvement is attained in the secondary hardening peak on increasing carbon content beyond about 0.4%[46].

(3) Other factors, mentioned earlier, suggest the advantages of using the lowest possible carbon content.

Secondary Carbide Forming Elements

Molybdenum was chosen as the main carbide forming alloying element. The following factors were considered.

(1) Molybdenum carbides lead to a high hardness at the secondary hardening peak[47], and high toughness is attainable in molybdenum secondary hardening steels[48,49].

(2) Molybdenum carbides are more resistant to overaging than chromium carbides[50].

(3) At commercially feasible austenitizing temperatures, molybdenum carbides are thermodynamically less stable than the carbides of vanadium, niobium, and titanium (which are some of the other elements that form secondary carbides) thus reducing the tendency for toughness loss due to large undissolved carbides[51].

(4) Molybdenum carbides appear to enhance wear resistance[35].

(5) Molybdenum enhances elevated temperature strength when present in solid solution in ferrite[52].

(6) Molybdenum enhances hardenability of steels thus permitting lower quenching rates to be used following austenitization[53].

(7) A minimum of 2% molybdenum is needed for appreciable secondary hardening.

(8) The amount of molybdenum should be the minimum needed since large amounts restrict the stable austenite region, particularly in the presence of other ferrite stabilizing elements.

The following considerations were important in the selection of vanadium.

(1) Small amounts of vanadium increase the peak hardness attainable on secondary hardening[54].

(2) Vanadium enhances the resistance to overaging of molybdenum-base secondary hardening steels.

(3) Vanadium carbides have been reported to increase wear resistance[35].

(4) The secondary hardening response of vanadium is maximum at vanadium to carbon ratios of 4[55]. However, the minimum possible amount of vanadium should be used since high amounts increase the tendency to produce large undissolved vanadium carbides in the steel.

Other Alloying Elements

(1) Silicon additions were used for enhancing the solid solution strength, retarding the low temperature response[56], and for improving secondary peak hardness[57]. The retardation of low temperature tempering response leads to a relatively flat tempering temperature vs hardness curve. This in turn permits the study of wear resistance of the steel as a function of microstructure for the same hardness.

(2) Aluminum additions were used since it is known that aluminum, in combination with silicon, can not only be effective in retarding low temperature tempering reactions, but it can also enhance the fracture toughness of steels as has been shown for AISI 4340-type steels[58].

(3) Nickel additions were selected to balance the ferrite stabilizing elements, and to permit austenitizing in a single phase austenite region.

(4) Chromium additions were made for enhancing hardenability and for increasing the resistance to corrosion and oxidation.

The design of secondary hardening matrix steels was based on the information available on the commercially-developed Vasco-MA composition which is claimed as a matrix steel[59], The term "matrix steel" resulted from developmental work on tool steels where the objective was to obtain a tool steel whose composition was similar to that of the "matrix" of a standard tool steel. By utilizing such a composition, it was hoped to avoid undissolved primary carbides at the austenitization temperature. However, recent investigations established that the commercial Vasco-MA matrix steel contained undissolved carbides[60]. It was believed that the information already available on the

mechanical properties and the nature of the carbides in this steel would benefit the alloy design of new "matrix steels".

The series C steels are low alloy steels whose selection was based on the past work of Bhat[58] who showed that combinations of high hardness and toughness were attained in AISI 4340-type steels containing high amounts of aluminum and silicon. An additional increase in hardness levels could be achieved by a slight increase in carbon content.

The choice of composition of the Cr-Si-Mo class of steels was based on past experience at ESCO Corporation where such low alloy steels are produced for wear-resistant applications such as drag line bucket points[61]. Major compositional modifications included the addition of carbon for further increases in hardness and the addition of chromium for improvements in hardenability and wear resistance.

The progress accomplished in alloy screening and testing is presented below for each of the alloy families which were selcted.

3.2.2 Secondary Hardening Martensitic Steels (Series A Steels - Continuously Cooled)

Twenty-two alloys were screened under this class of steels. Preliminary work in this class of steels involved a steel containing 0.4C, 4Mo, 1V, 1.5Al, and 1.5Si. An ingot of the above nominal chemical composition was vacuum induction melted, upset- and cross-forged into 1-1/8-in.-thick and 2-3/4-in.-wide plate, and vacuum homogenized for 24 hours at 1200 ^{o}C. Microstructural studies and hardness measurements were performed on specimens of the steel austenitized for one hour at several different temperatures and ice-brine quenched. It was found that the steel was characterized by soft ferrite-martensite duplex structures. The duplex microstructures resulted because, at the austenitizing temperatures used, austenite plus ferrite mixtures were thermodynamically stable. In order to obtain a single phase

austenite phase region at temperatures normally used for austenitizing (900 ^{o}C - 1200 ^{o}C), it was deemed necessary to modify the composition of the steel. The principal modification was the addition of Ni to expand the austenite phase field. Subsequent composition selections were influenced by these preliminary results.

The nominal chemical compositions of steels A1 through A21 are shown in Table IV. Also shown in the Table are actual chemical compositions which were determined for some of the steels. Steels A1 - A6 were cast as 22-lb ingots and steels A7 - A21 were cast as 10-lb ingots. The first set of steels A1-A6 contained higher amounts of C, Mo, and V than the steels A7 - A21; the compositions of these latter steels were arrived at following the investigation on steels A1 - A6.

An examination of the microstructure and hardness of steels A1 - A6 was conducted to establish the austenitization temperatures. For this purpose, cubes of approximately 1/2-in. side were austenitized for one hour in argon at several temperatures in the range 1050 ^{o}C - 1300 ^{o}C and ice-brine quenched. The hardness of the as-quenched steels (averaged over several measurements) is plotted in Figure 9 as a function of austenitization temperature. The as-quenched hardness of steels A3 - A6 increased by substantial amounts between austenitizing temperatures of 1050 ^{o}C to 1150 ^{o}C, and somewhat less so at higher temperatures. The hardness of steels A1 and A2 did not vary with austenitization temperature.

The increase in hardness with austenitization temperature indicated that more carbon dissolved in the austenite due to dissolution of carbides at the higher temperatures. The microstructure of the as-quenched steels austenitized in the range 1050 ^{o}C - 1250 ^{o}C was observed using optical microscopy. No undissolved carbides were observed in steels A1 and A2 austenitized at or above 1150 ^{o}C. However, large undissolved carbides were clearly revealed in optical micrographs of the steels A4 and A5 austenitized at 1150 ^{o}C, as shown by arrows

in Figures 10(a) and 10(c), respectively. The carbide dispersion was finer in the steel A5 than in the steel A4. Undissolved carbides were not revealed in optical micrographs of the same steels when they were austenitized at 1250 ^{o}C, the microstructures of which are shown in Figures 10(b) and 10(d).

The tempering response of steels A1 - A6 was determined following austenitization at 1150 ^{o}C and an ice-brine quench. The steels were tempered for one hour at temperatures in the range 200 ^{o}C to 700 ^{o}C. The results of hardness measurements are plotted in Figure 11 for the steels A1 and A2 and in Figure 12 for steels A3 to A6. All the steels exhibited typical secondary hardening behavior, with steels A3 - A6 in general achieving higher hardnesses than either steel A1 or A2.

The alloys A1 - A6 exhibited poor room temperature impact energies in the ice-brine quenched and tempered conditions. Some of the results obtained are shown in Table V. Some secondary cracking was observed in the fracture surfaces of the Charpy bars which could have been due to quench cracks produced by the severe quench. It was resolved to oil quench in order to avoid quench cracking. However, it was found that none of the alloys, A1 - A6, had sufficient hardenability to obtain fully martensitic structures by the slower quench. To overcome this problem, additions of Cr were made to a new batch of ingots whose compositions are shown in Table IV as alloys A7 - A13. In addition to the Cr modification, other changes in the composition were made and the rationale behind these modifications is discussed below.

One of the problems encountered in the steels A3 through A6 was the presence of undissolved carbides at austenitization temperatures below 1250 ^{o}C. Austenitization at 1250 ^{o}C led to a large grain size which severely impaired the impact toughness. It was decided to modify the composition in

in Figures 10(a) and 10(c), respectively. The carbide dispersion was finer in the steel A5 than in the steel A4. Undissolved carbides were not revealed in optical micrographs of the same steels when they were austenitized at 1250 ^{o}C, the microstructures of which are shown in Figures 10(b) and 10(d).

The tempering response of steels A1 - A6 was determined following austenitization at 1150 ^{o}C and an ice-brine quench. The steels were tempered for one hour at temperatures in the range 200 ^{o}C to 700 ^{o}C. The results of hardness measurements are plotted in Figure 11 for the steels A1 and A2 and in Figure 12 for steels A3 to A6. All the steels exhibited typical secondary hardening behavior, with steels A3 - A6 in general achieving higher hardnesses than either steel A1 or A2.

The alloys A1 - A6 exhibited poor room temperature impact energies in the ice-brine quenched and tempered conditions. Some of the results obtained are shown in Table V. Some secondary cracking was observed in the fracture surfaces of the Charpy bars which could have been due to quench cracks produced by the severe quench. It was resolved to oil quench in order to avoid quench cracking. However, it was found that none of the alloys, A1 - A6, had sufficient hardenability to obtain fully martensitic structures by the slower quench. To overcome this problem, additions of Cr were made to a new batch of ingots whose compositions are shown in Table IV as alloys A7 - A13. In addition to the Cr modification, other changes in the composition were made and the rationale behind these modifications is discussed below.

One of the problems encountered in the steels A3 through A6 was the presence of undissolved carbides at austenitization temperatures below 1250 ^{o}C. Austenitization at 1250 ^{o}C led to a large grain size which severely impaired the impact toughness. It was decided to modify the composition in

A further series of alloys were cast and their compositions are shown in Table IV (steels A14 to A21). These alloy compositions were designed mainly to study the effect of Si and Al additions. Alloys A20 and A21 were also cast to study the effect of minor amounts of V on the secondary hardening response with and without Si + Al additions. Although it was intended to obtain a C level of 0.35 in all the steels, some of the steels ended up with lower C contents. This factor was taken into account in analyzing the results which are discussed below.

The alloys A14 through A21 were all austenitized at 1100 ^{o}C to ensure that there was no free ferrite in the microstructure and were oil quenched. (It is not implied that all the alloys required an austenitization temperature of 1100 ^{o}C; this temperature was chosen so as to allow a comparison among the alloys.) Tempering temperatures up to 650 ^{o}C were used. The hardness values are shown in Table VII and also plotted in Figures 20 through 25. The effect of Si additions was analyzed by studying the tempering response of steels A14 through A17 and the results are shown in Figures 20-22. It was found that Si raised the hardness levels substantially, especially in the secondary hardening range; the increase in hardness was dependent on the amount of Si added with the highest hardnesses obtained in the alloy with the highest amount of Si. Silicon also shifted the secondary hardness peak to lower temperatures; the more Si added, the lower was the peak hardness temperature. In addition, Si helped in obtaining a flat tempering response over the entire range of tempering as shown in Figure 21.

The tempering response of the alloy containing Al is shown in Figure 23. It was found that the addition of Al also raised the secondary hardness although not to as great an extent as with an equivalent amount of

Si addition. The peak was also shifted to lower temperatures. The effect of combined additions of Si + Al proved to be interesting. Alloy A19 contained 1Si + 1Al. The hardening response is compared to that of another secondary hardening steel (obtained from the literature[49]) in Figure 24. It appeared that the combined addition resulted in a hardness level, at the peak, which was higher than can be expected by just adding the increases in hardness obtained by Si and Al individually. This effect is also observed on comparing steels A20 and A21, as shown in Figure 25. The flatness of the tempering behavior should allow the study of varying microstructure and toughness at the same hardness level. The addition of a small quantity of V resulted in an increase in the secondary hardening levels and also shifted the peak to higher temperatures.

Preliminary tests have indicated that in order to obtain higher hardness in some of the alloys (say, around R_c55) longer aging times at temperatures slightly below the peak temperatures can be used.

Some preliminary data on Charpy energies at room temperature have been obtained for some of the alloys in selected tempered conditions and the data are presented in Table VIII. These preliminary results indicate that good combinations of hardness and impact toughness can be obtained in some of the experimental alloys. For example, Cv-Rc combinations of 15-58 and 13-53.2 have been obtained. At this point, no detailed analysis of this data has been made because a more complete evaluation is being obtained with materials obtained from larger (22-lb) ingots.

3.2.3 Secondary Hardening Bainitic Steels (Series A Steels - Isothermally Transformed)

The compositions of steels studied under this classification are given in Table IX.

When these steels were austenitized and isothermally transformed at temperatures intermediate between room temperature and the austenitizing temperature, microstructures containing different relative proportions of bainite, martensite, and untransformed austenite were obtained. Isothermal transformation treatments were of interest because they permitted microstructural variations that might enhance abrasive wear resistance. In addition, in higher carbon steels (containing greater than about 0.5 percent C), isothermal treatments can promote a reduction in the amount of internally twinned martensite which is believed to have a deleterious effect on toughness[62]. Accordingly, the steels of series A were examined with regard to their isothermal transformation response.

Dilatometric specimens of the steels A1 and A2 were austenitized at 1150 ^{o}C for 15 min, (heating rate 10 ^{o}C/sec), quenched at 187 ^{o}C/sec to several different temperatures in the 400 ^{o}C - 520 ^{o}C range, and held at the temperatures for monitoring the progress of the austenite transformation. A typical time-temperature-transformation (TTT) diagram determined by this procedure is illustrated in Figure 26, which was obtained for a specimen of the steel A2. For the steel A2, the TTT data showed an austenite bay at 520 ^{o}C where austenite remained untransformed for 3 hours. The bainite reaction began in 6 to 7 seconds at 420 ^{o}C. Transformation data of this type were useful in selecting the temperatures and hold times for isothermal heat treatments.

Following determination of the TTT diagram, specimen blanks of the steels A1 and A2 were austenitized at 1150 ^{o}C for one hour, quenched to 437 ^{o}C and 450 ^{o}C, respectively, held at the respective temperatures for one hour to attain maximum transformation to bainite, and oil quenched. The steels were then tempered for one hour at several temperatures in the

range 200 ^{o}C - 700 ^{o}C. In Figure 27 is shown plots of Rockwell C hardness vs tempering temperature for the steels A1 and A2. Although both steels exhibited secondary hardening behavior, the steel A1 had a relatively low hardness and was therefore eliminated from the bainitic steel series. The steel A2 exhibited higher hardness levels at tempering temperatures between 500 ^{o}C and 600 ^{o}C.

Room temperature Charpy V-notch impact tests of isothermally transformed steel A2 specimens, tempered at temperatures in the range 450 ^{o}C - 600 ^{o}C, were conducted, and the results are plotted in Figure 28. Beyond a tempering temperature of 500 ^{o}C, an apparent drop in the Charpy energy was observed. The impact energy of the isothermally transformed steel was relatively low even at lower tempering temperatures.

Fracture surface examination of Charpy specimens suggested one possible means of improving the impact energy of the steel A2 with a bainitic microstructure. As illustrated in Figure 29(a) by the scanning electron fractograph of a Charpy specimen of steel A2 (isothermally transformed for one hour at 450 ^{o}C and tempered for one hour at 500 ^{o}C), the fracture mode was predominantly quasi-cleavage with some dimpled rupture. Undissolved carbides (left in the steel after austenitizing) were observed on the fracture surfaces and were analyzed using energy dispersive x-ray chemical analysis. The analysis gave rise to a pattern illustrated in Figure 29(b), indicating that the undissolved carbides were primarily those of vanadium and titanium. The low Charpy impact energy was believed to have been due in part to the presence of large undissolved carbides and also partly due to cleavage of the matrix. There is evidence[49] to believe that undissolved carbides may be detrimental to toughness if they are larger than a critical size. In attempts to eliminate large

undissolved carbides, specimens of the steel A2 were subsequently austenitized at 1215 ^{o}C prior to carrying out the isothermal treatments in the usual manner. It was found that although the higher austenitization temperature reduced the amount of undissolved carbides, it increased the grain size substantially, and consequently there was a slight decrease in the impact energies obtained. In any case, the Charpy values obtained for specimens austenitized at either temperature were only around 4-6 ft-lbs corresponding to hardnesses of around R_c50. It was decided to drop the steel A2 also from further investigation.

The TTT diagram of steel A5 was determined and is shown in Figure 30 for the lower bainite range. The M_s of the steel was determined to be 300 ^{o}C and the M_f was 100 ^{o}C. At a temperature just above 420 ^{o}C, the isothermal transformations did not go to completion, even on holding for periods up to four hours, indicating that the B_s temperature was approached, and the presence of an austenite bay. Charpy blanks were austenitized at 1210 ^{o}C for one hour, quenched in a salt pot to a temperature just above the M_s, i.e., 325 ^{o}C, isothermally transformed for one hour, and oil quenched to room temperature. The blanks were tempered at different temperatures up to the secondary hardening peak. Charpy specimens were obtained from these blanks and tested at room temperature. The results are shown in Table X and also plotted in Figure 31. Impact energies of 12-14 ft-lbs were obtained from specimens tempered to temperatures up to 400 ^{o}C, beyond which there was a steep drop in Charpy values and an increase in hardness to R_c60 at the peak. At the present time, the exact reasons for the drop in Charpy energies beyond a tempering temperature of 400 ^{o}C have not been identified. However, it was observed from x-ray measurements of untempered specimens that substantial amounts of retained austenite were present. Hence, the transformation of

this relatively higher carbon austenite to brittle decomposition products at higher tempering temperatures, could be responsible for the initial drop in toughness. The fracture surfaces of the broken Charpy bars were examined in a scanning electron microscope and are shown in Figure 32. The fracture surfaces showed different amounts of dimple rupture and quasi-cleavage with the specimen tempered at 450 ^{o}C showing the maximum amount of cleavage surfaces.

Because alloy A5 did not have the target C content of 0.4 and contained a lower amount of Al than planned initially, a new ingot was cast (alloy A22). Two other ingots (alloys A23 and A24) with minor variations in the C and Si contents were also cast and their compositions are shown in Table IX. The as-quenched hardness of these alloys as a function of the austenitization temperature is shown in Figure 33. The increase in hardness with austenitization temperature was an indication that undissolved carbides were going into solution in the austenite. There did not appear to be any substantial differences in hardnesses between the steel austenitized at 1150 ^{o}C and 1200 ^{o}C.

The hardening response of alloy A22 in the quenched and tempered condition is shown in Figure 34. The tempering response of the alloy following austenitization at 1150 ^{o}C and 1200 ^{o}C was similar although slightly higher hardnesses were obtained for the 1200 ^{o}C specimens. The tempering behavior of alloys A23 and A24 were also similar to that of A22 and are shown in Figure 35 and Figure 36. Although no large change in hardness was observed on austenitizing at 1200 ^{o}C as compared to 1150 ^{o}C, it was found that there were more undissolved carbides present in the 1150 ^{o}C specimens as compared to those in the 1200 ^{o}C specimens as shown in Figure 37 for alloy A24.

Using an austenitization temperature of 1200 ^{o}C, the steels A22, A23, and A24 were isothermally transformed at 275 ^{o}C and 350 ^{o}C and tempered at different temperatures. The plots of hardness versus tempering temperature for the three steels are shown in Figures 38, 39, and 40. Although the quenched and tempered heat treatment resulted in the highest hardness, the steels transformed isothermally also possessed high hardness levels on tempering beyond 400 ^{o}C.

The results of Charpy tests conducted at room temperature are shown in Table XI for steels A22, A23, and A24. The austenitization temperatures used are indicated in the table. The isothermal transformation temperature was 275 ^{o}C. It was observed that, for all three steels, there was a drastic drop in Charpy values on tempering at temperatures beyond 400 ^{o}C just as in the case of steel A5. The steels A22 and A24 which contained higher amounts of C and Si, respectively, as compared to A23 showed poorer Charpy impact resistance. Although the amounts of retained austenite in these steels following the different heat treated conditions have yet to be determined, it appeared that the transformation products of the retained austenite (which were surely present in these steels) had a major role in the embrittlement observed. This observation was supported by the fact that the Charpy values did not recover beyond the peak hardness temperature which indicated that the undesirable morphology of the transformation product of the initial retained austenite was responsible for the loss in Charpy energies. If the drop had been only due to the secondary hardening reaction, the properties should have recovered beyond the peak hardness treatment. More experiments are underway to clarify this behavior.

Based on the above results, it was decided to obtain a new set of alloy compositions to obtain bainite and combinations of bainite and

other microconstituents which would have superior combinations of hardness and toughness. As it appeared that the presence of retained austenite is undesirable in isothermally transformed secondary hardening steels, it was decided not to add the alloying elements Al and Si to the new set of alloys. The reason for this was because Al and Si are known to promote the retention of large amounts of austenite in isothermally transformed steels[58,63]. The preliminary compositions of these alloys are shown in Table XII. These compositions are essentially similar to the steels developed for the quenched and tempered heat treatments except for the absence of Al and Si. The amounts of the secondary hardening elements present are expected to allow the lowest possible austenitization temperatures with a minimum amount of undissolved carbides.

For applications involving ambient temperatures where secondary hardening steels are not necessary, it was decided to study isothermally transformed low alloy steels containing Al and Si. Such a study was deemed to be desirable because it has been reported in the literature[35] that both bainite and retained austenite can be beneficial for wear resistance. The series C steels were investigated initially and the compositions used are shown in Table XIII. Three isothermal transformations were chosen and the results of hardness and Charpy tests are shown in Tables XIV and XV. The retained austenite contents were measured by standard x-ray techniques[64]. The results showed that good combinations of hardness and toughness were obtained in such steels although the hardnesses themselves were not as high as R_C55. However, hardnesses of R_C51-52 have been obtained with C_V values which are considered excellent for this class of steels. These experimental steels have toughnesses which compare very favorably with those of maraging steels in this hardness/strength regime.

3.2.4 Secondary Hardening Matrix Steels (Series B Steels)

Matrix steels are steels that are derived from tool steels by reducing the alloy element content sufficiently so that all carbides are in solution after an austenitization treatment. Several of these steels exhibit a secondary hardening response when they are tempered. One such steel, the commercial steel Vasco MA, which has been previously claimed as a matrix steel was recently investigated at LBL[60]. The investigations indicated that, contrary to the definition of a matrix steel, Vasco MA contained coarse, undissolved carbides after austenitizing at a temperature as high as 1350 ^{o}C. It has been reported [49] that the presence of such coarse carbides can be the prime cause of low fracture toughness in steels. When high austenitizing temperatures are used in order to eliminate the coarse, undissolved carbides in steels of this type, grain growth commonly occurs, leading to an increase of the ductile-brittle transition temperature and to temper embrittlement. In addition, when more carbon goes into solution in the austenite, the martensite that forms during subsequent quenching has an increased tendency for internal twinning which further lowers fracture toughness. Therefore, a new approach was used for designing matrix steels. The approach involved, (1) chemical analysis and statistical estimation of the volume fraction of the complex alloy carbides after each of several austenitization treatments, and (2) similar studies using steels in which carbon and the significant carbide forming alloying elements were systematically varied.

This approach was expected to help in establishing the phase stabilities of the alloy carbides and thus aid in designing other similar steels.

For preliminary experiments under the current program, the steel of nominal composition B1 in Table XVI (same composition as Vasco MA)

was chosen. Specimens of the steel were austenitized for one hour in argon atmosphere at 900 ^{o}C, 1000 ^{o}C, 1100 ^{o}C, and 1200 ^{o}C, and ice-brine quenched. Rockwell C hardness measurements indicated that the as-quenched hardness increased when the austenitizing temperature was raised, as illustrated in Figure 41. As expected, optical microscopy of the as-quenched steel showed that there were undissolved carbides following all of the austenitizing treatments. A typical microstructure is illustrated by the optical micrograph in Figure 42(a), which was obtained from the specimen austenitized at 900 ^{o}C. Scanning electron microscopic examination in conjunction with energy dispersive x-ray analysis of the same specimen established that tungsten was the major alloy constituent of the carbides while smaller amounts of vanadium and molybdenum were also present.

The above results formed the basis for the design of additional alloy compositions of Series B steels listed in Table XVI. In subsequent investigations, experimental heats of the steels B4 and B5 were examined. Because the carbides in the steel B1 contained large amounts of tungsten, it was evident that it would be most logical to reduce the tungsten if undissolved carbides were to be minimized or eliminated. In addition, it is also known that large amounts of vanadium results in the formation of carbides that are stable up to at least 1300 ^{o}C, so vanadium was reduced in steel B5. Both steels were austenitized at the same temperatures as the steel B1 and the as-quenched Rockwell C hardness was determined. The results are plotted in Figure 41. Two conclusions were arrived at from the data presented in the figure. First, the hardness generally increased with increase in austenitizing temperature. Secondly, for the 900 ^{o}C austenitizing treatment, the hardness of the steel B4 was greater than that of the steel B5, which in turn was harder than the steel B1. The greater

hardness reflected greater amounts of carbon and alloying elements in solution in the austenite.

Optical micrographs of the steels B1, B4, and B5 are presented in Figure 42(a), (b), and (c), respectively, for the 900°C austenitizing treatment. A comparison of the three microstructures clearly shows that undissolved carbides were present in all three steels with the volume fraction of carbides being the maximum in the steel B1. In Figure 43 is shown the optical pictures of steels B1, B4, and B5 in the as-quenched condition. It was observed that the base steel B1 had large quantities of undissolved carbides following austenitization at 1000°C. The amount of undissolved carbides, and their size was much smaller in the as-quenched B4 and B5 alloys. Some kind of grain boundary precipitate was present in the steels B1 and B4 as seen clearly in Figure 44, which contains optical micrographs of the tempered alloys. These precipitates were associated with a precipitate-free zone as pointed out by the arrow in the figure. An analysis of the elements present in these precipitates using the energy dispersive x-ray analysis unit showed that they were rich in V, W, and Mo. The possible influence of these precipitates on the fracture behavior will be discussed in a following section. Within the grains, fine secondary carbides were observed. An analysis of their composition proved to be difficult as they were very small. The fine, undissolved primary carbides present in steels B4 and B5 were revealed by scanning electron microscopy as shown in Figure 45 for steel B4, which shows microstructures in the as-quenched condition.

The hardness of steels B1, B4, and B5 austenitized at 1000°C, and tempered at different temperatures following an oil quench, were determined and the results are shown in Table XVII. Also shown in the table are the hardness values obtained from steels austenitized at 1200°C. From

Figure 46, it is observed that steel B5 maintained the highest level of hardness over the secondary hardening range. The peak in hardness appeared to occur at a lower temperature (500 ^{o}C) as compared to that of steel B1 which was located at 550 ^{o}C. Steel B4, with lower W, also exhibited higher hardnesses than steel B1 on either side of the peak which was located at 550 ^{o}C. The increased hardness levels in steels B4 and B5 was due to the greater amount of C and secondary carbide forming elements in solution following austenitization which allowed more secondary carbides to precipitate. No tempering data of steel B1 following austenitization at 1200 ^{o}C was available. As seen from Table XVII, the hardness of the steels B4 and B5, tempered following austenitization at the higher temperature, was higher as compared to those obtained following austenitization at 1000 ^{o}C. This result was undoubtedly due to more complete dissolution of the fine, undissolved carbides which led to higher amounts of C and secondary carbide formers being available for secondary hardening.

Charpy impact tests were performed at room temperature on alloys B1, B4, and B5 austenitized at 1000 ^{o}C and also on alloy B4 and B5, austenitized at 1200 ^{o}C. The results are shown in Table XVII. Figure 47 shows the variation of Charpy impact energy with tempering temperature for steels B4 and B5 austenitized at 1000 ^{o}C and 1200 ^{o}C. Both the steels exhibited poor impact values for the 1200 ^{o}C austenitization treatment although the hardness levels were higher for this austenitization temperature. Alloy B4 had much better C_v values than alloy B5 when a 1000-^{o}C austenitization temperature was used. The differences in Charpy energies are possibly explained by the difference in grain sizes. In Figure 48 is plotted the variation of Charpy impact energy with tempering temperature of steels B1, B4, and B5 for an austenitization temperature of 1000 ^{o}C. It is seen

from the figure that the base alloy B1 had the poorest impact energies and alloy B4 had the highest energy values. The poor impact energies shown for alloy B1 can be attributed to the presence of undissolved carbides (see Figure 43(a)). Alloy B4 had almost the same Charpy values (around 15 ft-lbs) over the tempering range 450 ^{o}C to 600 ^{o}C. Alloy B5 had Charpy values intermediate between those of B1 and B4. There appeared to be some kind of an embrittlement reaction in both alloy B5 and B1 on tempering between 450 ^{o}C and 600 ^{o}C; this may be related to the slight increase in hardness of those alloys in this temperature range of 500 ^{o}C - 550 ^{o}C. Figure 49 shows scanning electron fractographs taken from broken Charpy specimens of steel B4 and B5 austenitized at 1000 ^{o}C and tempered at 600 ^{o}C. A grain boundary failure mode is present which could have been due to the presence of the precipitate and the associated precipitate-free zone as was shown in Figure 44 . Within the grains the fracture mode appeared to be a combination of dimple rupture and quasi-cleavage. As shown in Figure 50 the dimples were associated with carbide particles which were analyzed to be rich in W and Mo.

Some preliminary results have been obtained on alloys in which W and Cr were reduced below that of the base composition. In Figure 51 is plotted the hardness of as-quenched alloys versus the austenitization temperature (one hour at temperature and ice-brine quenched) for the series of alloys in which the W was reduced below that of the base alloy B1. Both B4 and B6 showed higher hardnesses than B1 at austenitization temperatures below 1200 ^{o}C. This was because more C was in solution in the lower W alloys. There did not appear to be too significant a difference in the hardness of B4 and B6 quenched from either 1000 ^{o}C or 1100 ^{o}C. However, this does not necessarily mean that an alloy with 0.5W would be optimum because it might not have an adequate secondary hardening response. A similar behavior was observed for the series of alloys in which the Cr was varied. The results

are plotted in Figure 52. The alloy with the lowest Cr content had the highest as-quenched hardness following austenitization at temperatures of 1000 ^{o}C, 1100 ^{o}C, and 1200 ^{o}C.

The secondary hardening response of steels B6, B9 and B10 were determined and the Charpy impact energies at room temperature were obtained. The results are shown in Table XVIII. Steel B6, which contained the lowest W content among the steels studied (0.5W) could not achieve the hardnesses possible with the higher W grades. However, good combinations of toughness and hardness (20 ft-lbs - 51.8R_c) were obtained. It appeared that a minimum amount of W was necessary for achieving substantial secondary hardening in this class of steels. Steels B9 and B10, which were the lower Cr modifications showed similar tempering responses and also exhibited similar Charpy impact values at room temperature. The low value of C_v for steel B10 tempered at 600 ^{o}C was probably due to error.

From the data obtained to date, there is evidence that it would be possible to improve the toughness of the matrix steels through proper alloy modifications. These modifications will permit steels to be austenitized at lower temperatures than the base matrix steel, avoid the presence of undissolved carbides,and also obtain the required hardness levels.

3.2.5 Low Alloy Steels (Series C Steels)

The Series C steels are modifications involving additions of Al, Si, and C to AISI 4340 steel. The chemical compositions of these steels are given in Table XIII. (Note that the steel compositions have been renumbered and are not the same as reported in the last two quarterly reports.) The modified compositions were obtained by remelting commercial, vacuum arc remelt, aircraft quality AISI 4340 in an induction furnace backfilled with argon. Alloy additions of Al, Si and C were made to the remelted steel. The alloys,obtained as 22-lb, 2-1/2-in.-diameter ingots,were upset- and cross-forged into plates 1-in. thick and homogenized in argon for 24 hours at

1200 ^{o}C. The austenitization temperatures were determined metallographically (as shown in Figure 53) and were found to be 950 ^{o}C for steels C1, C2, and 1000 ^{o}C for steel C3. The steels were austenitized for one hour, oil quenched and tempered at various temperatures up to 600 ^{o}C. The hardness data is shown in Table XIX. The steels C2 and C3 exhibited a slight hardness peak around the tempering temperature of 300 ^{o}C. As expected, the hardness levels of these two steels were higher than that of steel C1 which had a lower C content. The tensile properties and Charpy impact energies of the three alloys were obtained at room temperature and are shown in Table XX. The values obtained for steel C1 duplicates results reported in a previous study[61]. Good combinations of strength and toughness were obtained in steels C1 and C2. The results indicated that the addition of 2.0Al + 2.0Si to 4340 increased strength, but lowered impact toughness. Compact tension specimens are being prepared for these steels, from which the fracture toughness will be determined.

3.2.6 Cr-Si-Mo Steels (Series D Steels)

The steels in Series D were selected not only for alloy screening in Task II, but also for microstructural studies of wear in Task I of the program. The compositions used in this series are shown in Table XXI. It was decided that the steel D-1 (an ESCO composition) would be initially characterized to examine the microstructural features and mechanical properties that may be responsible for its known wear resistance. The steels D2, D3, and D4 were selected in order to obtain additional improvements in wear resistance through alloying and through incorporating the beneficial microstructural features of the steel D1. Experimental quantities of the steel compositions were cast as 22-lb ingots following melting in an induction furnace using an argon atmosphere. The processing of the cast

ingots was similar to that of the series C steels. An austenitization temperature of 900 ^{o}C was used for steels D1, D2, and D3. They were oil quenched from 900 ^{o}C and tempered at temperatures to 500 ^{o}C. The time at temperature was one hour, following which they were air cooled to room temperature. The tempering data are plotted in Figure 54. Steel D2 with the higher C level had the highest hardness. It exhibited a slight hardening peak around 100 ^{o}C - 150 ^{o}C, which is characteristic of low alloy steels. Steels D2 and D3 had about the same hardness up to a tempering temperature of 350 ^{o}C; beyond 400°C, the steel with the higher Cr content showed higher hardnesses. The results obtained were expected, and further investigations of these steels involve routine determination of mechanical properties and microstructures.

The results of Charpy tests on the steels D1 - D3 are shown in Figure 55. It was observed that the higher C version (steel D2), although it exhibited high hardness levels (around R_C56 on tempering at 200 ^{o}C - 300 ^{o}C) showed the lowest C_V values around 10-12 ft-lbs. The higher Cr modification (D3), which had the same hardness levels as that of steel D1, showed much better impact resistance. For example, following tempering at 200 ^{o}C, a C_V of 30 ft-lbs was obtained corresponding to a hardness of R_C53. The other mechanical properties, such as yield and ultimate strength, K_{Ic}, and microstructure are being characterized presently.

4. CONCLUSIONS

The following conclusions were made from the Phase I studies.

1. The operating conditions in the principal coal transportation and fragmentation equipment that are within the scope of the current program include a wide range of service environments involving impact loading, ambient and elevated (500 ^{o}F - 1000 ^{o}F) temperatures, and abrasion from coal particles, which may either be in the form of particles ranging in size from very fine pieces to large chunks. Abrasive wear can occur by either two-body or three-body wear.
2. Abrasion in dry coal feeders will be predominantly of three-body type involving high stresses. Some adhesive wear can also occur.
3. Coal loader shovels and chutes are expected to undergo ambient temperature, relatively low stress abrasion of a two-body type.
4. Coal crushing and milling equipment encounter abrasion under high contact pressure and impact.
5. Some of the results obtained from studies within the scope of this program may also be applicable to mining equipment.
6. A literature survey of wear testers made it clear that a wide variety of testers are available which can simulate different service conditions in the laboratory. Based on this survey, different testers have been chosen to study abrasive wear situations expected in the different applications.
7. A pin-on-disk-type tester was designed and constructed which simulates high stress abrasion of a two-body type at ambient temperatures.

8. An abrasive particle size effect on wear rate was observed up to a size of 100 μ beyond which the wear rate appeared to be independent of particle size.

9. Jaw crusher tests results indicated that modified 4340 + 1.5Al + 1.5Si steels exhibited combinations of hardness and wear ratios which were as good as or better than those obtained for AISI 4340 steel.

The alloy design phase (Phase II) studies led to the following conclusions.

1. It was possible to obtain secondary hardness above Rc55 in the alloys A7-A12 which contained around 0.4C and lower amounts of the carbide formers Mo and V as compared with the alloy A5 which contained higher amounts of the carbide formers.

2. A further reduction in C level to 0.35 resulted in lower peak hardness levels (alloys A8-A21). However, hardnesses of Rc53 have been obtained and have been increased by using longer aging times (10 hours) at temperatures a little below the peak hardness temperature.

3. The addition of Si resulted in an increase in the secondary hardening response and also a shift of the peak to lower temperatures. The magnitude of the effect was dependent on the amount of Si added; the greater the amount of Si, the larger the effect.

4. The effect of Al additions was similar to Si except that the magnitude of the changes was lower..

5. The effect of adding Al + Si combinations was more potent than the effect of Al and Si additions individually.

6. It was possible to obtain steels which exhibited a "flat" tempering response from temperatures of 200°C to 600°C with the proper choice of alloy composition.

7. Good combinations of hardness and impact toughness were obtained in some of the experimental secondary hardening steels.

8. The addition of Al + Si to secondary hardening steels resulted in the retention of substantial amounts of retained austenite in isothermally transformed steels.

9. The presence of retained austenite can either be beneficial or detrimental to toughness, depending upon the temperature of tempering. Tempering at temperatures greater than 400°C of secondary hardening steels containing Al and Si caused a severe degradation of Charpy impact energies. This degradation was apparently related to the transformation products of the retained austenite. However, the presence of retained austenite in these steels tempered at lower temperatures could be beneficial to toughness.

10. Good combinations of strength and toughness were obtained in isothermally transformed and quenched and tempered 4340 + Al + Si steels.

11. It was possible to increase the as-quenched hardness, tempering response, and decrease the austenitization temperature and the amount of undissolved carbides of the so-called matrix steels through a reduction in the amount of the alloy elements such as W, V, and Cr.

12. Good hardness-toughness combinations were obtained in the modified matrix steels on tempering in the secondary hardening range.

13. An increase of Cr in the Cr-Si-Mo steels by one weight percent increased the impact toughness without loss in hardness.

5. WORK FORECAST

The work forecast for the following year is given below, with the contract being administered through the Campus Research Office of the University of California, Berkeley.

5.1 TASK I

Using the dry abrasive wear tester, a standard material for comparison will be obtained. Abrasives of different hardnesses and grit sizes will be used. Data on experimental alloys will be generated for different heat treated conditions. More of the 4340 + Al + Si alloys and the new Cr-Si-Mo steels will be tested using the ESCO jaw crusher. A three-body abrasive wear tester capable of ambient and elevated temperature testing will be constructed. A purchase order to run impact tests at the Albany Metallurgy Research Center will be set up.

5.2 TASK II

The metallurgical characterization, including hardness, tensile properties, impact toughness, fracture toughness, and microstructure will be completed on larger size (22-lb) ingots. A correlation between wear properties and metallurgical variables is expected following this study.

5.3 TASK III

Major equipment producers will be contacted for testing of components made from experimental alloys.

REFERENCES

1. Coal Feeder Development, Phase I Report, Report on Contract No. E(49-18)-1973, March 1976, Foster-Miller Associates, Inc., Waltham, Massachusetts.

2. Coal Demonstration Plants, Quarterly Report, April-June 1976, Office of Fossil Energy, Energy Research and Development Administration, Washington.

3. Proceedings of the Conference on Coal Feeding Systems, Held at Pasadena, June 21-23, 1977, JPL Publication 77-55, Jet Propulsion Laboratory, California Institute of Technology, Pasadena, California 91103.

4. R. L. Phen, W. K. Lucklow, L. Mattson, D. Otth and P. Tsou, ibid., p. 324.

5. S. F. Fields, ibid., p. 359.

6. A. H. Furman, ibid., p. 411.

7. G. A. Saltzman, Plastics Design and Processing, December, 1973, p. 9.

8. G. A. Saltzman, Proceedings of the International Conference on Wear of Materials, held at St. Louis, April 1977, ed. W. A. Glaeser, K. C. Ludema and S. K. Rhee, The American Society of Mechanical Engineers, New York, NY 10017, p. 217.

9. M. A. Moore, Wear, 27, 1974, p. 1.

10. S. Bhattacharya and F. C. Bock, Proceedings of the International Conference on Wear of Materials, held at St. Louis, April 1977, ed. W. A. Glaeser, K. C. Ludema and S. K. Rhee, The American Society of Mechanical Engineers, New York, NY 10017, p. 167.

11. F. Borik and D. L. Sponseller, J. Mater, 6 (3), 1971, p. 576.

12. R. C. D. Richardson, Engineering, Vol. 208(5401), 1969, p. 479.

13. A catalog of Friction and Wear Devices, 2nd Printing, 1972, American Society of Lubrication Engineers, Park Ridge, Illinois.

14. J. Muscara and M. J. Sinnot, Metals Eng. Quart., Vol. 12(2), 1972, p. 21.

15. R. G. Bayer, P. A. Engel, and J. L. Sirico, Wear, Vol. 19 (3), 1972, p. 343.

16. F. Borik, Metals Eng. Quart., Vol. 12 (2), 1972, p. 33.

17. F. Borik and W. G. Schalz, J. Mater., 6 (3), 1971, p. 576.

18. R. D. Haworth, Jr., Trans. ASM, 41, 1949, p. 819.

19. F. Borik, SAE Reprint No. 700687, September 14, 1970.

20. D. E. Diesburg and F. Borik, "Materials for the Mining Industry", Climax Molybdenum Company, U.S.A., 1974, p. 15.

21. R. C. Tucker, Jr., and A. E. Miller, "Selection and Use of Wear Tests for Metals", ASTM STP615, R. A. Bayer, Ed., American Society for Testing and Materials, 1976, p. 68.

22. K. J. Bhansali and W. L. Silence, Metal Progress, 112 (6), 1977, p. 39.

23. R. Blickensderfer, D. K. Deardorff, and J. E. Kelley, Report of Investigations 7930, U.S. Department of the Interior, Bureau of Mines, Albany Metallurgy Research Center, Albany, Oregon, 1974.

24. R. A. Beal, J. E. Kelley, and J. S. Hansen, Quarterly Progress Report, Development of Wear-Resistant Valve Materials, October 1977, U.S. Bureau of Mines, Albany Metallurgy Research Center, Albany, Oregon, 97321.

25. N. F. Fiore, "Microstructural Effects in Abrasive Wear", Proposal submitted to ERDA, University of Notre Dame, Notre Dame, Indiana, 46556, 1976.

26. S. W. Date and S. Malkin, Wear, 40, 1976, p. 223.

27. I. Finnie, Wear, 19, 1972, p. 81.

28. R. L. Aghan and L. E. Samuels, Wear, 16, 1970, p. 293.

29. J. Larsen-Badse, Wear, 11, 1968, p. 213.

30. M. M. Khruschov and M. A. Babishev, Friction and Wear in Machinery, 19, 1965, p. 1.

31. N. F. Fiore, Quarterly Progress Report on "Microstructural Effects in Abrasive Wear", Department of Metallurgical Engineering and Materials Science, Notre Dame, IN 46556, October, 1977.

32. V. F. Zackay and E. R. Parker, "Wear Resistant Alloys for Coal Handling Equipment", proposal submitted to ERDA, Materials and Molecular Research Division, Lawrence Berkeley Laboratory, University of California, Berkeley, November 1976.

33. W. Fuller, ESCO Corporation, Portland, Oregon, Private communication.

34. E. Hornbogen, Wear, 33, 1975, p. 251.

35. P. L. Hurricks, Wear, 26, 1973, p. 285.

36. A. Kasak and T. A. Neumeyer, Wear, 14, 1969, p. 445.

37. R. W. Durman, Foundry Trade Journal, May 1973, p. 645.

38. J. Larsen-Badse and K. G. Mathew, Wear, 14, 1969, p. 199.

39. W. L. Silence, Proceedings of the International Conference on Wear of Materials, held in St. Louis, April 1977, eds. W. A. Glaser, K. C. Ludema, and S. K. Rhee, The American Society of Mechanical Engineers, p. 77.

40. K. G. Budinski, ibid., p. 100.

41. R. B. Gundlach and J. L. Parks, ibid., p. 211.

42. H. S. Avery, Discussion to paper by D. E. Diesburg and F. Borik (Reference 20).

43. M. M. Kruschov, Wear, 28, 1974, p. 69.

44. R. C. D. Richardson, Wear, 11, 1968, p. 245.

45. H. S. Avery, "Materials for the Mining Industry", Climax Molybdenum Company, USA, p. 43.

46. J. D. Murray, "High Strength Steels", Iron Steel Inst. Spec. Report #76, 1963, p. 41.

47. K. Kuo, J. Iron Steel Inst., 184, 1956, p. 258.

48. R. D. Goolsby, Ph.D. Thesis, University of California, LBL-405, Lawrence Berkeley Laboratory, Berkeley, CA 94720, November 1971.

49. T. Tom, Ph.D. Thesis, University of California, LBL-1856, Lawrence Berkeley Laboratory, Berkeley, CA 94720, September 1973.

50. E. C. Bain and H. W. Paxton, "Alloying Elements in Steel", American Soc. Metals, Metals Park, Ohio.

51. B. Aronsson, Proc. Climax Molybdenum Symp., Zurich, 1969, p. 77.

52. C. R. Austin, C. R. St. John, and R. W. Lindsay, Trans. AIME, 162, 1945, p. 84.

53. W. W. Cias and D. V. Doane, Met. Trans, 4 (10), 1973, p. 2257.

54. R. W. K. Honeycombe, "Structure and Strength of Alloy Steels", Climax Molybdenum Company, Ltd., London.

55. F. B. Pickering, Iron and Steel Inst., Spec. Report, 64, 1959.

56. A. G. Allten and P. Payson, Trans. ASM, Vol. 45, 1953, p. 498.

57. K. J. Irvine, J. Iron and Steel Inst., 200, 1962, p. 820.

58. M. S. Bhat, "Microstructure and Mechanical Properties of Ultra-High Strength Steels Containing Aluminum and Silicon", Ph.D. Thesis, University of California, LBL-6046, Lawrence Berkeley Laboratory, Berkeley, California, February 1977.

59. "VASCO Matrix Steels", Information Booklet published by VASCO, Latrobe, Pennsylvania.

60. N. J. Kar, "Interrelationships Between Thermal History and Mechanical Properties of a Secondary Hardening Steel", M.S. Thesis, University of California, LBL-5449, Lawrence Berkeley Laboratory, Berkeley, California, December 1976.

61. L. J. Venne, W. Fuller, ESCO Corporation, Portland, Oregon, Private Communication.

62. D. Huang and G. Thomas, Met. Trans. 2, 1971, p. 1587.

63. G. Kohn, "Effects of the TRIP Phenomenon on the Toughness of Heat Treatable Alloy Steels", Ph.D. Thesis, University of California, LBL-5466, Lawrence Berkeley Laboratory, Berkeley, California, November 1976.

64. B. D. Cullity, "Elements of X-Ray Diffraction", Addison Wesley, Reading, Massachusetts, 1956, p. 391.

Table I Hardness of 7075 Al and AISI 4340 Wear Specimens

Alloy	Aging (Tempering) Temp (°F)	Vicker's Hardness Kg/mm^2
7075 Al (Underaged)	202	158.0
	209	163.0
	223	167.0
	254	179.0
7075 Al (Overaged)	250	180.5
	254	181.0
	264	179.5
	305	167.0
	318	134.0
	332	122.5
	359	106.0
	371	102.0
AISI 4340	392	602.0
	662	498.0
	932	407.0
	1202	318.0

Table II Chemical Compositions of Modified 4340 Steels Melted by ESCO Corporation for Jaw Crusher Tests

Heat No.	Composition (Wt.pct)									
	C	Mn	Si	Cr	Ni	Mo	Cu	Al	S	P
X-3574	0.44	0.74	1.92	0.89	1.78	0.27	0.12	1.61	0.013	0.026
X-3584	0.41	0.80	2.03	0.89	1.76	0.23	0.13	1.60	0.009	0.018
X-3585	0.45	0.95	2.09	0.97	1.65	0.29	0.13	1.31	0.013	0.028

Table III Hardness and Wear Ratios of Modified 4340 Steels and Some Commercial Steels

Steel	Aust. Temp. (°F)	Tempering Temp. (°F)	Hardness BHN	Wear Ratio*
4340+1.5Al+1.5Si (#X-3574)	1832	572 (1 hour)	578	0.232
4340+1.5Al+1.5Si (#X-3584)	1832	572 (2 hours)	555	0.220
4340+1.5Al+1.5Si (#X-3585)	1832	572 (1 hour)	514	0.248
12S	-	-	514	0.266
HiC/12S	-	-	555	0.242
AISI4340 #22A	1750	Normalized	320	0.67
AISI4340 #22B	1600	1200 (1 hour)	340	0.72
AISI4340 #22C	1600	400 (1 hour)	520	0.23

* Wear ratio = $\frac{\text{Wt. loss of test specimen}}{\text{Wt. loss of standard}}$

The standard used was Steel T1, heat-treated to 269BHN.

The data on steels 12S and HiC/12S was provided by ESCO Corporation.

The data on the AISI4340 steels was obtained from Reference 20.

Table IV Compositions of Series A Steels

Designation	Composition (Wt. pct)*									
	C		Mn	Mo		V	Cr	Ni	Al	Si	Fe
A1	0.4	(0.37)	-	4.0	(3.81)	-	-	-	-	-	bal
A2	0.4	(0.4)	-	4.0	(3.80)	1 (1.00)	-	-	-	-	"
A3	0.42	(0.47)	0.5	4.0	(3.80)	0.75 (0.43)	-	3 (3.28)	1 (0.96)	1(0.96)	"
A4	0.42	(0.47)	0.5	4.0	(4.40)	0.75 (1.08)	-	2 (1.94)	1.5 (1.29)	1.5(1.57)	"
A5	0.42	(0.47)	0.5	4.0	(3.61)	0.75 (1.00)	-	3 (3.05)	1.5 (1.18)	1.5(1.36)	"
A6	0.42	(0.45)	0.5	4.0	(4.24)	0.75 (0.95)	-	3 (3.08)	2 (1.77)	2(2.13)	"
A7	0.4	(0.43)	0.5	2.5		0.5	1.0	3	1.5	1.5	"
A8	0.35	(0.34)	0.5	2.5		0.5	1.0	3	1.5	1.5	"
A9	0.40	(0.37)	0.5	1.75		0.4	1.0	3	1.5	1.5	"
A10	0.35	(0.35)	0.5	2.0		0.4	1.0	3	1.5	1.5	"
A11	0.40	(0.38)	0.5	1.75		0.4	1.0	5	1.5	1.5	"
A12	0.35	(0.33)	0.5	2.5		0.4	1.0	5	1.5	1.5	"
A13	0.40	(0.42)	0.5	4.0		0.75	-	2	-	-	"
A14	0.35	(0.28)	0.5	2.0		-	1.0	3	-	-	"
A15	0.35	(0.35)	0.5	2.0		-	1.0	3	-	1.0	"
A16	0.35	(0.29)	0.5	2.0		-	1.0	3	-	2.0	"
A17	0.35	(0.31)	0.5	2.0		-	1.0	3	-	3.0	"
A18	0.35	(0.35)	0.5	2.0		-	1.0	3	1.0	-	"
A19	0.35	(0.34)	0.5	2.0		-	1.0	3	1.0	1.0	"
A20	0.35	(0.33)	0.5	2.0		0.25	1.0	3	-	-	"
A21	0.35	(0.36)	0.5	2.0		0.25	1.0	3	1.0	1.0	"

* The numbers in parenthesis are from results of chemical analysis.

Table V Results of Room Temperature Charpy V-Notch Impact Tests on Quenched and Tempered Series A Steels

Steel	Tempering Temperature, °C	Rockwell C Hardness	Impact Energy, Ft-lbs
A2	500	49	4.3
	550	52	4.0
	600	57	1.8
	650	50	2.5
A4	500	62	2.3
	550	62	2.0
	600	59	2.3
	650	53	6.8

Note: All specimens were austenitized for one hour at 1150 °C followed by ice-brine quenching, and tempering for one hour.

The charpy data was obtained in the L-T direction.

Table VI Tempering Response (Rockwell C Hardness) of Series A Alloys Austenitized at 1250°C for 1 Hour and Oil Quenched

Alloy Number	Tempering Temperature, °C							
	AQ	200	300	400	500	550	600	650
A7	60	54.6	53	56.3	61	61.4	58.6	54.6
A8	54	52.5	53	53.2	59	58.6	54.6	51.5
A9	56.7	54.8	55	55	57	55.7	53.5	50
A10	56.5	54	54.8	55	58	56	53.8	50
A11	57.7	53	55.5	53.3	59.8	60	56.3	52.7
A12	57	53	55.3	54.8	59.3	60	56.5	52.6
A13	61	52.5	51.7	50.5	53	57	57.4	55

Table VII Tempering Response (Rockwell C Hardness) of Series A Alloys Austenitized at 1100°C for 1 Hour and Oil Quenched

	Tempering Temperature, °C							
Alloy	A.Q.	200	300	400	500	550	600	650
A14	49.6	47.5	44.7	43.1	43.2	42.1	43.3	35.4
A15	55.4	51.8	51.4	49.7	47.0	49.5	47.9	39.1
A16	51.2	51.5	50.9	50.5	50.8	50.2	47.5	39.4
A17	55.4	53.0	53.7	54.4	54.6	53.1	49.0	42.4
A18	53.4	50.3	46.0	47.8	47.1	47.7	46.4	39.9
A19	54.1	52.9	49.0	52.3	51.8	52.5	49.5	42.0
A20	52.5	50.6	47.0	45.0	46.7	47.3	48.6	44.7
A21	52.71	53.5	52.8	53.1	53.0	53.2	52.7	48.7

Table VIII Preliminary Room Temperature Charpy Impact Energies of Some Quenched and Tempered Series A Steels

Alloy No.	Tempering Temperature (C°) 500	550	600	650
A7	-	-	2.8 (59)	6.3
A9	-	9.5 (57)	8.8 (54)	-
A10	-	15.0 (58)	11.0 (55)	-
A11	-	-	5.8 (57.5)	4.8 (51)
A14	-	-	35.0 (43)	54.0 (35.4)
A15	16.5 (50)	18.0 (49.5)	12.5 (47)	-
A16	18.0 (50)	26.0 (50.0)	4.0 (47.5)	-
A17	5.5 (54)	5.5 (53.0)	-	-
A18	-	17.7 (47.5)	16.3 (46.5)	-
A19	-	11.0 (52.5)	10.0 (49.5)	-
A20	-	-	30.0 (49.1)	13.3 (44.7)
A21	8.0 (54.3)	13.0 (53.2)	12.5 (52.8)	

Charpy impact energy in ft-lbs

Numbers in parenthesis refer to R_c hardness.
Austenitization temperature for alloys A7-A11 was 1100 ^{o}C and for alloys A14-A21 was 1050 ^{o}C.

Table IX Compositions of Series A Steels Used for Isothermal Transformation Studies

Alloy No.	Composition (wt.pct)								
	C*	Mn	Si	Al	Cr	Mo	V	Ni	Fe
A1	0.37	-	-	-	-	4.0	-	-	Bal
A2	0.4	-	-	-	-	4.0	1.0	-	"
A5	0.47	0.5	1.5	1.5	-	4.0	0.75	3	"
A22	0.45	"	"	"	-	"	"	"	"
A23	0.36	"	"	"	-	"	"	"	"
A24	0.47	"	"	"	-	"	"	"	"

* The C percentages are from actual chemical analysis.

Table X Hardness and Room-temperature Charpy V-Notch Energy Values of Steel A5 Austenitized at 1210°C (1 hour), Isothermally Transformed at 325°C (1 hour), and Oil Quenched.

Tempering Temperature (°C)	Hardness (Rockwell 'C')	Room-Temp, Charpy V-Notch Energy (ft-lbs)
Untempered	49.5	12
325	50.4	10
400	50.4	14
450	50.3	9
500	55.0	5
550	60.0	2

Table XI Hardness and Room Temperature Charpy Data of Series A Secondary Hardening Bainitic Steels

Steel	Austenitization Temp. (°C)	Tempering Temp. (°C)	Hardness (Rc)	Room Temp. Charpy Energy (ft-lbs)
A22	1225	untempered	51.3	9.3
		400	52.5	10.3
		500	54.6	6.5
		550	53.7	4.3
		650	34.7	3.0
A23	1150	untempered	48.5	12.0
		400	47.5	11.8
		500	53.3	6.0
		550	57.9	4.3
		650	46.9	2.0
A23	1200	untempered	50.1	12.8
		400	49.9	11.0
		500	53.0	5.0
		550	56.0	2.3
		650	50.0	2.3
A24	1225	untempered	50.7	5.5
		400	51.0	8.0
		500	58.1	4.5
		550	59.5	2.3
		650	53.6	2.5

The heat treatment consisted of austenitizing at 1200°C (1 hour), isothermally transforming at 275°C (1 hour) and oil quenching.

Table XII Nominal Composition of New Series A Steels to be Used for Isothermal Transformation Studies

	Composition, wt. pet.						
Alloy No.	C	Cr	Mo	V	Mn	Ni	Fe
1	0.35	-	2	0.25	0.5	3	Bal
2	0.35	2	2	0.25	0.5	3	"
3	0.35	2	2	0.25	0.5	3	"
4	0.35	3	2	0.25	0.5	3	"
5	0.35	4	2	0.25	0.5	3	"

Table XIII Nominal Composition of Series C Steels *

Alloy No.	Chemical Composition (wt. pct)								
	C	Mn	Si	Al	Cr	Mo	V	Ni	Fe
C1	0.4	0.7	1.8	1.5	0.8	0.3	-	1.8	bal
C2	0.5	0.7	1.8	1.5	0.8	0.3	-	1.8	"
C3	0.5	0.7	2.3	2.0	0.8	0.3	-	1.8	"

* The Series C steels were obtained by making the necessary alloy additions to remelted vacuum arc melted AISI 4340 steel.

Table XIV Hardness, Charpy Impact Energies and Retained Austenite Contents of Isothermally Transformed 4340 + 1.5 Al + 1.5 Si Steel Austenitized at 1000°C.

Isothermal* Transformation Temp. (°C)	Tempering ** Temp. (°C)	Hardness (R_c)	Charpy Energy (ft. lbs.)	% Ret. Austenite
350°	As Quenched	43.4	53.5	14.7
	200	42.8	56.3	7.9
	300	43.3	57.8	5.7
	400	42.8	53.8	-
315°	As Quenched	48.5	36.5	7.0
	300	48.1	35.0	7.2
250°	As Quenched	51.3	20.5	1.4
	200	51.5	26.8	-
	300	50.9	25.0	-
	400	51.5	27.8	-

* Isothermally transformed 1 hour at temperature and oil quenched to room temperature.

** Tempered 1 hour at temperature and air cooled to room temperature.

Table XV Hardness, Charpy Impact Energies and Retained Austenite Contents of Isothermally Transformed 4350 + 1.5 Al + 1.5 Si Steel Austenitized at 1000°C.

Isothermal* Transformation Temp. (°C)	Tempering** Temp. (°C)	Hardness (R_C)	Charpy Energy (ft. lbs.)	% Ret. Austenite
350°	As quenched	45.1	51.0	11.2
	200	45.1	47.5	6.9
	300	45.2	52.3	8.6
	400	45.7	45.5	10.5
315°	As quenched	48.1	35.8	15.2
	300	48.3	36.8	12.6
250°	As quenched	52.0	22.0	9.1
	300	50.6	24.5	

* Isothermally transformed 1 hour at temperature and oil quenched to room temperature.

** Tempered 1 hour at temperature and air cooled to room temperature.

Table XVI Nominal Composition of Series B Steels

Alloy No.	Composition (wt. pct)						
	C	Si	Cr	Mo	V	W	Fe
B1	0.5	0.2	4.5	2.8	1	2	bal
B2	0.4	0.2	4.5	2.8	1	2	"
B3	0.5	0.2	4.5	2.0	1	2	"
B4	0.5	0.2	4.5	2.8	1	1	"
B5	0.5	0.2	4.5	2.8	0.5	2	"
B6	0.5	0.2	4.5	2.8	1	0.5	"
B9	0.5	0.2	3.5	2.8	1	2	"
B10	0.5	0.2	2.5	2.8	1	2	"

Table XVII Hardness and Room Temperature Charpy Results of Quenched and Tempered Series B Steels

Alloy	Austenitizing Temperature (°C)	Tempering Temperature (°C)	R_C	C_V(ft-lb)
B1	1000	450	49.0	9.0
		500	52.0	6.8
		550	53.0	6.0
		600	50.0	6.3
		650	43.0	7.0
B4	1000	450	52.5	14.8
		500	53.5	15.3
		550	54.0	15.5
		600	52.0	15.5
		650	45.0	17.0
	1200	450	57.0	2.0
		500	58.0	2.0
		550	58.5	3.3
		600	57.5	2.3
		650	53.0	2.3
B5	1000	450	55.0	13.3
		500	56.0	12.3
		550	55.5	10.5
		600	53.5	10.3
		650	46.0	15.3
	1200	450	58.0	3.5
		500	57.5	3.0
		550	59.5	2.5
		600	57.0	3.0
		650	52.5	2.8

Charpy data obtained for L-T direction.

Table XVIII Hardness and room temperature Charpy Impact Energies of Quenched and Tempered Series B Steels

Alloy No.	Tempering Temp.(°C)	Hardness (Rc)	Charpy Energy (ft.lbs)
B6	450	50.5	16.3
	500	50.5	17.3
	550	51.8	20.0
	600	50.0	17.8
	650	47.8	23.5
B9	450	51.0	14.3
	500	51.8	17.0
	550	53.3	15.5
	600	49.5	16.8
	650	46.5	16.5
B10	450	51.5	14.8
	500	50.3	13.3
	550	53.0	15.0
	600	50.0	9.8
	650	47.5	16.0

The steels were austenitized at 1000°C for 1 hour and oil quenched prior to tempering.

Table XIX Tempering response (Rockwell R_C Hardness) of Series C Steels

Alloy No.	Tempering Temperature (°C)					
	As Quenched	200	300	400	500	600
C1	55.9	53.7	53.2	52.4	48.0	41.1
C2	60.8	55.2	56.2	54.4	49.3	43.1
C3	59.5	54.3	55.0	54.3	50.7	41.1

Table XX Room Temperature Tensile and Charpy Data of Series C Steels

Alloy No.	Tempering Temp. (°C)	0.2 pct yield strength (KSI)	Ultimate Strength (KSI)	Reduction in Area (pct.)	Charpy Energy (ft.lbs)
C1 (Austenitized at 950°C oil quenched)	As quenched	223	330	22	11.0
	200	-	-	-	20.5
	300	238	285	40	18.5
	350	246	288	42	16.0
	400	246	278	48	16.0
	500	-	-	-	10.0
	600	-	-	-	19.0
C2 (Austenitized at 950°C, oil quenched)	As quenched	258	361	2	5.0
	200	-	-	-	12.0
	300	261	302	37	14.5
	350	263	306	34	8.5
	400	259	292	43	8.5
	500	-	-	-	8.0
	600	-	-	-	8.0
C3 (Austenitized at 1000°C, oil quenched)	As quenched	258	345	0	3.0
	200	-	-	-	9.0
	300	255	304	8	8.0
	350	261	312	24	8.5
	400	270	303	29	6.5
	500	-	-	-	4.0
	600	-	-	-	8.0

Charpy data obtained for L-T direction.

Table XXI Nominal Composition of Series D Steels

Alloy No.	Composition (wt.pct)				
	C	Si	Cr	Mo	Fe
D1	0.3	1.5	2	0.3	bal
D2	0.4	1.5	2	0.3	"
D3	0.3	1.5	3	0.3	"

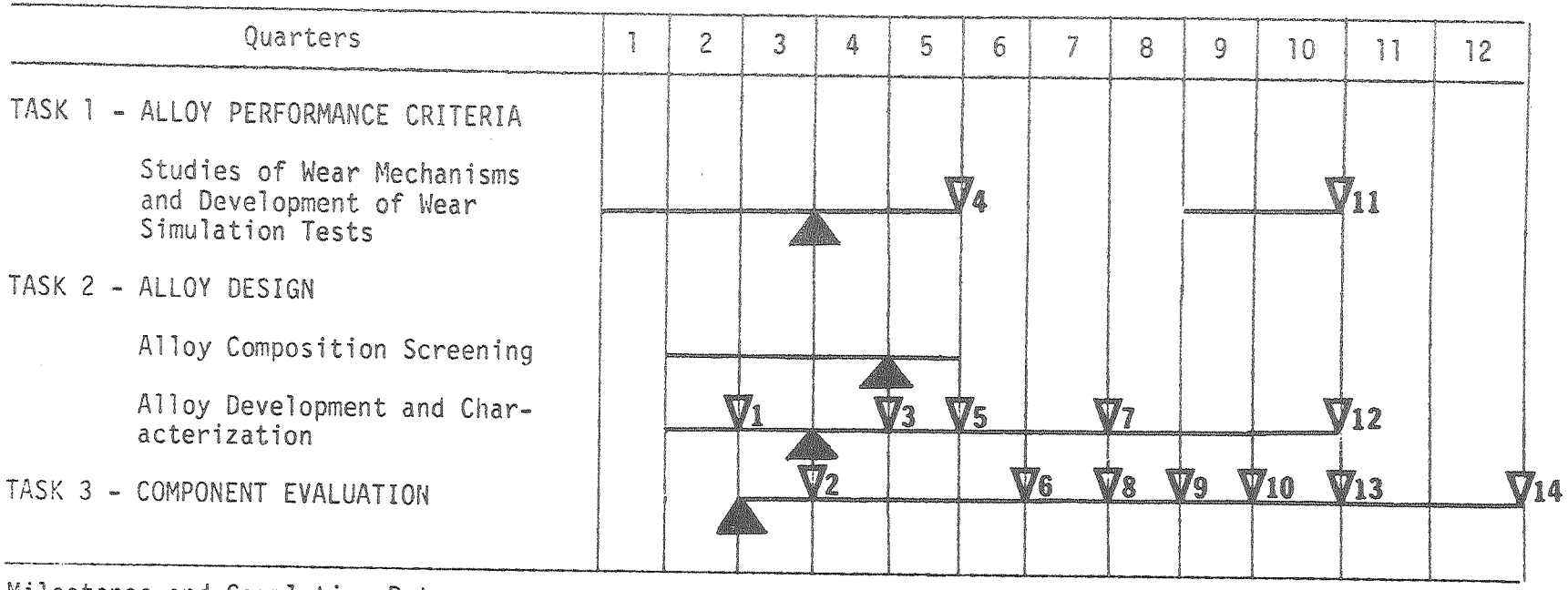

Milestones and Completion Dates

1. Scale-up development of AISI 4340 + 1.5% Si + 1.5% Al steel.
2. Evaluation of AISI 4340 + 1.5% Si + 1.5% Al steel components.
3. Initial compositions of experimental wrought low alloy and secondary hardening steels.
4. Wear mechanisms in simulated tests.
5. Final compositions of wrought low alloy steels for component evaluation.
6. Room temperature evaluation of dry coal feeder components - low alloy steels.
7. Final compositions of wrought secondary hardening steels for component evaluation.
8. Room temperature evaluation of slurry feeder components - low alloy steels.
9. Evaluation of jaw crusher plates.
10. Room temperature evaluation of wrought secondary hardening steel components.
11. Wear mechanism studies of wrought components.
12. Final cast and PM alloys.
13. Elevated temperature evaluation of feeder components.
14. Evaluation of cast and PM components.

Figure 1. Program Schedule and Progress. The dar triangles indicate progress to date.

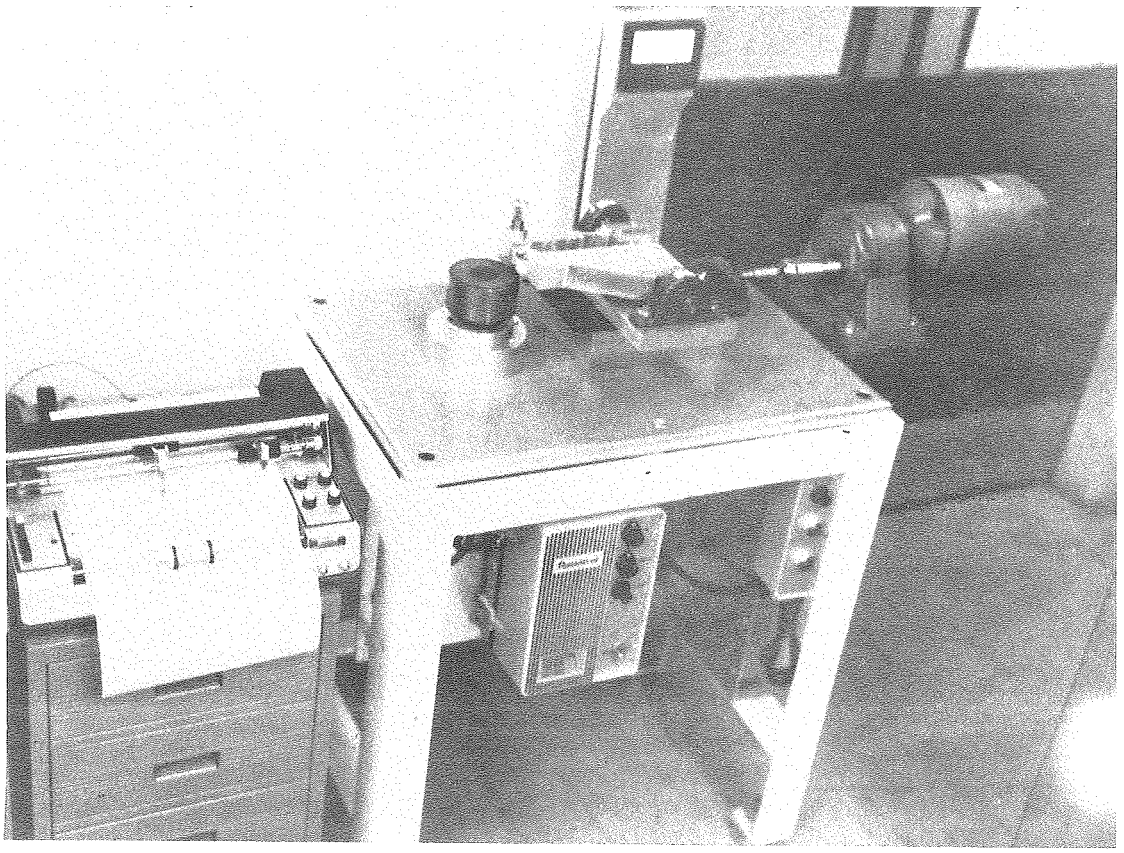

XBB-777-6580

Figure 2. Overall view of dry abrasive wear tester.

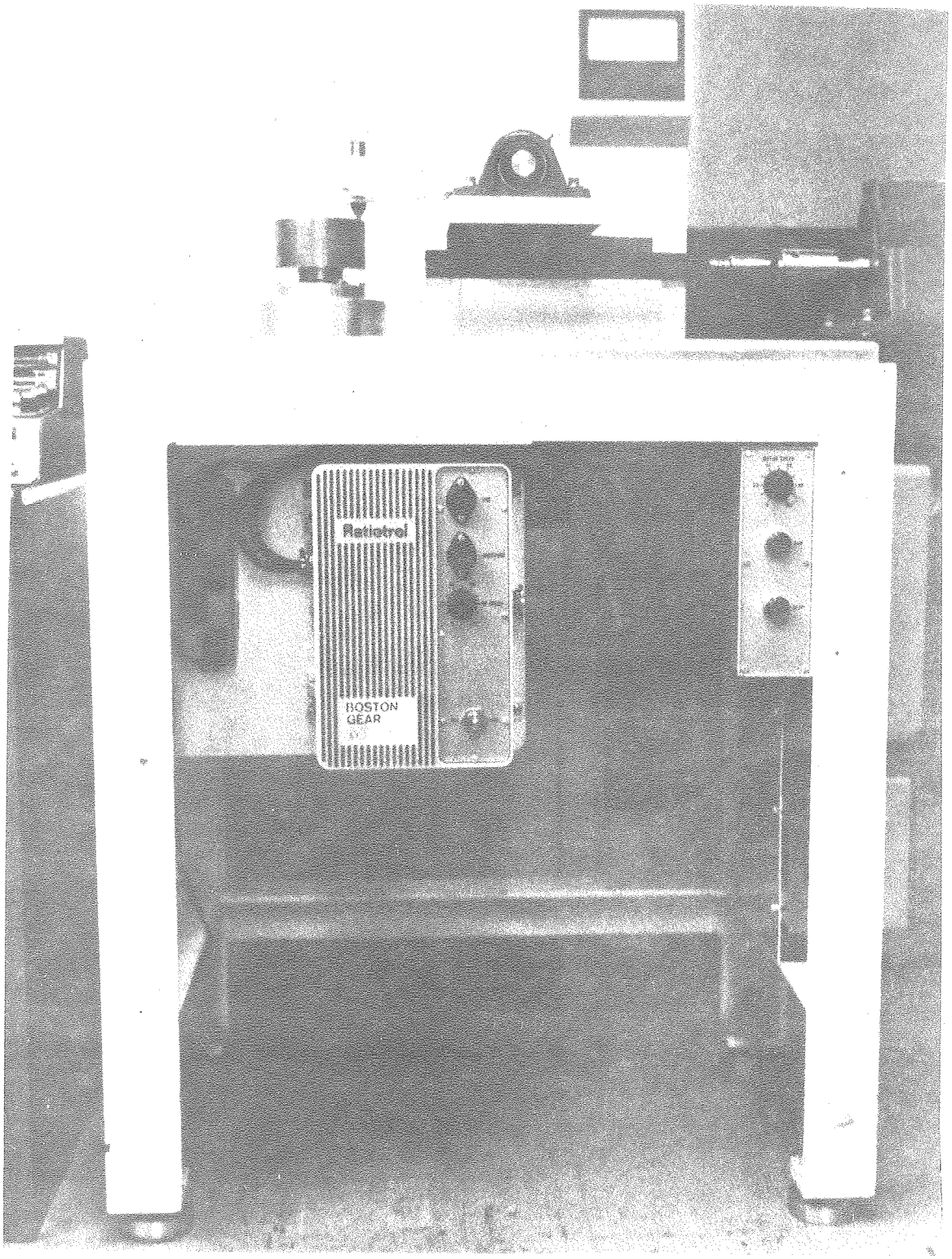

XBB-777-6581

Figure 3. Side view of wear tester.

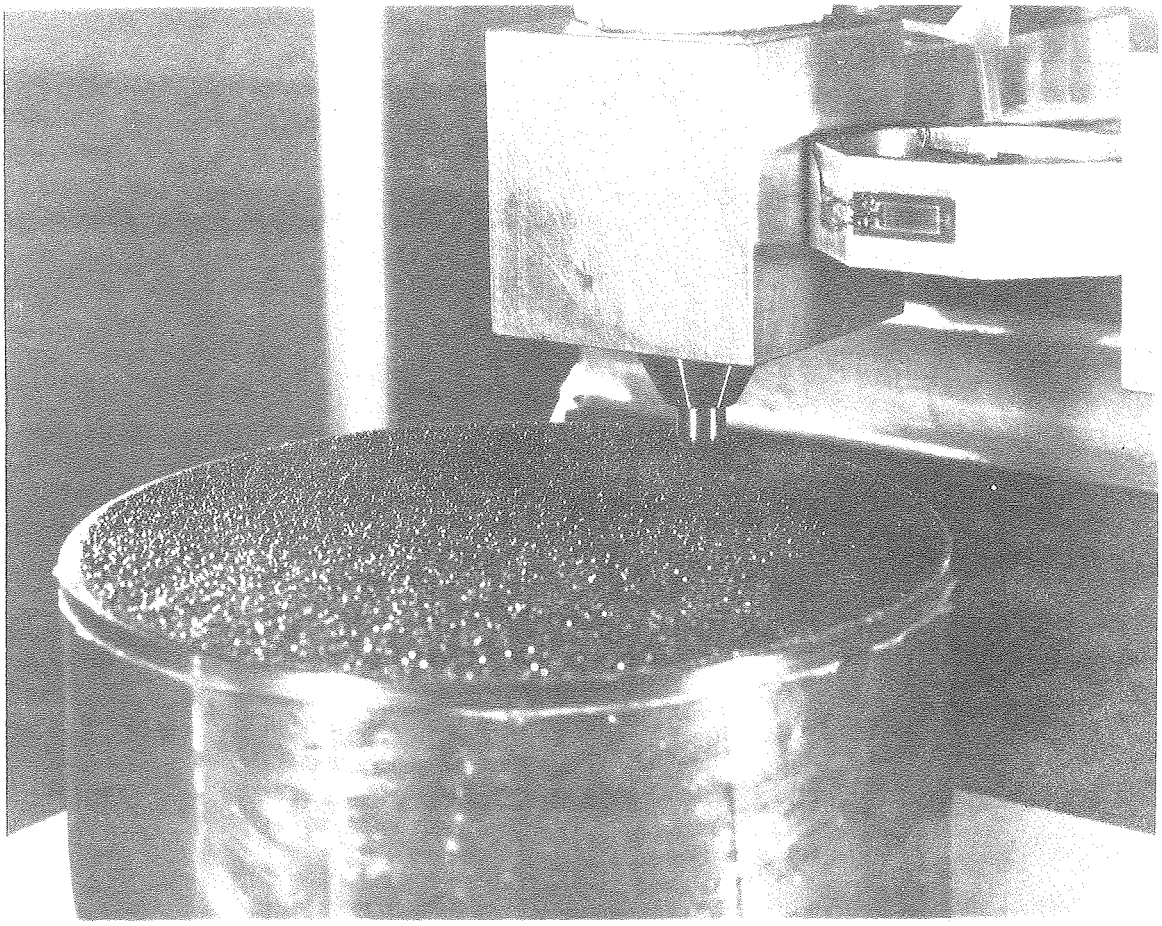

XBB777-7276

Figure 4. Close-up view of pin and disk.

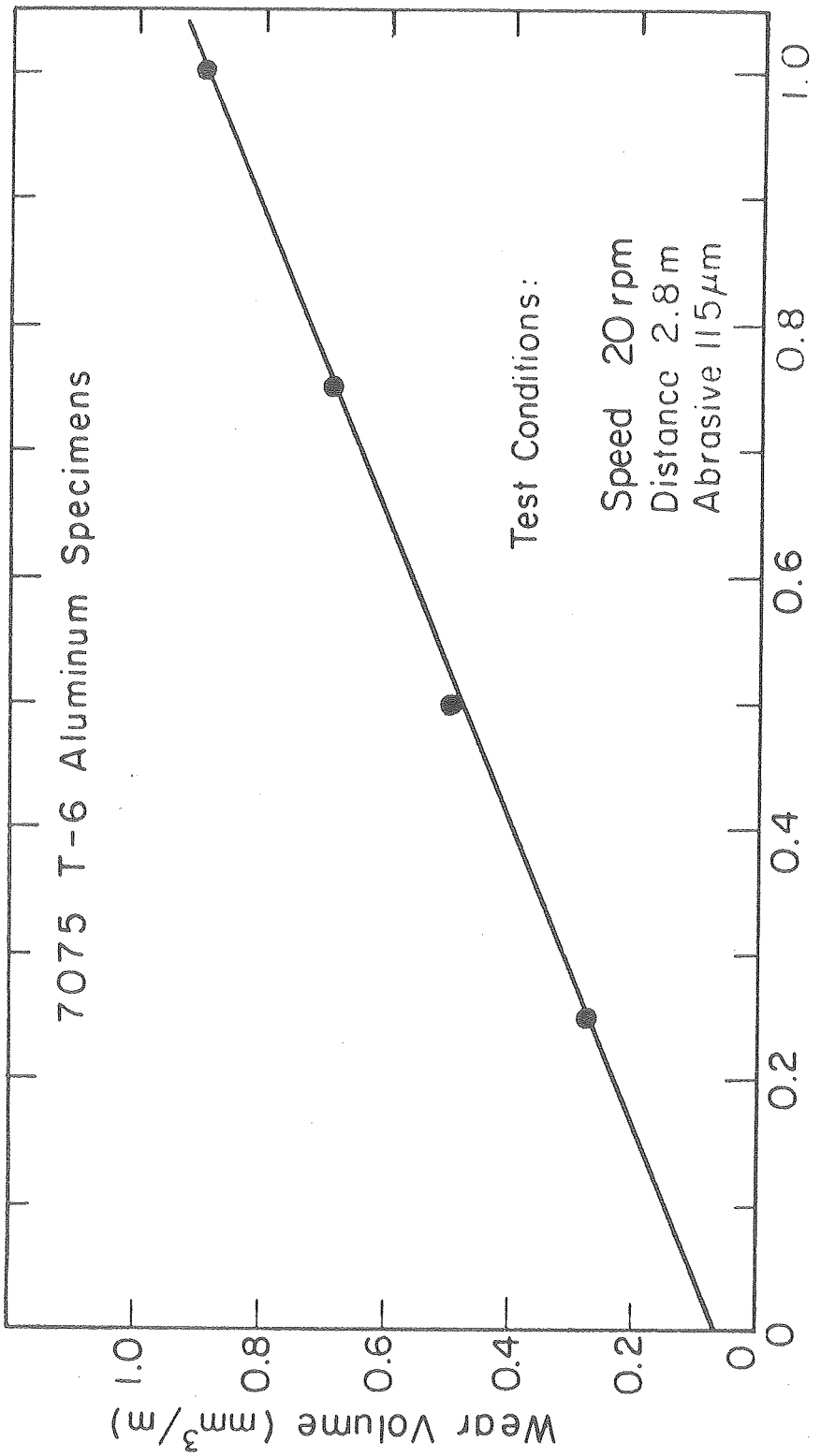

XBL 7711-6440A

Figure 5. Plot of volume wear rate versus load for 7075 Aluminum as measured on abrasive wear tester.

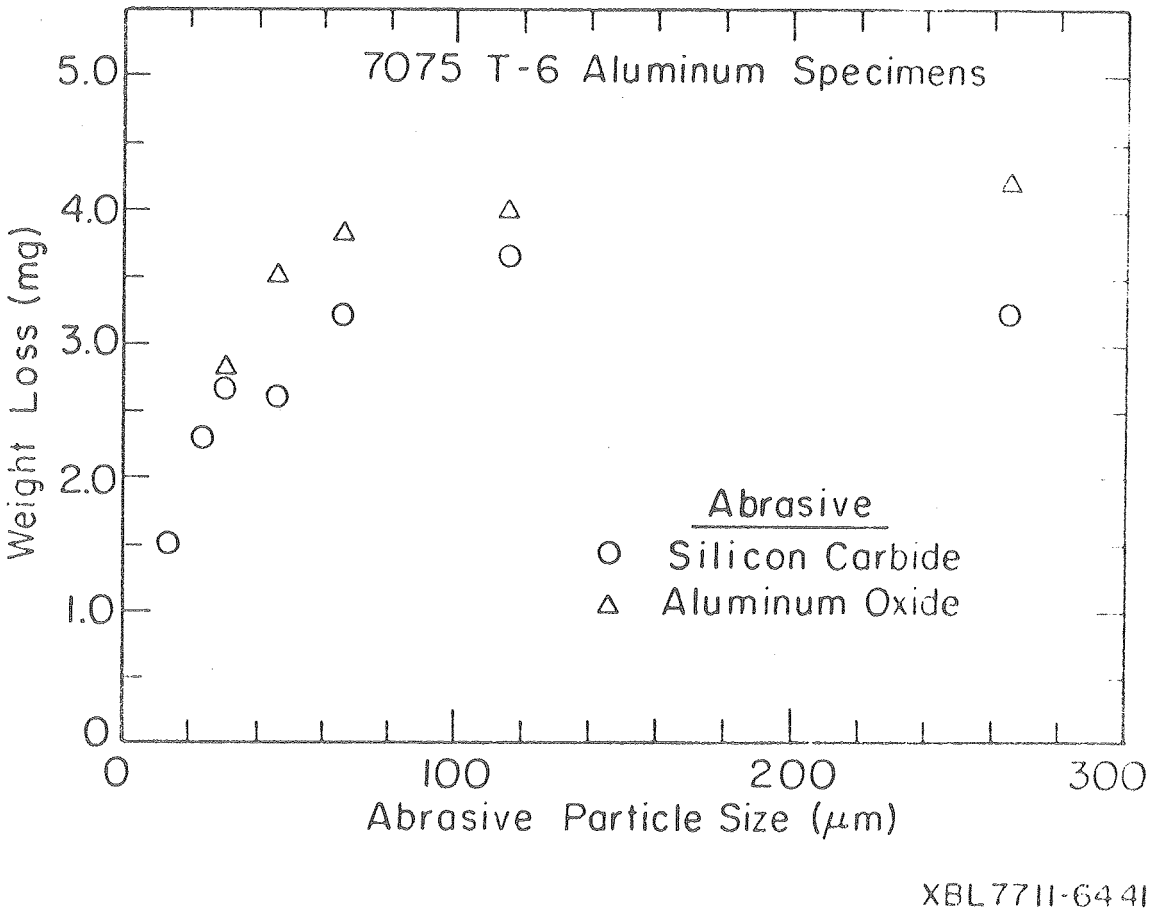

Figure 6. Plot of weight loss versus abrasive particle size for 7075 Aluminum specimens.

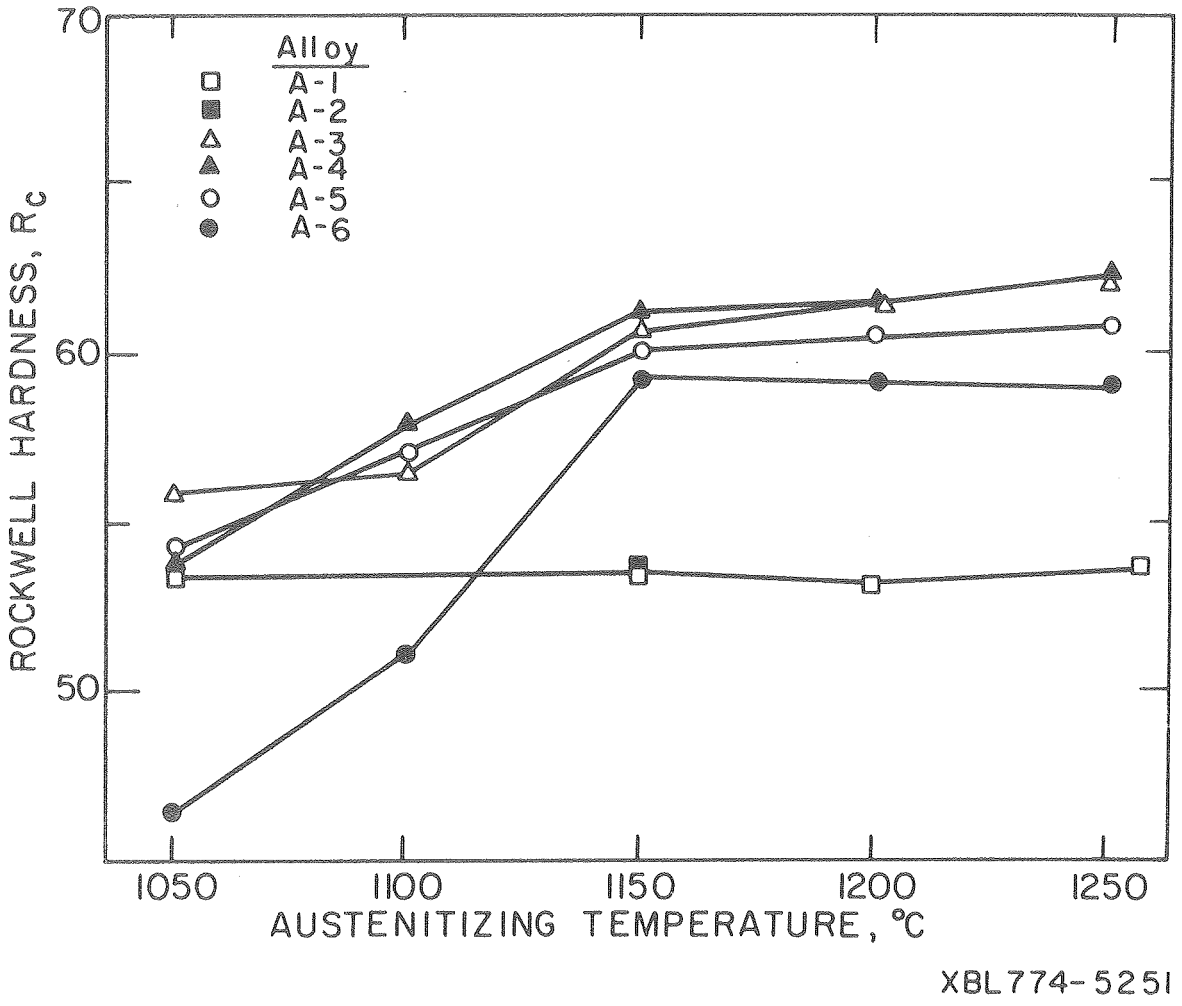

Figure 9. Plots of hardness versus austenitizing temperature for alloys A1-A6.

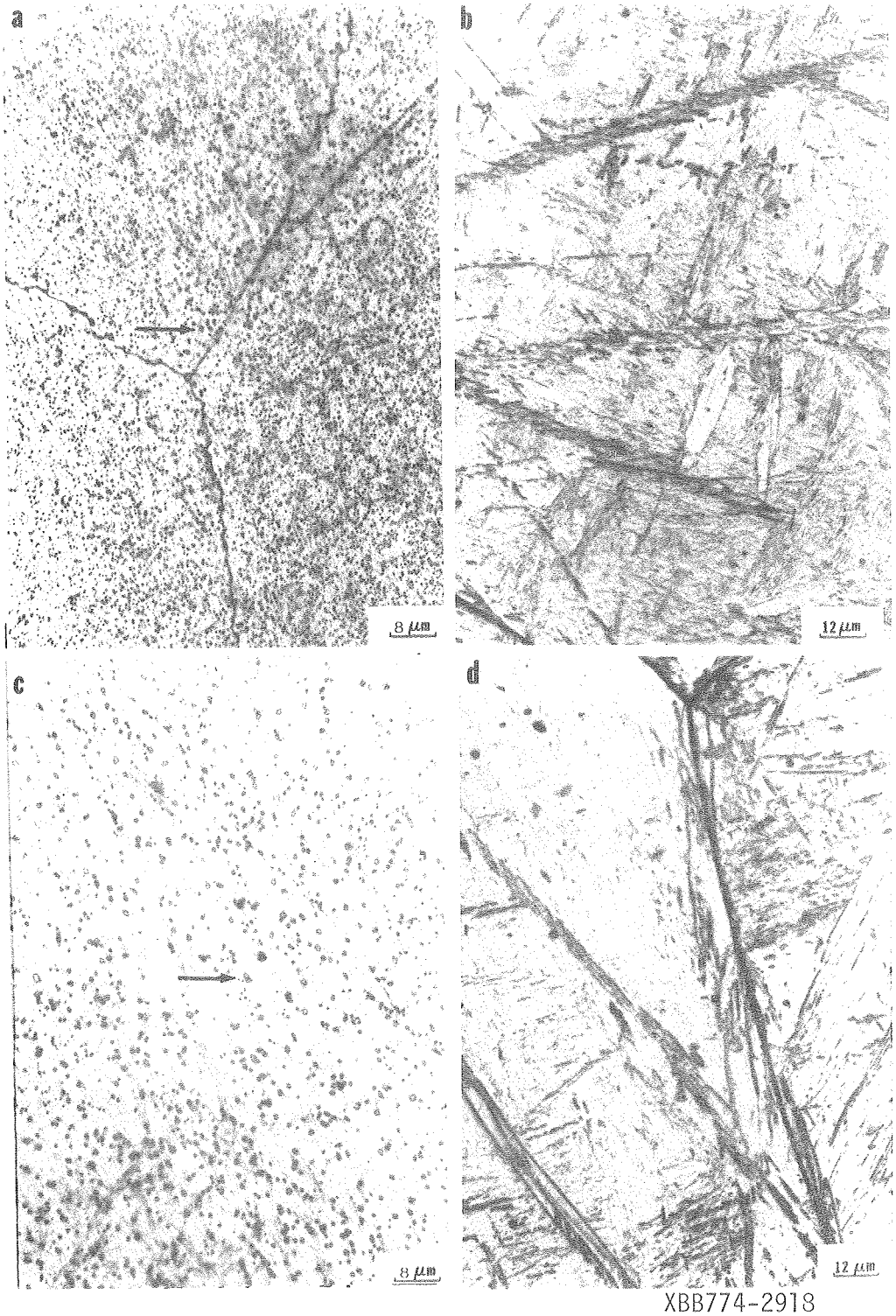

Figure 10. Optical micrographs of steel A4 austenitized for 1 hour at (a) 1150°C, and (b) 1250°C, and steel A5 austenitized for 1 hour at (c) 1150°C, and (d) 1250°C.

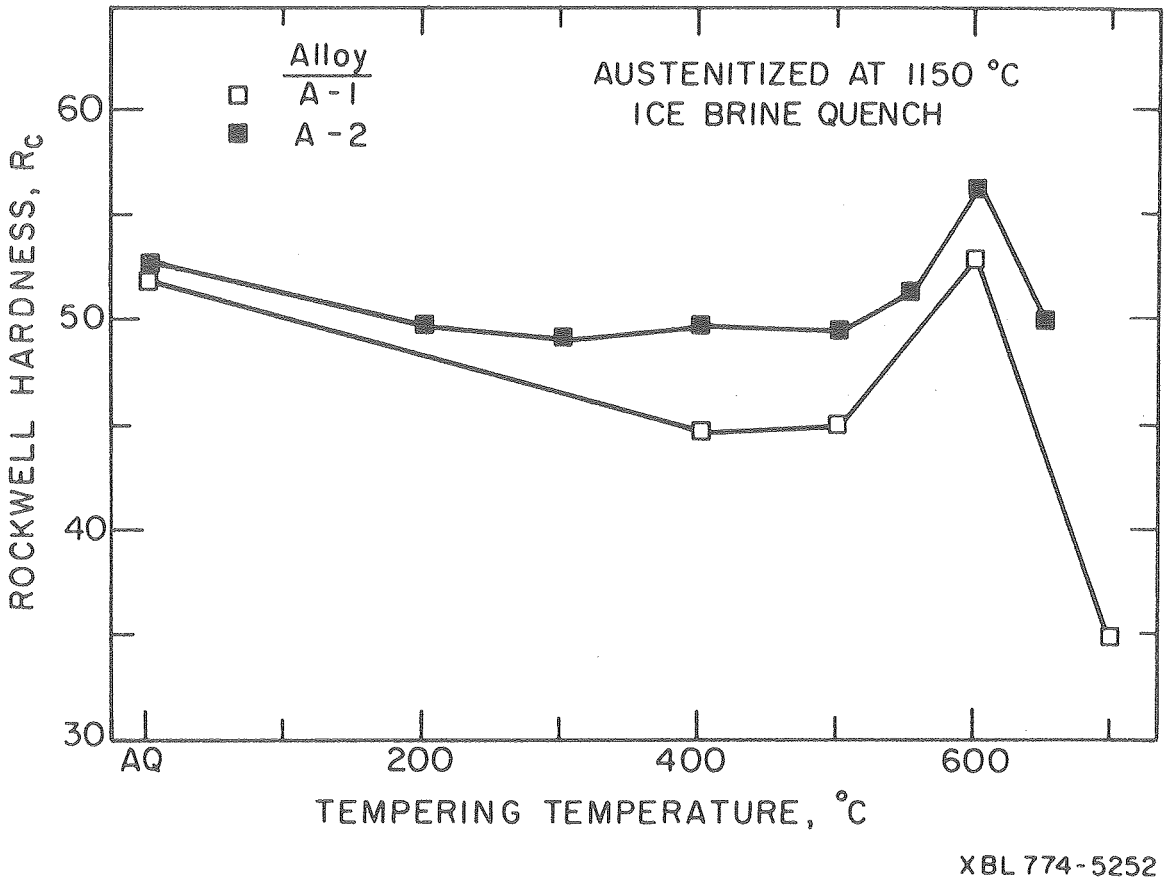

Figure 11. Plots of hardness versus tempering temperature for steels A1 and A2.

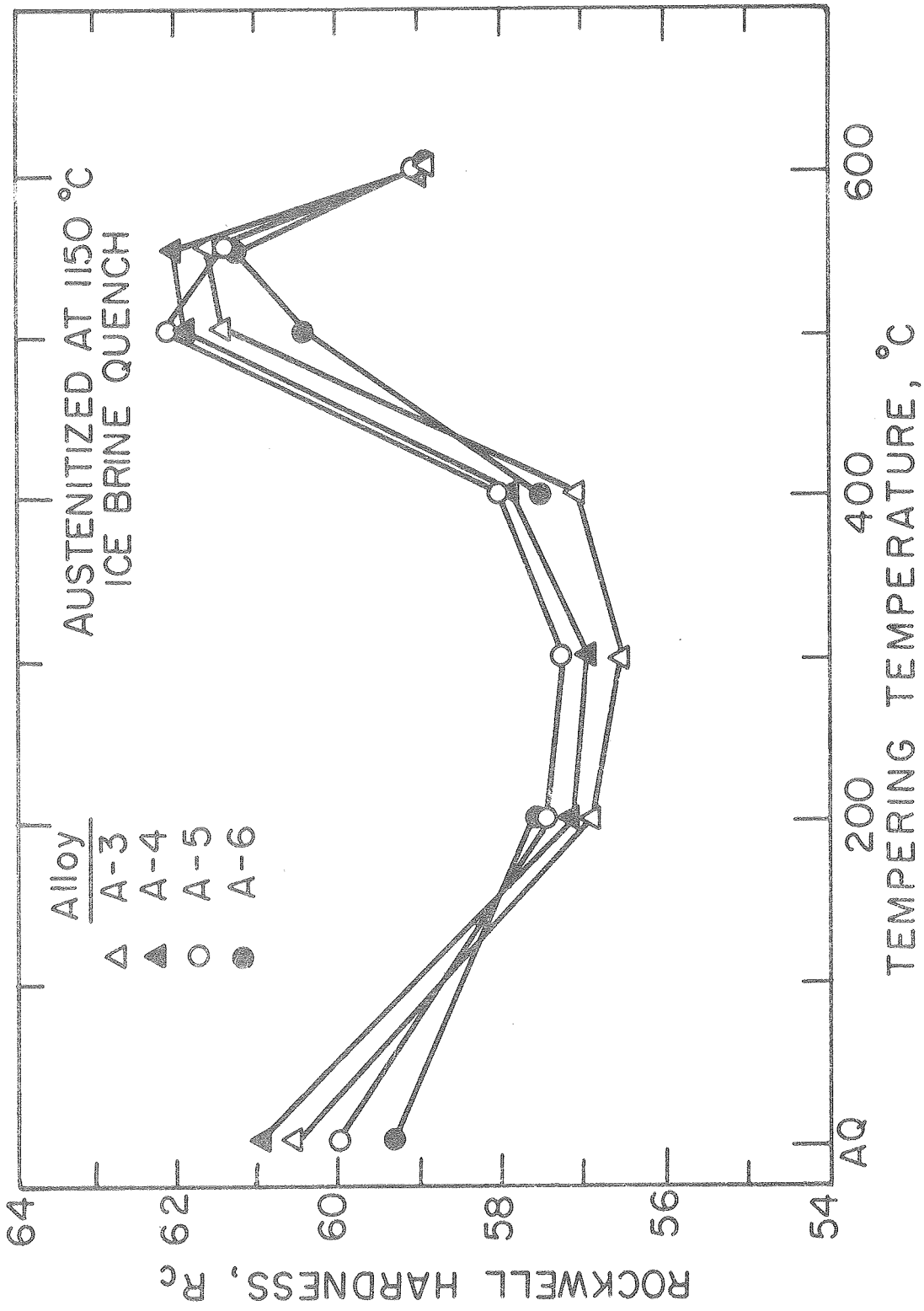

XBL 774-5253

Figure 12. Plots of hardness versus tempering temperature for steels A3-A6.

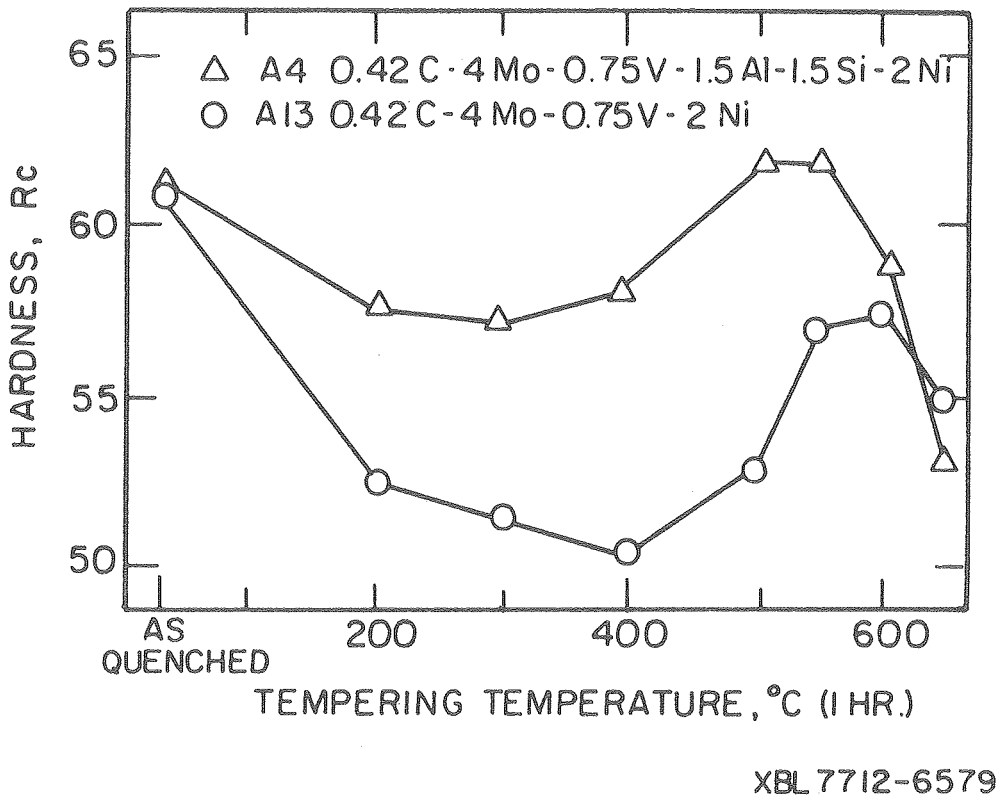

Figure 13. Plots of hardness versus tempering temperature for steels A4 and A13, austenitized at 1100°C.

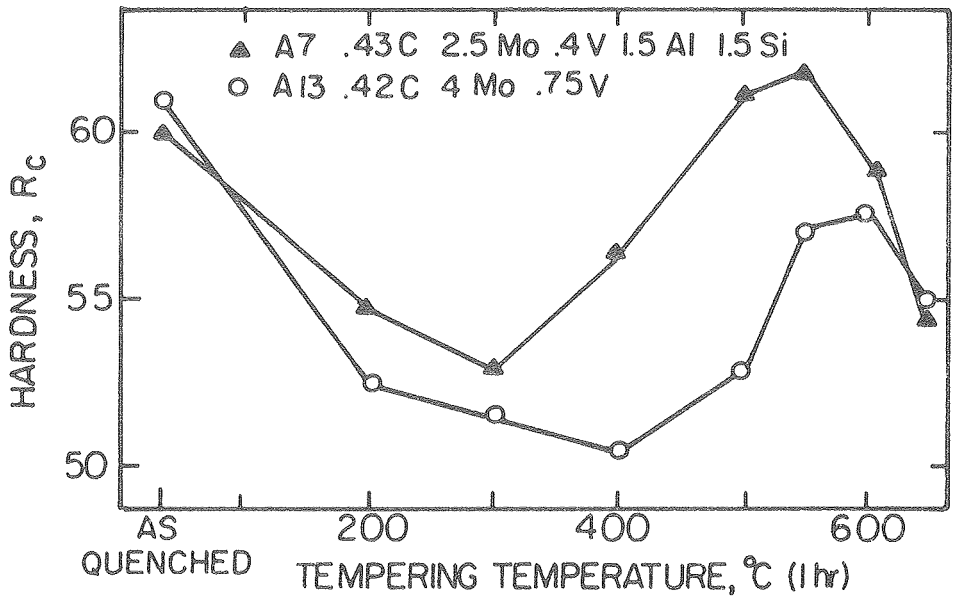

XBL 776-5662B

Figure 14. Plots of hardness versus tempering temperature for steels A7 and A13, austenitized at 1100°C.

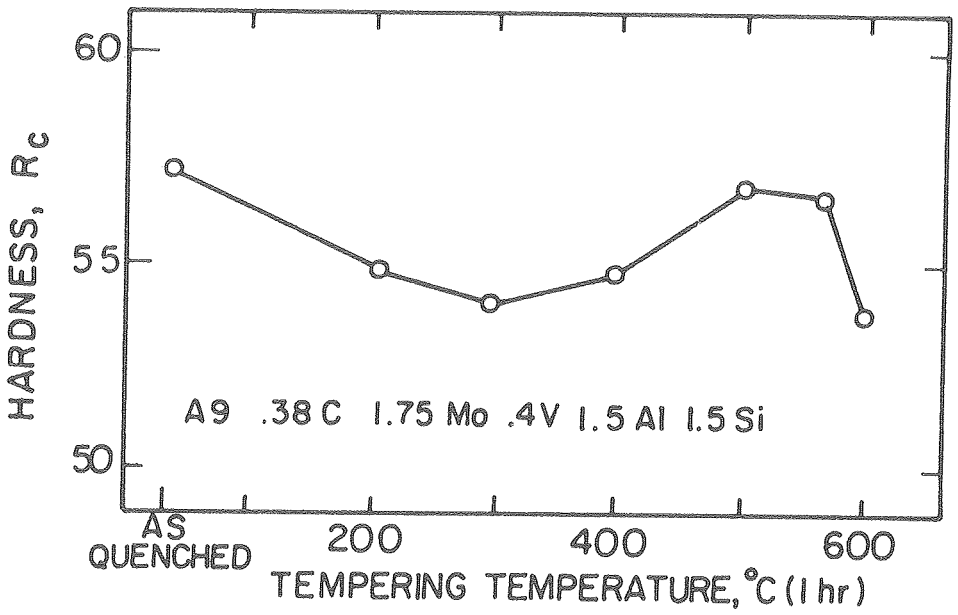

XBL 776-5666B

Figure 15. Plot of hardness versus tempering temperature for steel A9, austenitized at 1100°C.

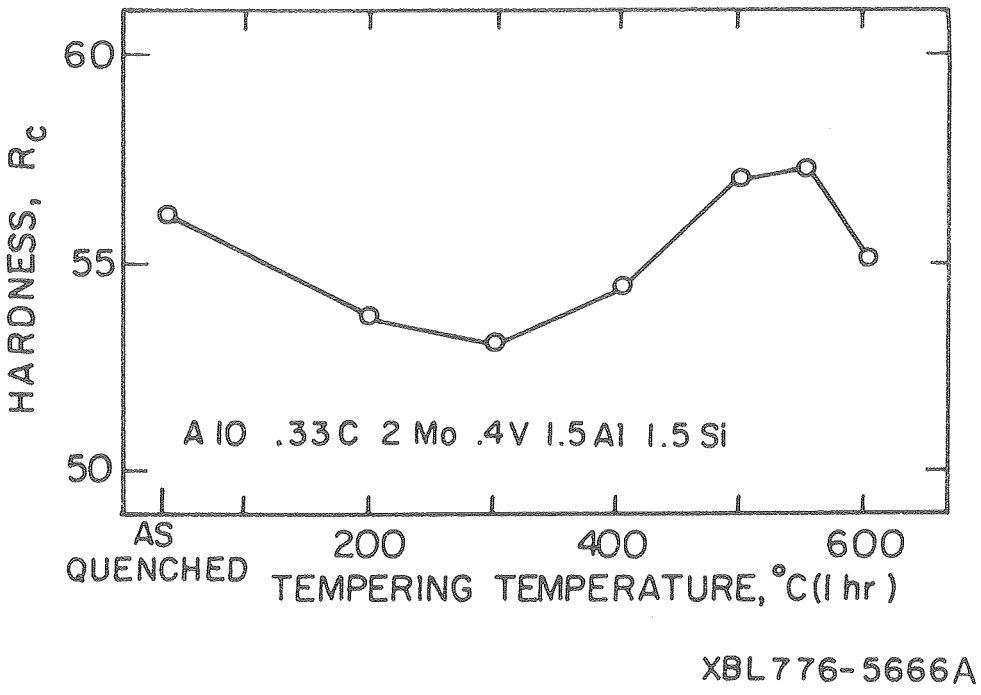

Figure 16. Plot of hardness versus tempering temperature for steel A10, austenitized at 1100°C.

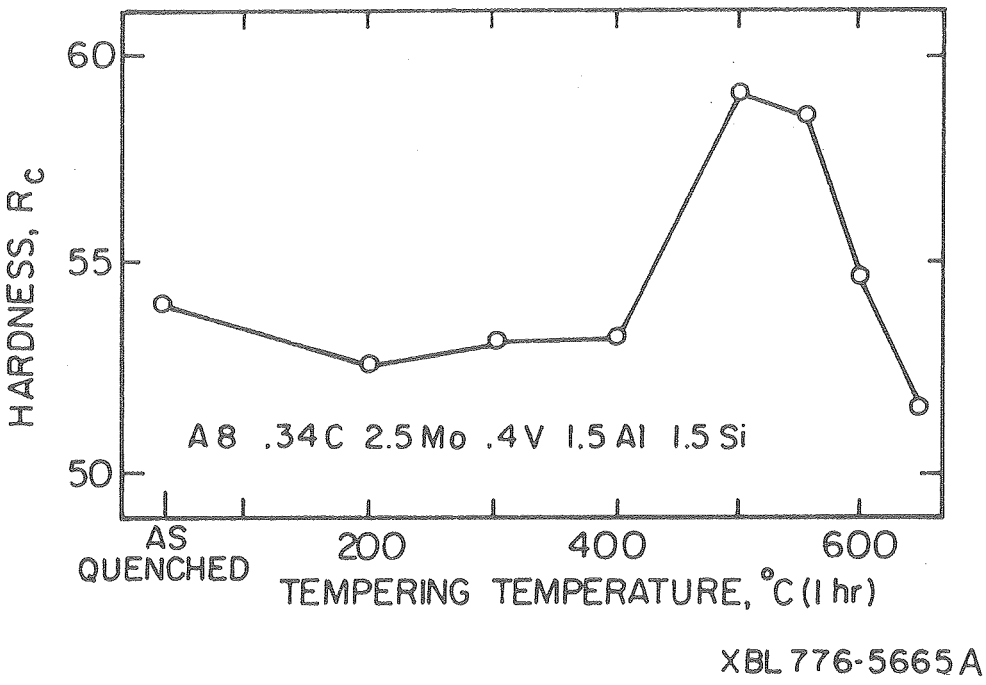

Figure 17. Plot of hardness versus tempering temperature for steel A8, austenitized at 1100°C.

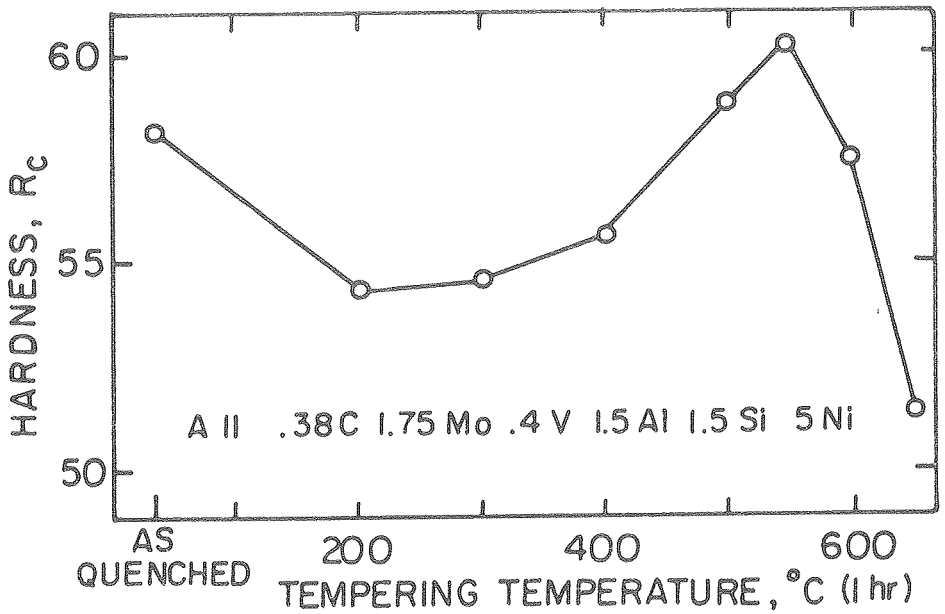

XBL 776-5667B

Figure 18. Plot of hardness versus tempering temperature for steel A11, austenitized at 1100°C.

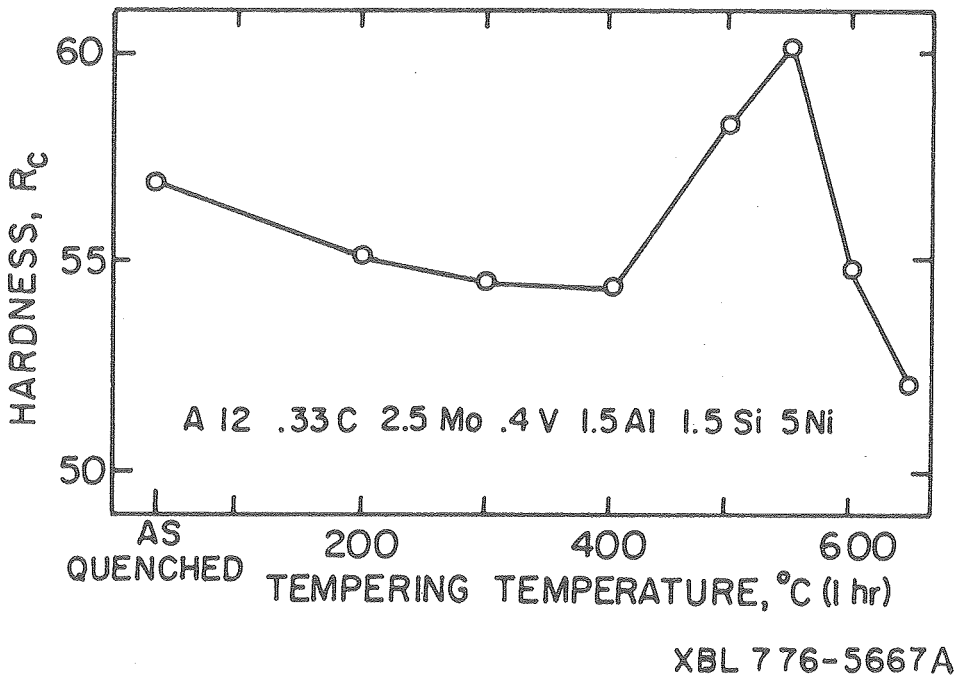

Figure 19. Plot of hardness versus tempering temperature for steel A12, austenitized at 1100°C.

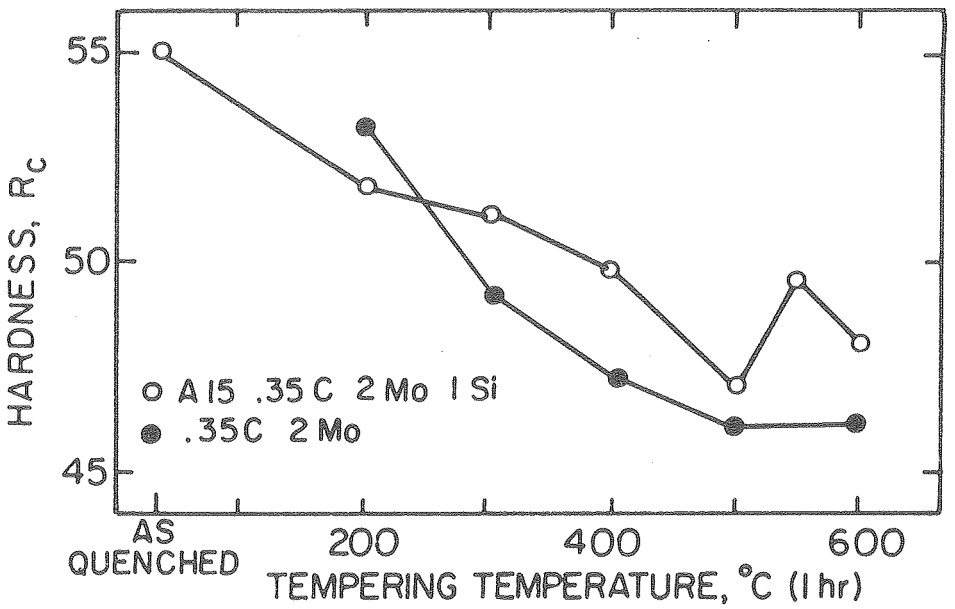

XBL 776-5663B

Figure 20. Plots of hardness versus tempering temperature for steel A15 and an Fe-0.35C-2Mo-3Ni steel, obtained from the literature (ref. 49).

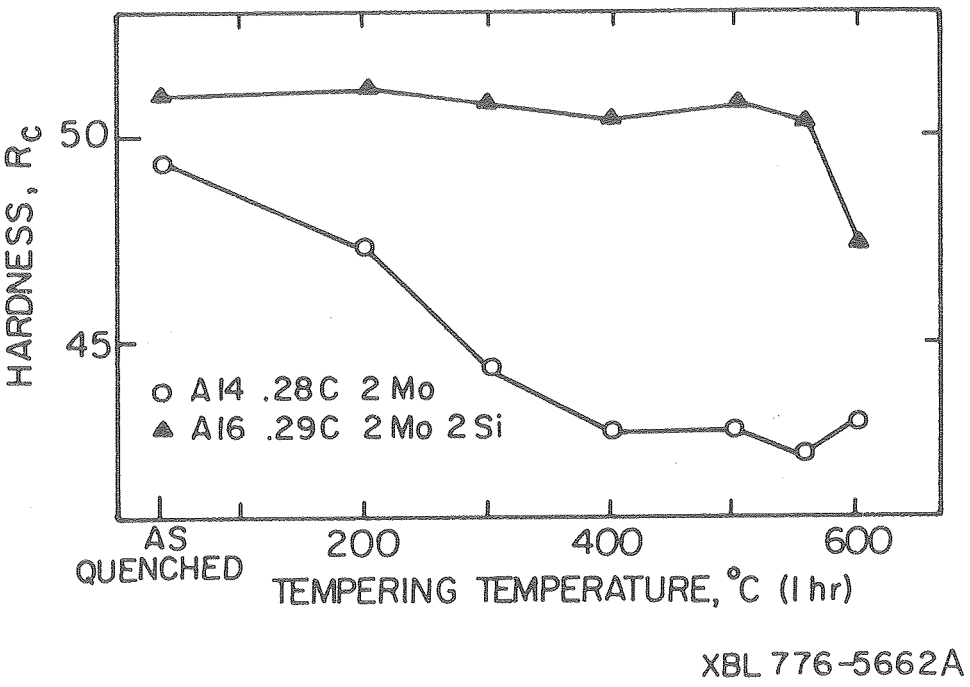

Figure 21. Plots of hardness versus tempering temperature for steels A14 and A16, austenitized at 1100°C.

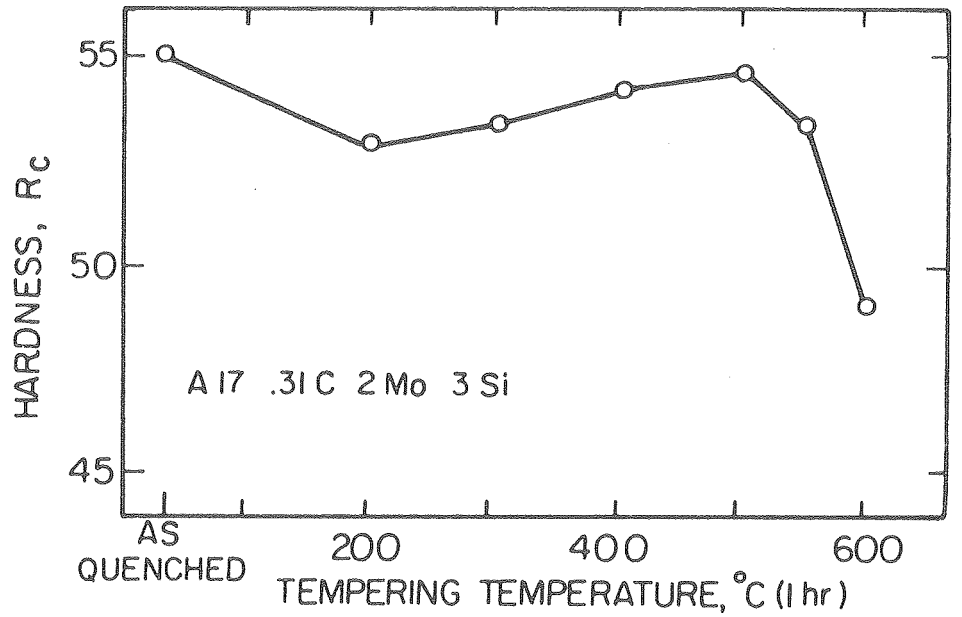

Figure 22. Plot of hardness versus tempering temperature for steel A17, austenitized at 1100°C.

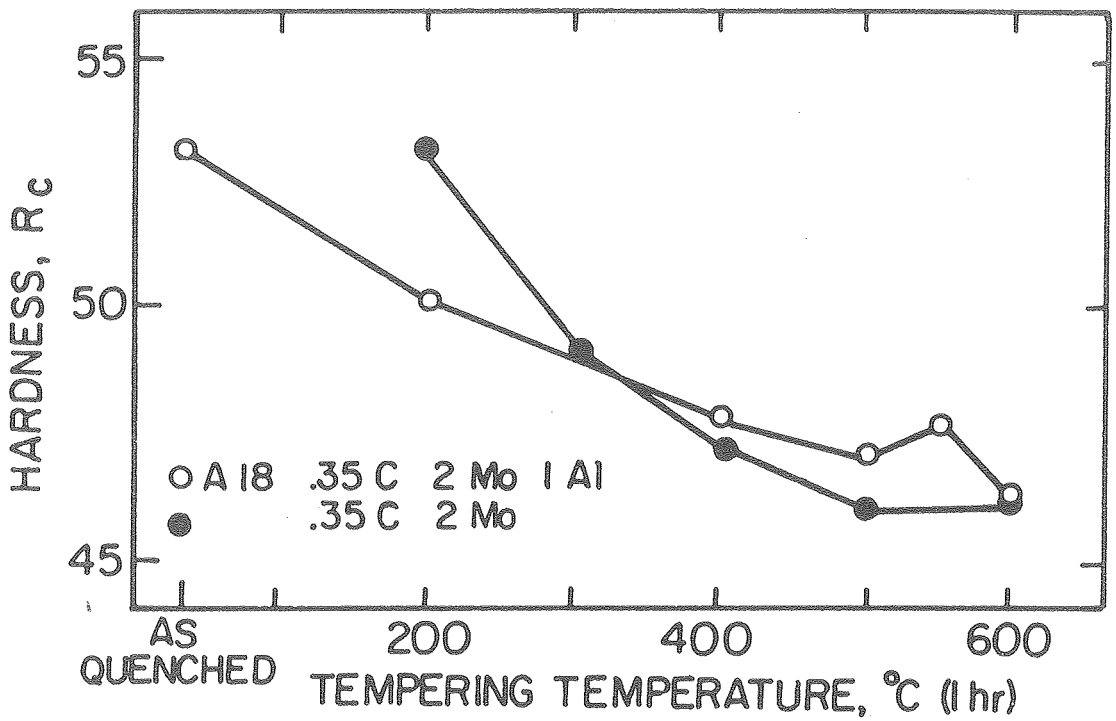

Figure 23. Plots of hardness versus tempering temperature for steel A18 and an Fe-0.35C-2Mo-3Ni steel, obtained from the literature (ref. 49).

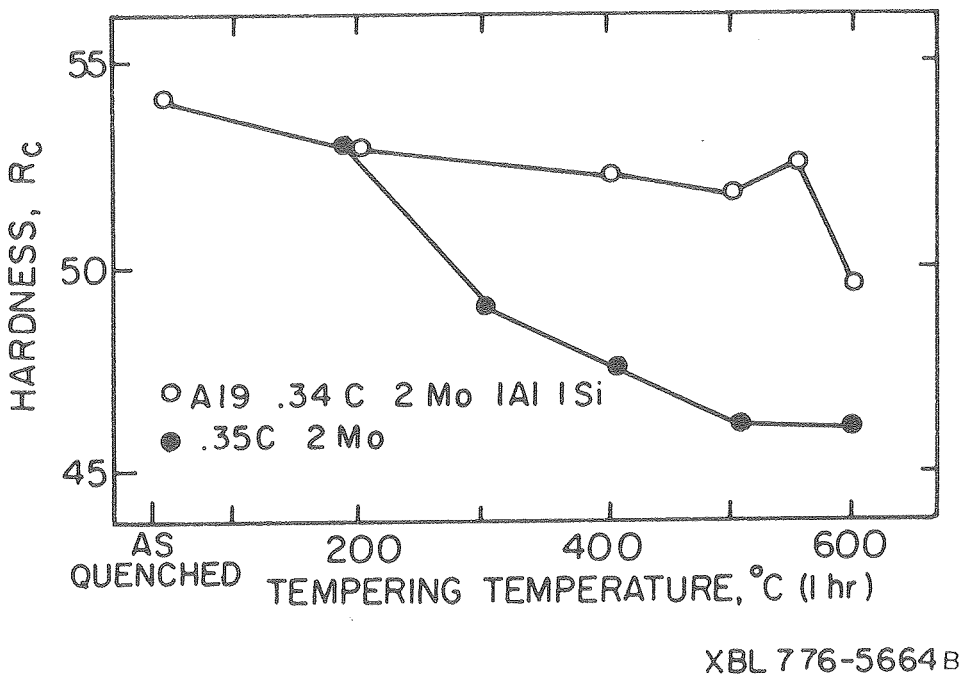

Figure 24. Plots of hardness versus tempering temperature for steel A19 and an Fe-0.35C-2Mo-3Ni steel, obtained from the literature (ref. 49).

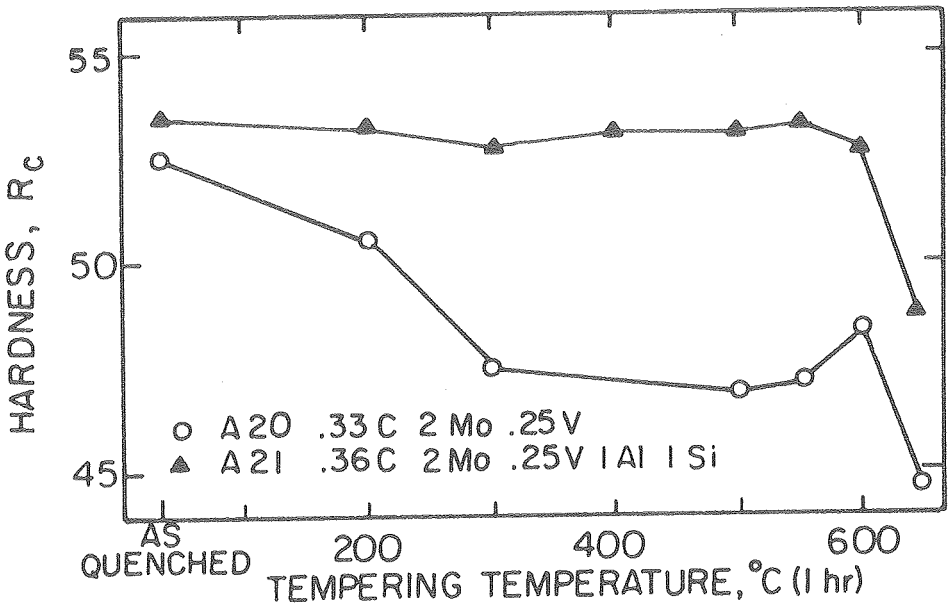

XBL 776-5665B

Figure 25. Plots of hardness versus tempering temperature for steels A20 and A21, austenitized at 1100°C.

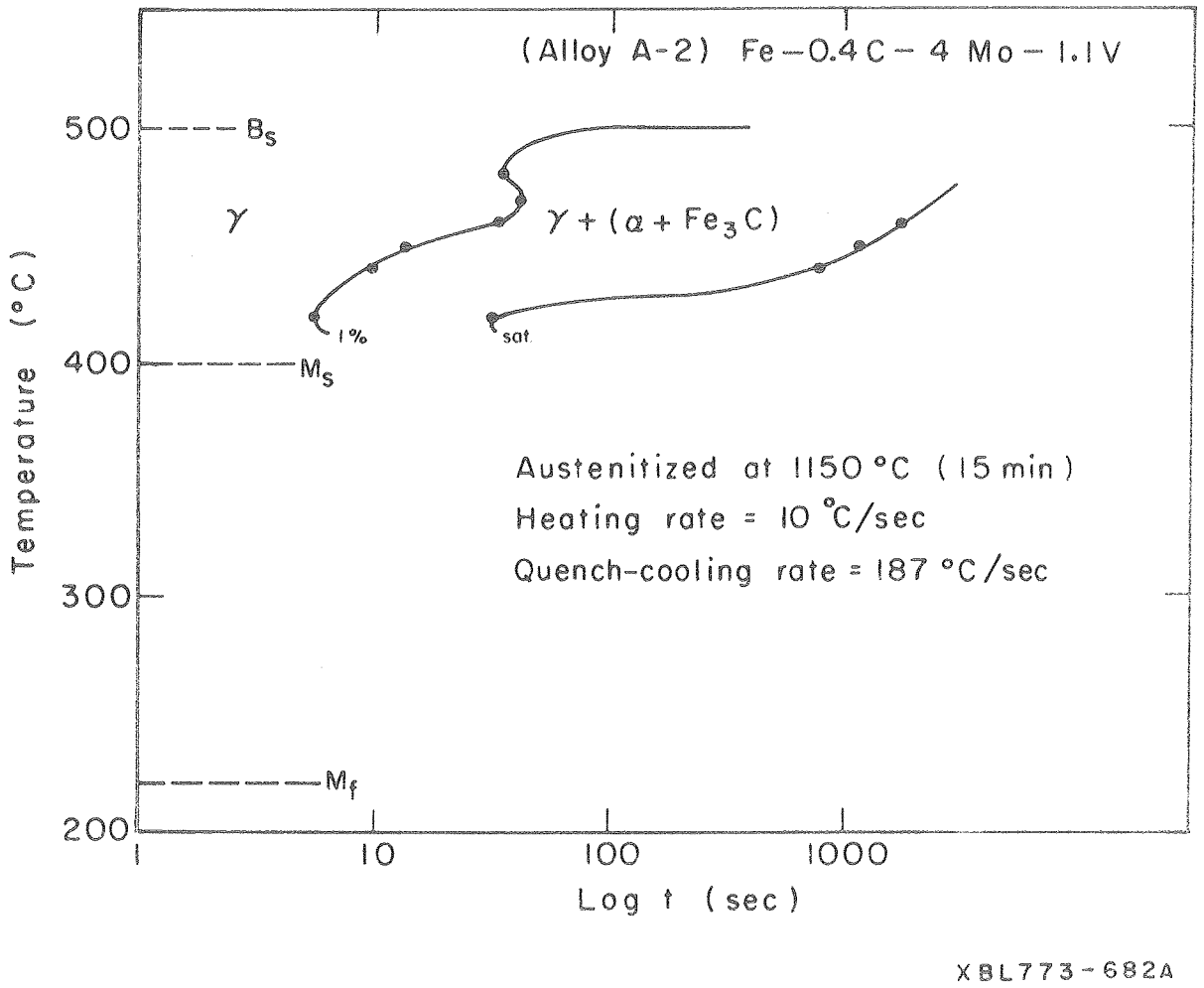

Figure 26. Time-Temperature-Transformation diagram of steel A2, obtained by dilatometry.

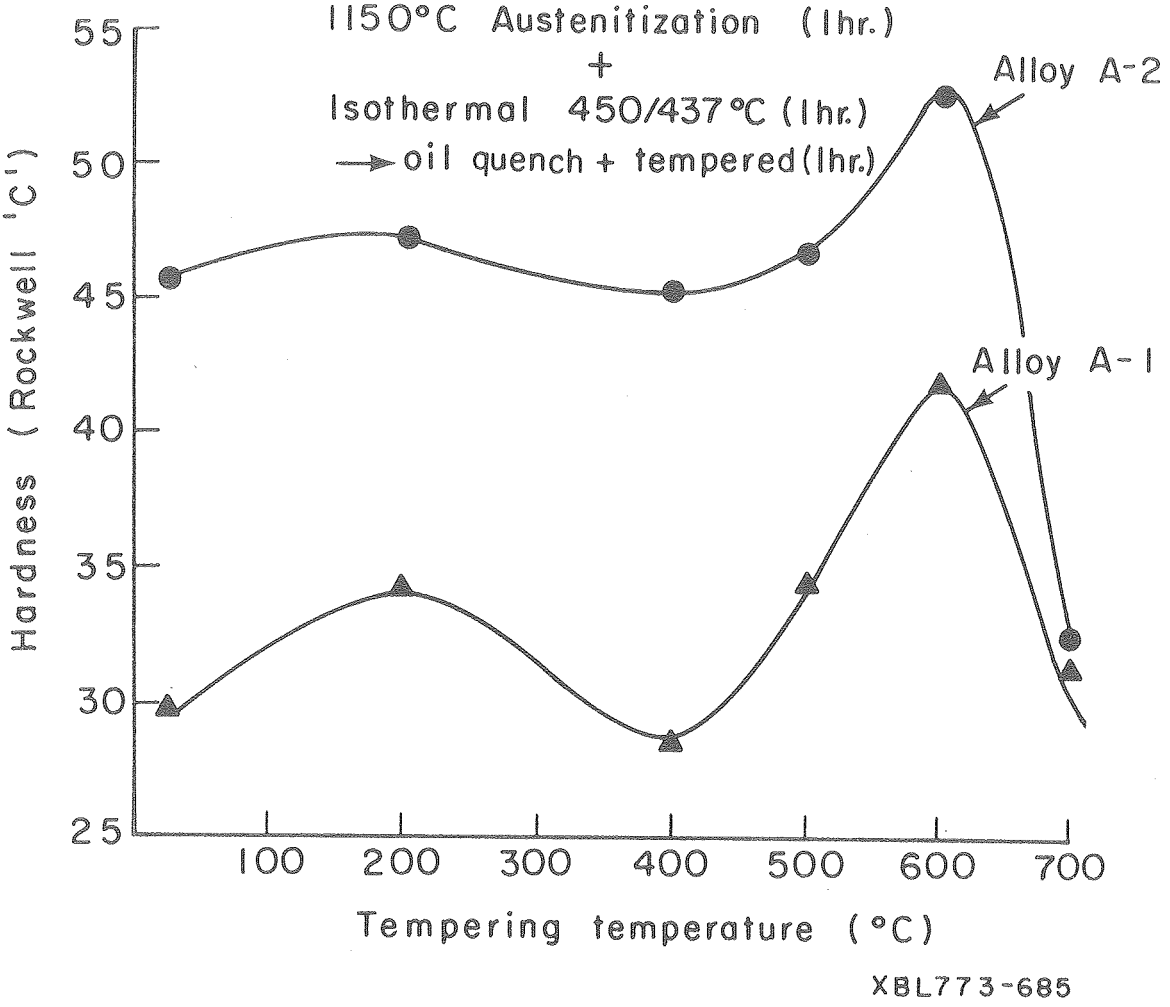

Figure 27. Plots of hardness versus tempering temperature of alloys A1 and A2, isothermally transformed at 437°C and 450°C, respectively.

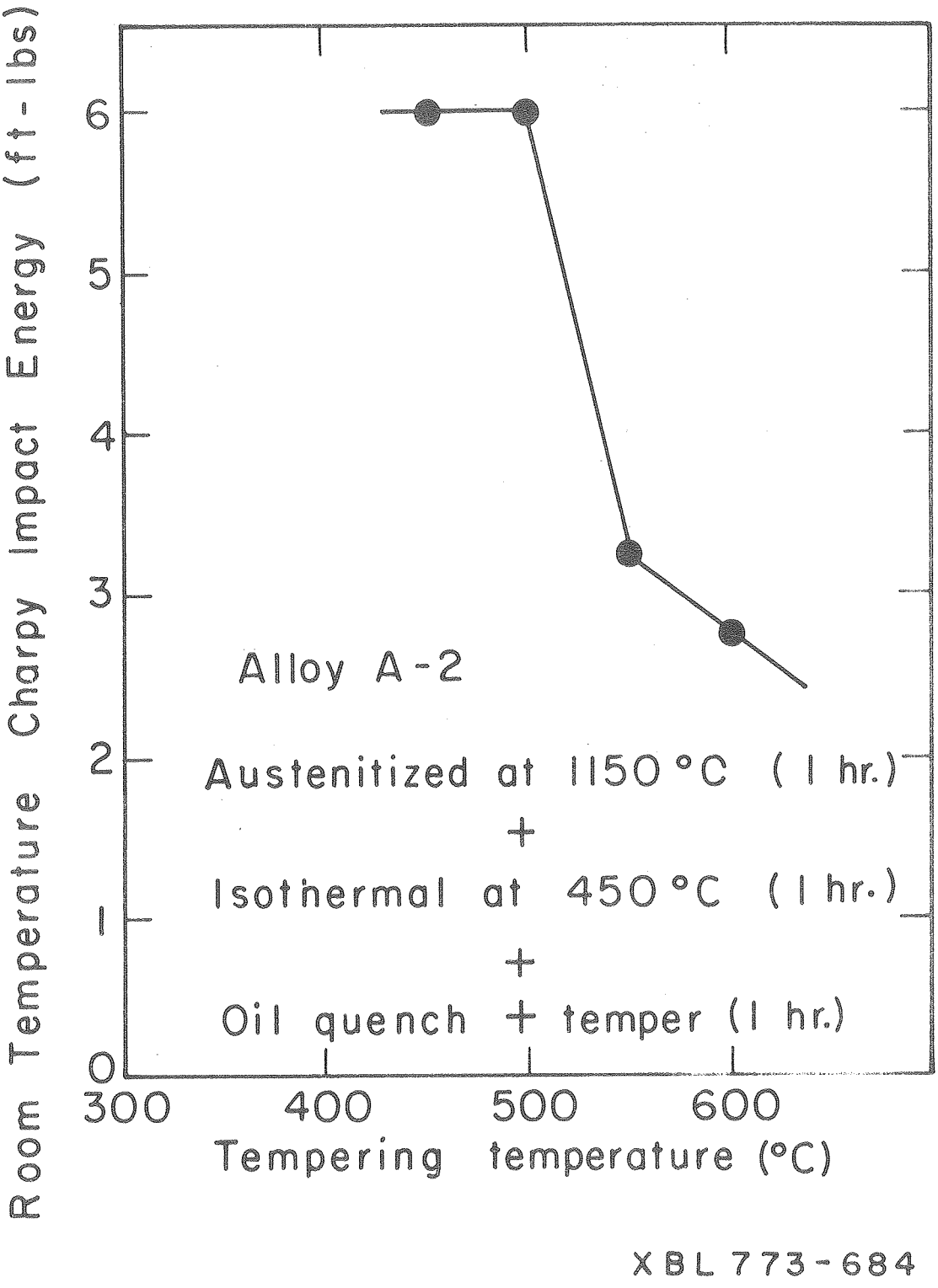

Figure 28. Plot of room temperature Charpy impact energy versus tempering temperature for alloy A2.

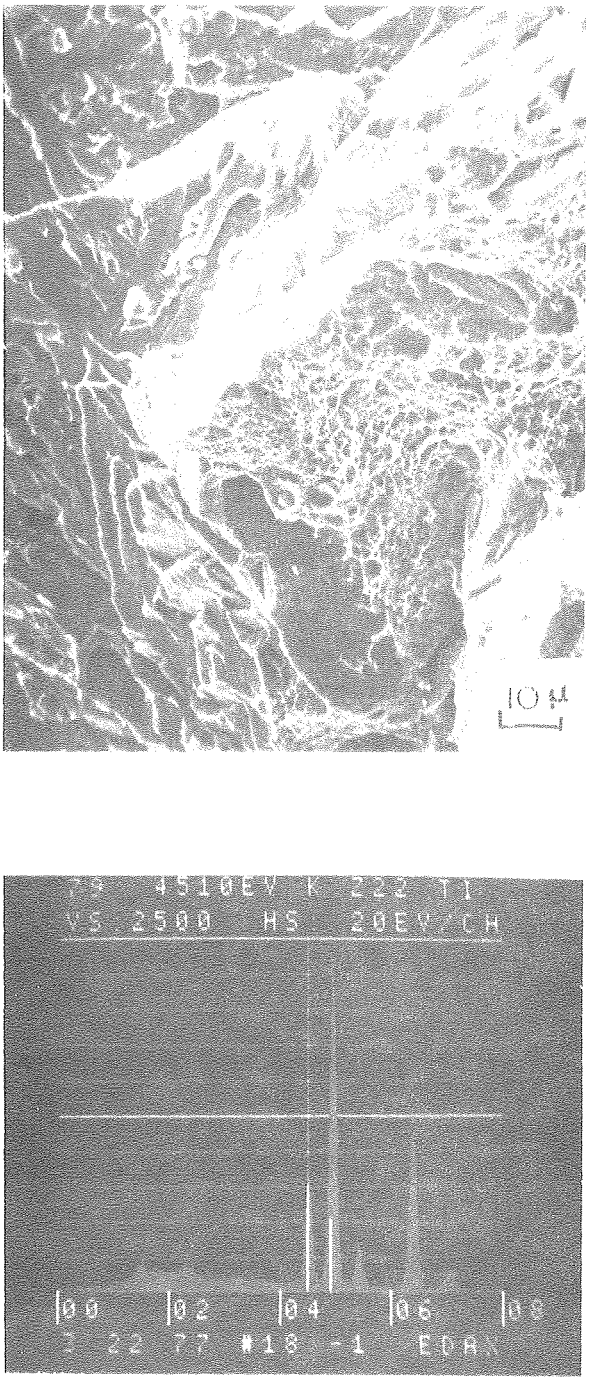

XBB-773-2683

Figure 29. Scanning electron fractograph obtained from broken surface of Charpy bar of steel A2 austenitized at 1150°C, isothermally transformed at 450°C, and tempered at 500°C. The energy dispersive x-ray analysis picture was obtained from the large carbide particle in the middle of the fractograph.

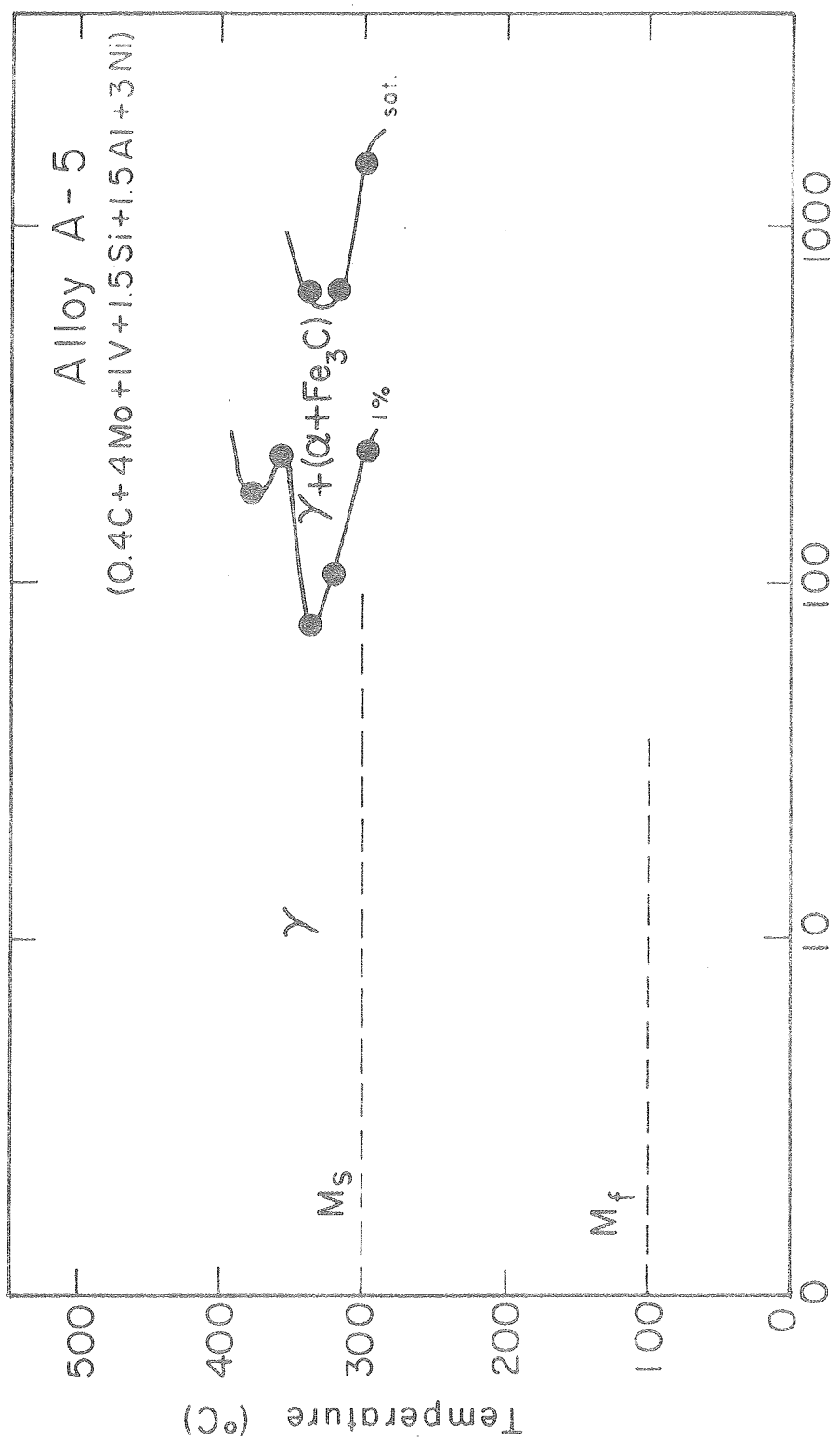

XBL776-12384

Figure 30. Time-Temperature-Transformation diagram of steel A5 obtained by dilatometry.

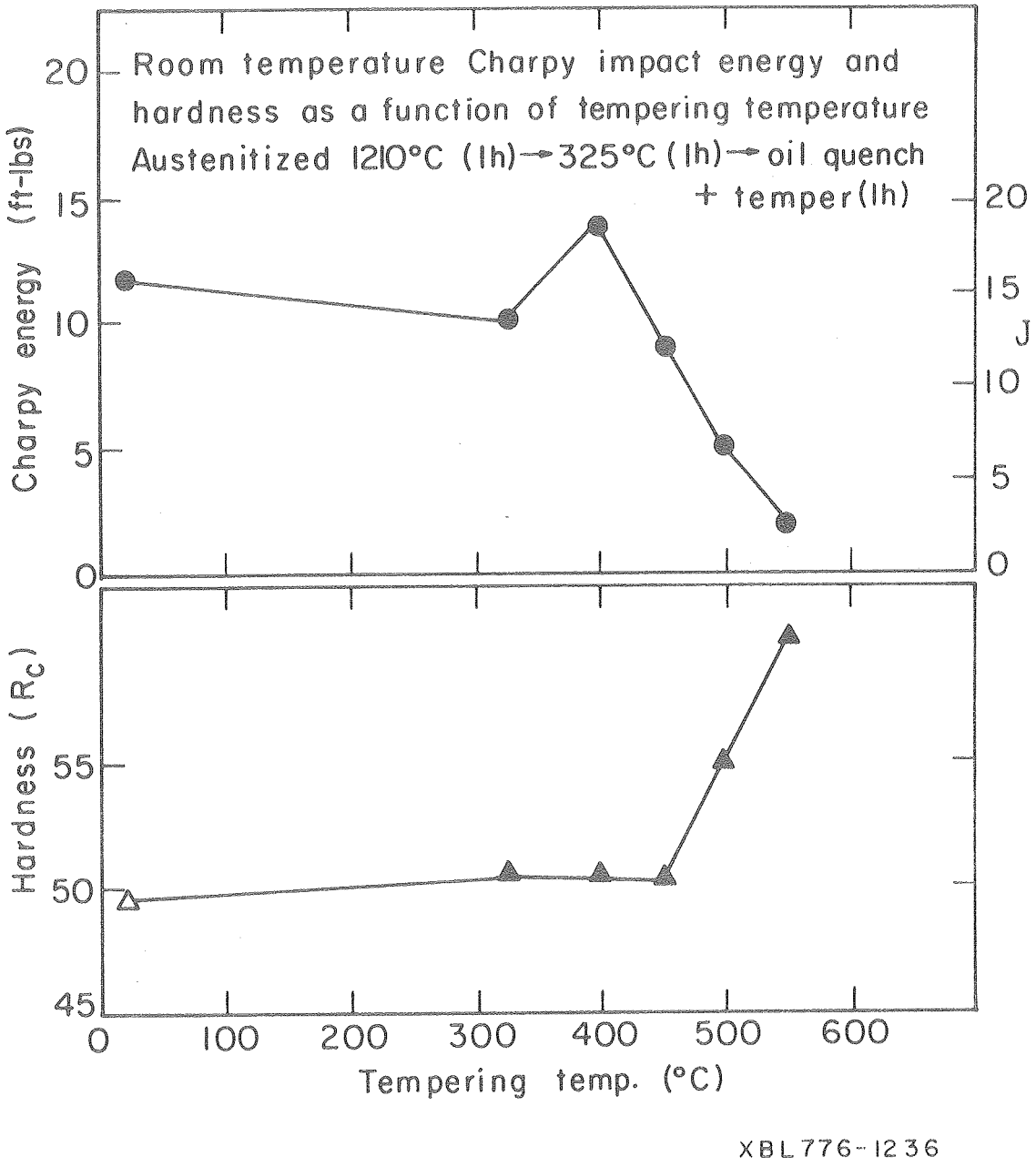

Figure 31. Plots of hardness and room temperature Charpy energy versus tempering temperature for steel A5.

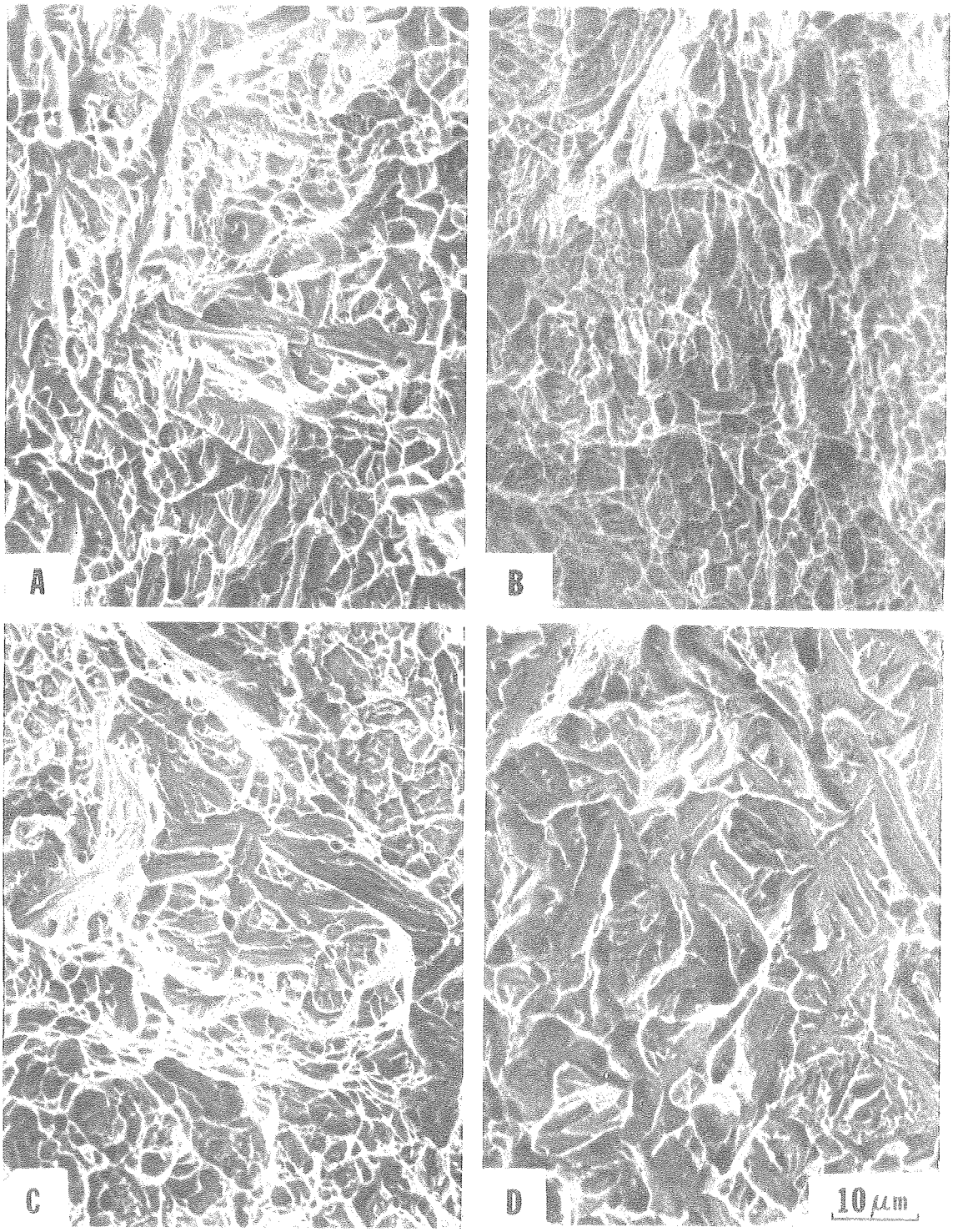

Figure 32. Scanning electron fractographs of broken Charpy specimens of steel A5 isothermally transformed at 325°C (a) untempered, and tempered one hour at (b) 300°C, (c) 400°C, and (d) 450°C.

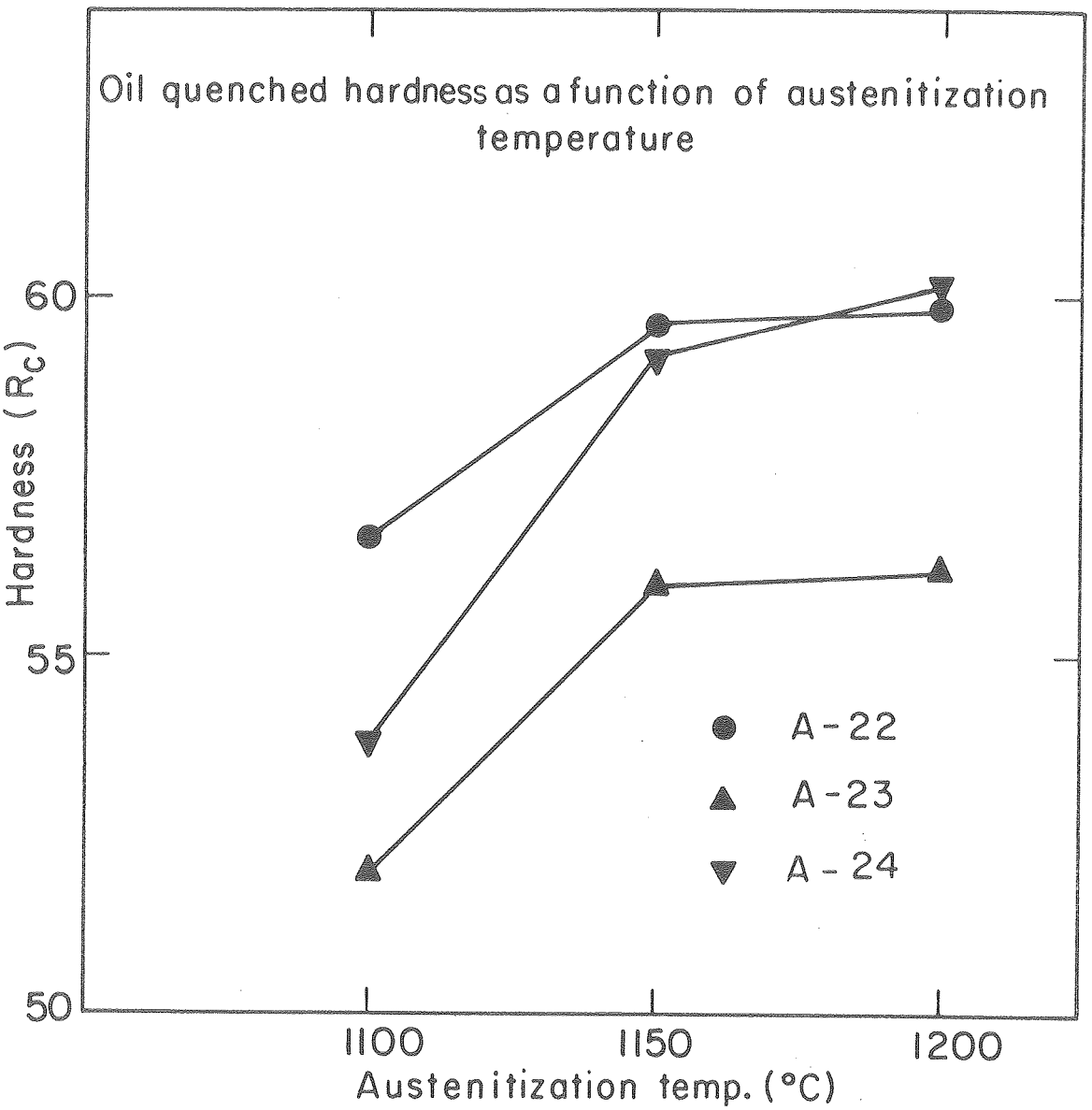

XBL 776-1230

Figure 33. Plots of hardness versus austenitization temperature of as-quenched steels A22, A23, and A24.

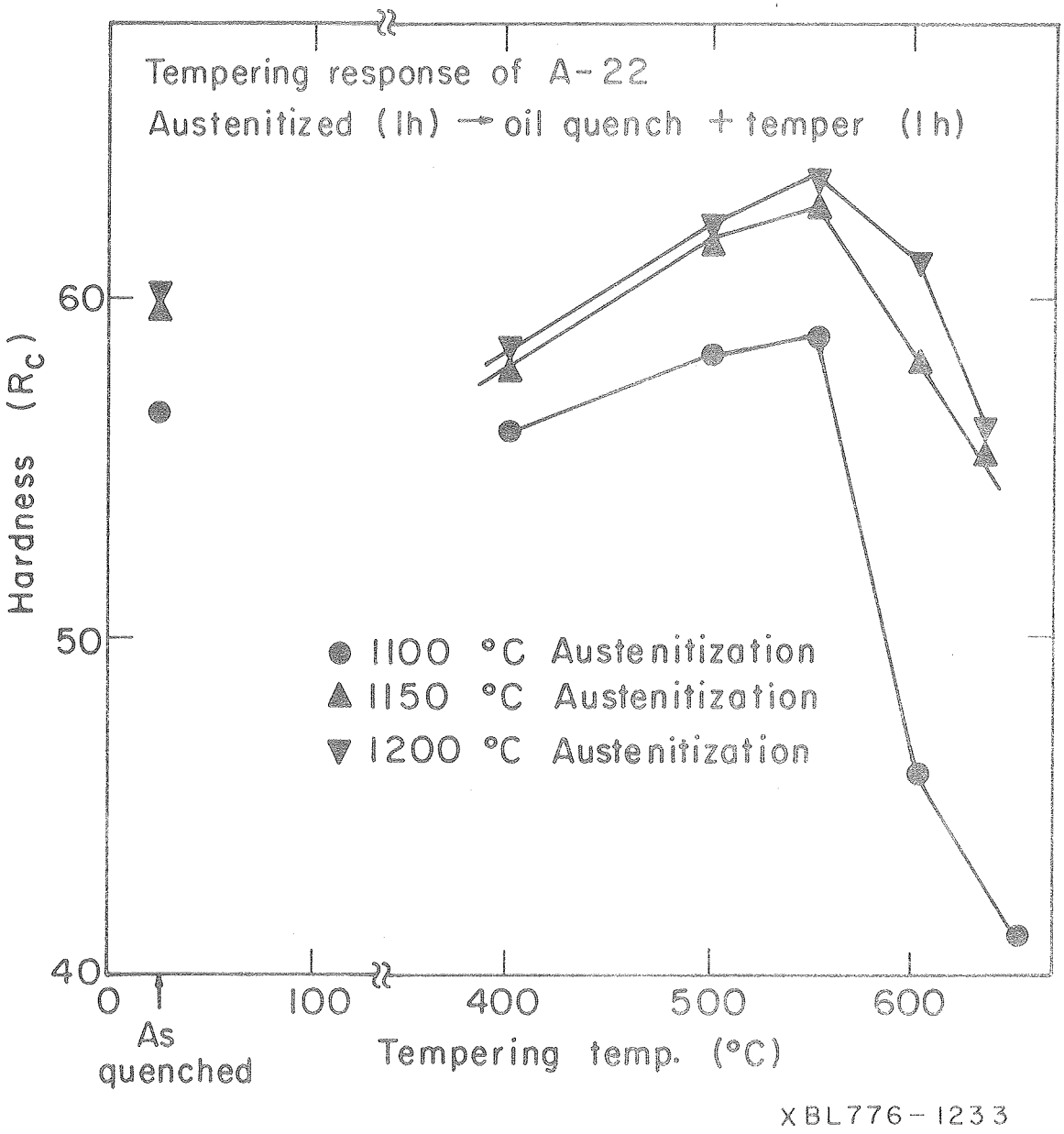

Figure 34. Plots of hardness versus tempering temperature of steel A22, quenched from different austenitization temperatures.

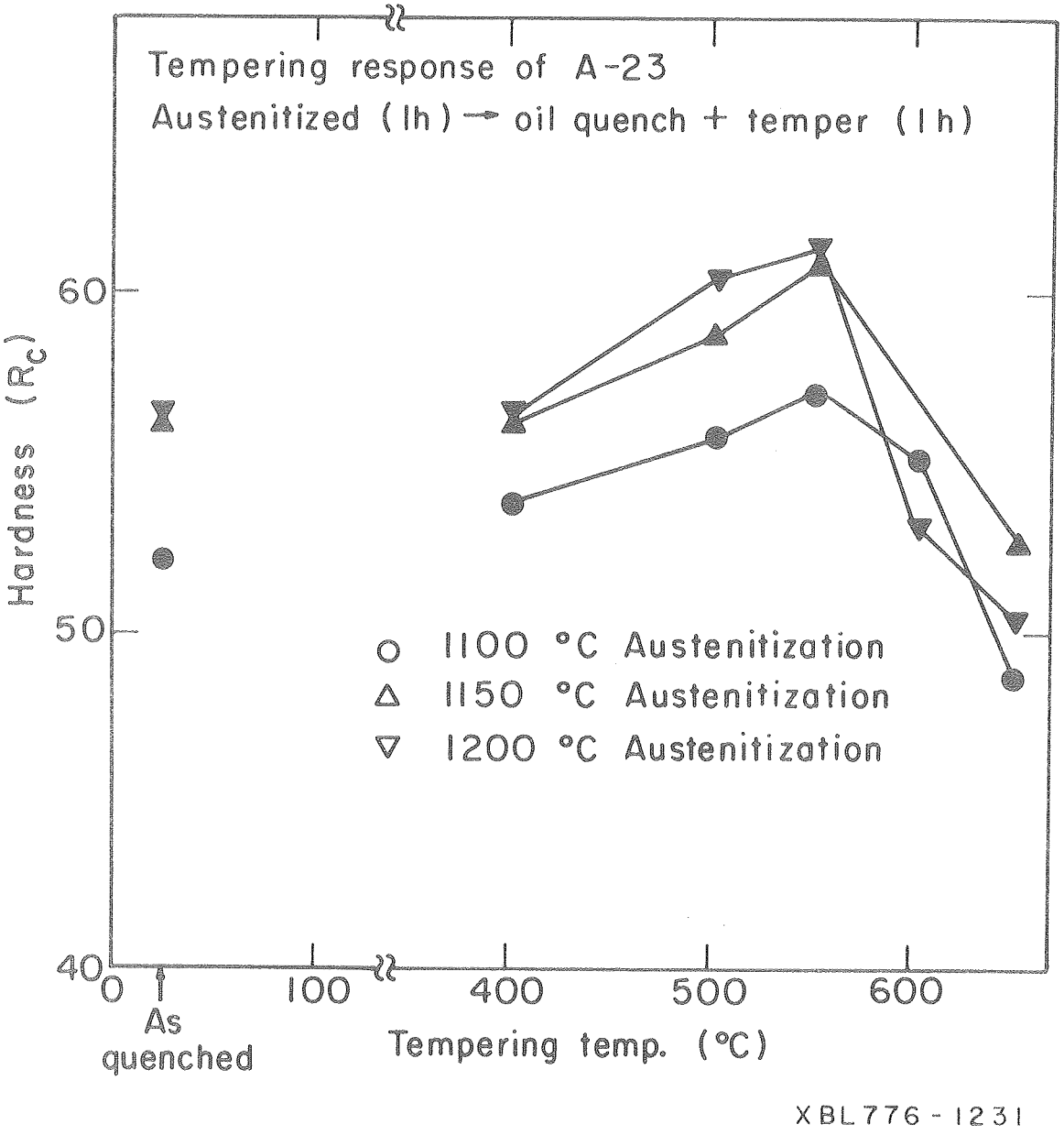

Figure 35. Plots of hardness versus tempering temperature of steel A23, quenched from different austenitization temperatures.

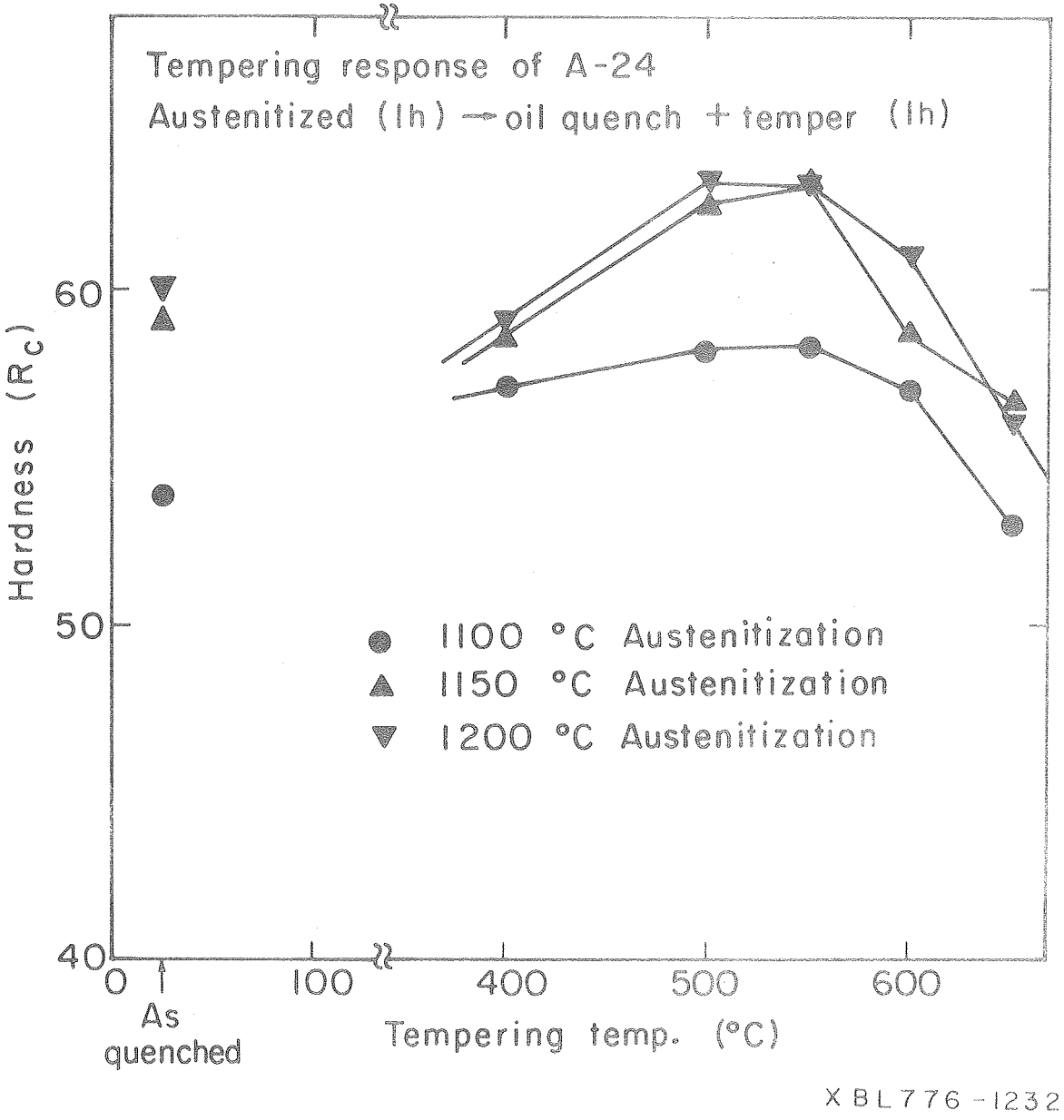

Figure 36. Plots of hardness versus tempering temperature of steel A24, quenched from different austenitization temperatures.

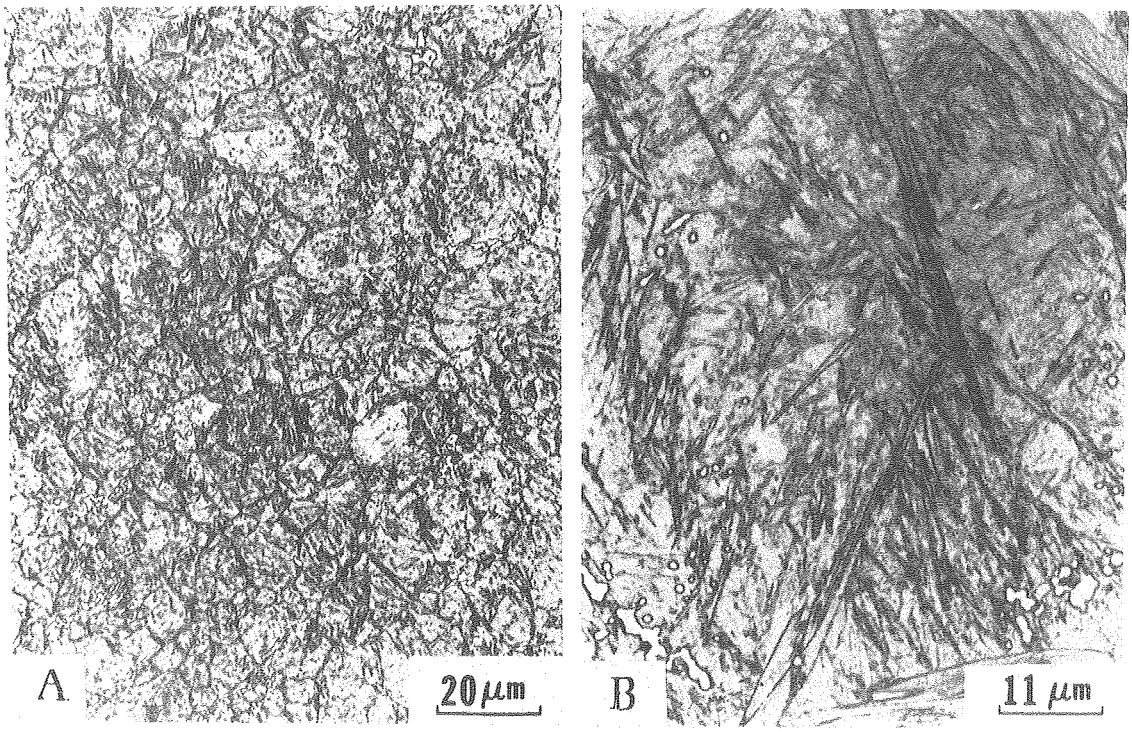

XBB766-6146

Figure 37. Optical micrographs of steel A24, austenitized at (a) 1150°C, and (b) 1200°C.

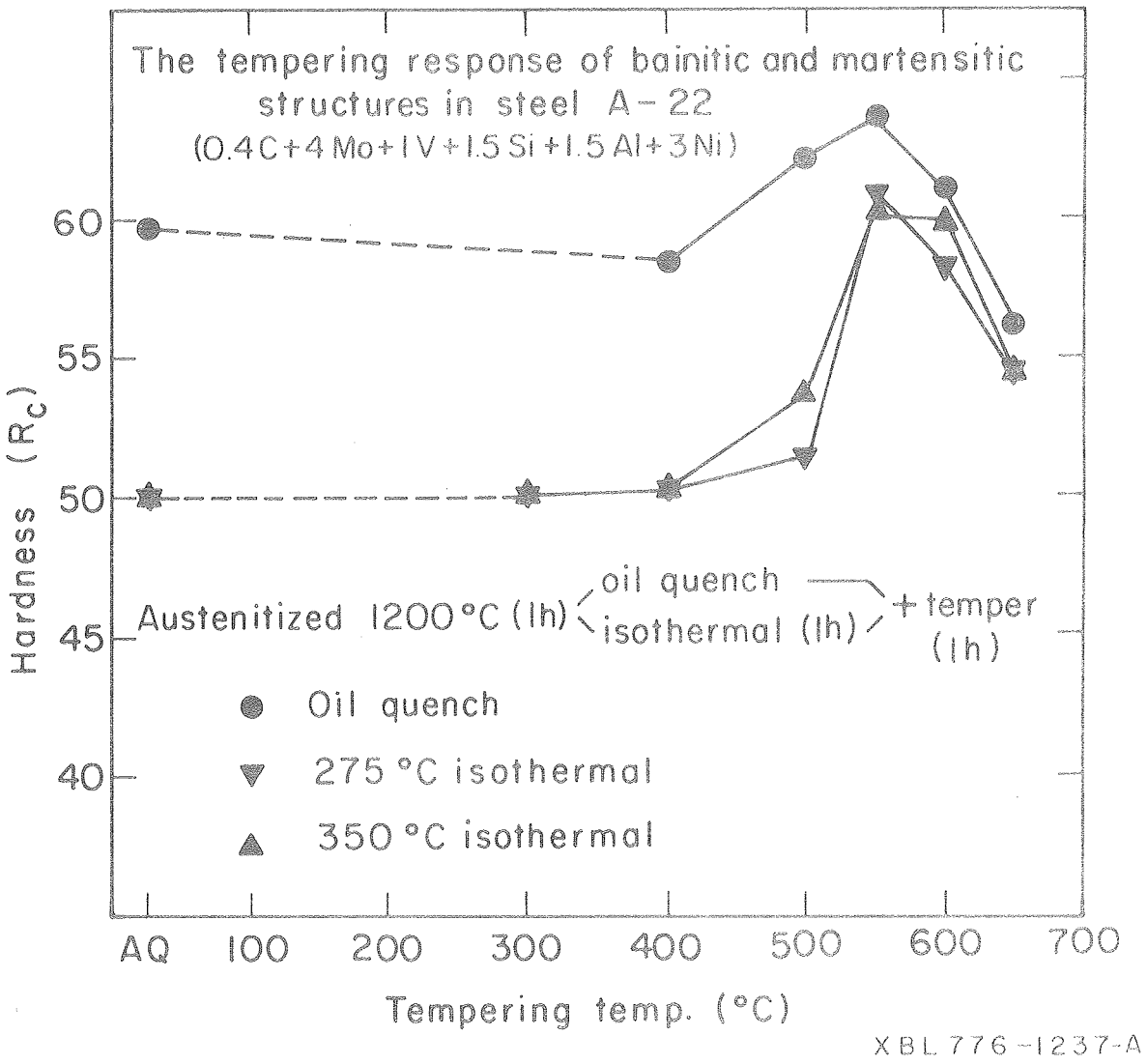

Figure 38. Plots of hardness versus tempering temperature of steel A22 in the quenched and tempered condition, and also isothermally transformed at 275°C and 350°C.

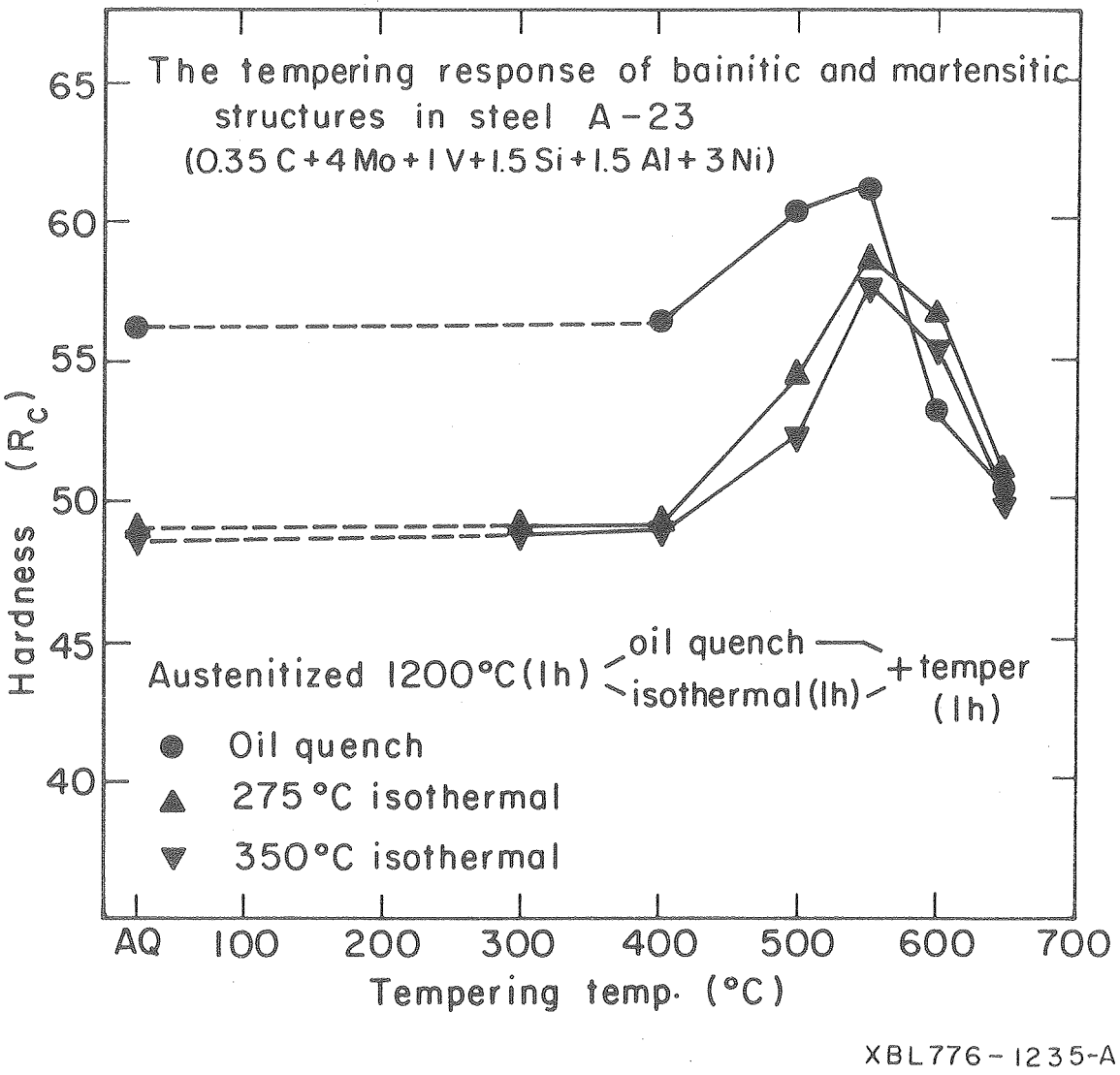

Figure 39. Plots of hardness versus tempering temperature of steel A23 in the quenched and tempered condition, and also isothermally transformed at 275°C and 350°C.

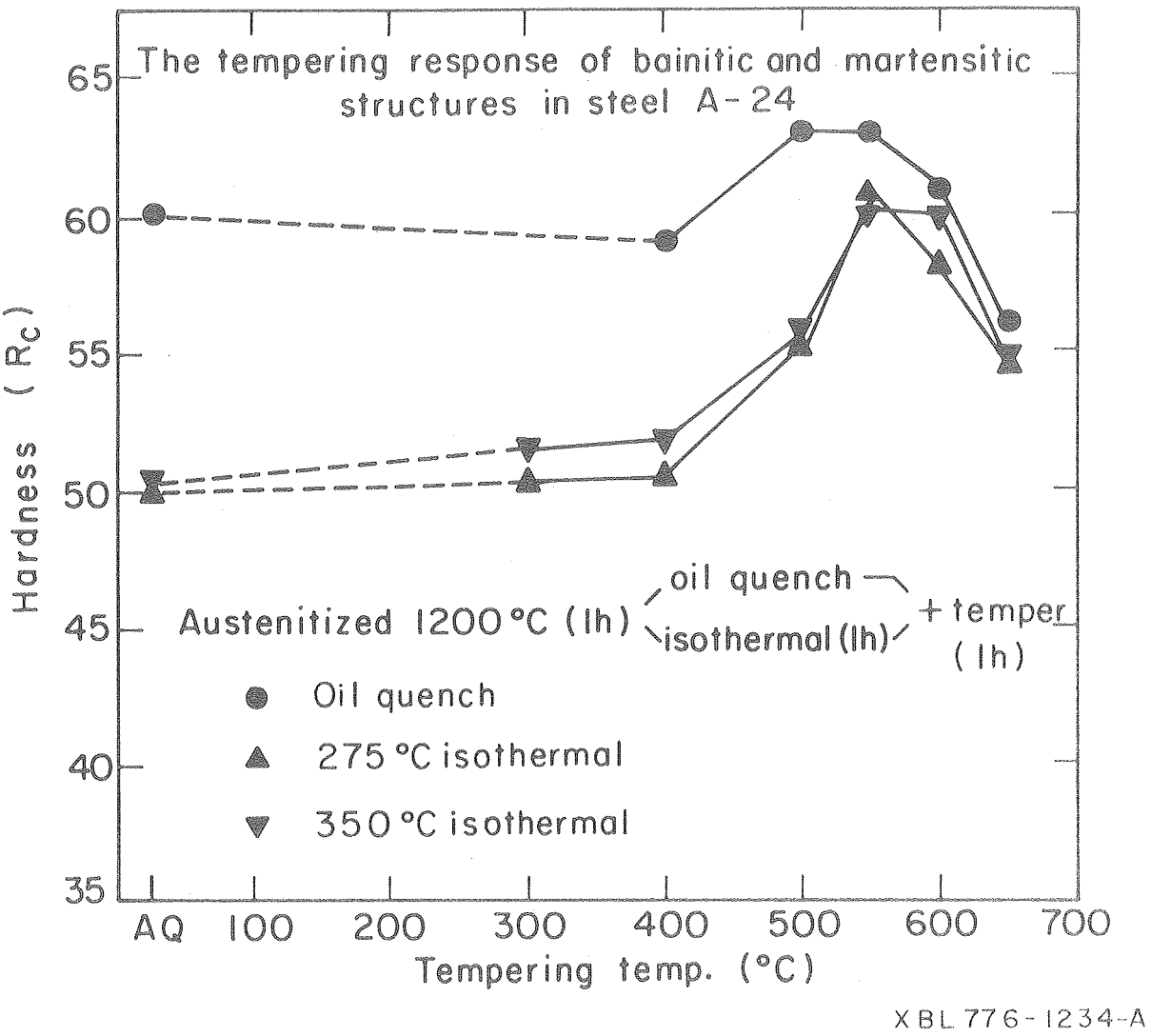

Figure 40. Plots of hardness versus tempering temperature of steel A24 in the quenched at tempered condition, and also isothermally transformed at 275°C and 350°C.

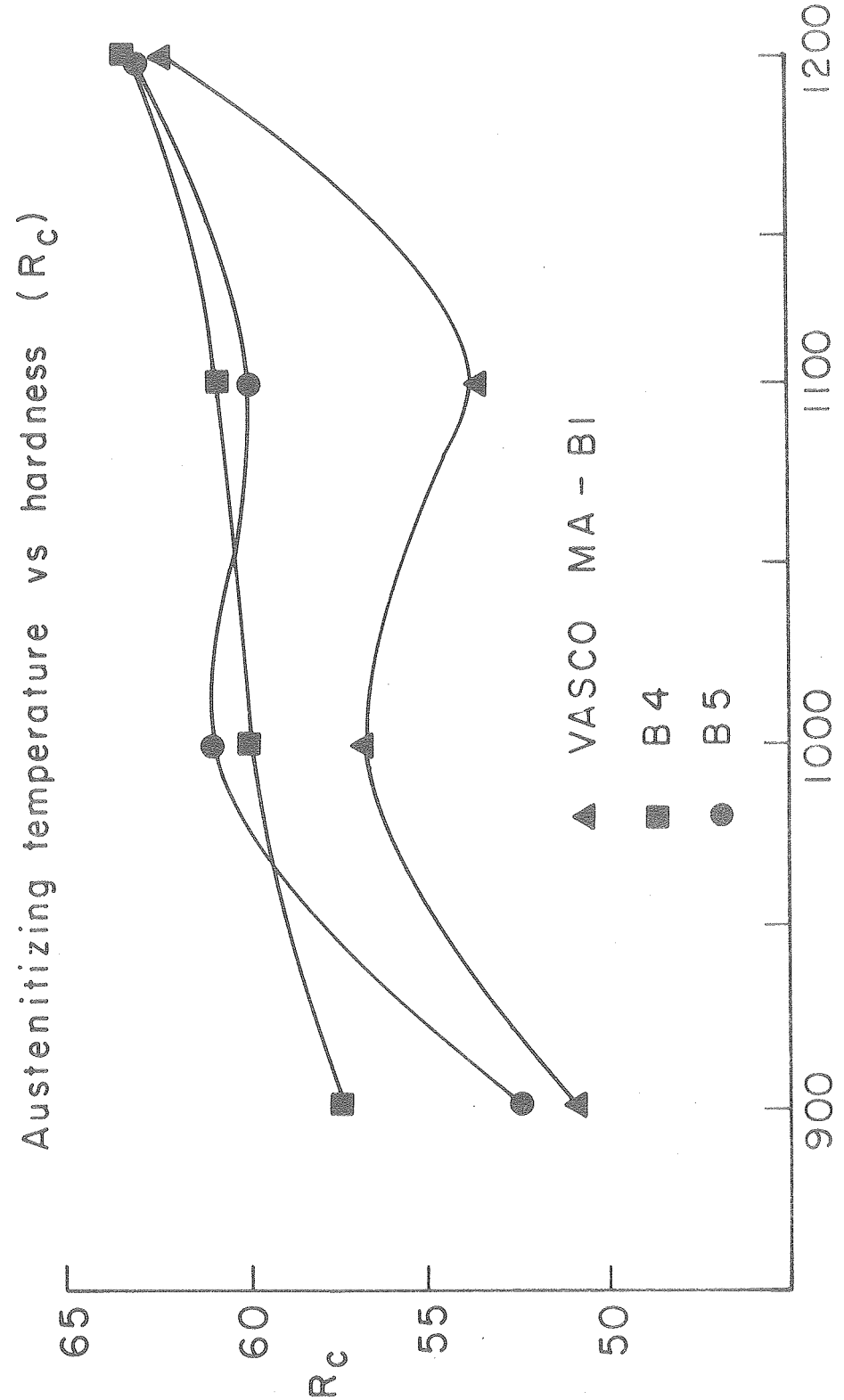

Figure 41. Plots of hardness versus austenitizing temperature for ice-brine quenched steel B1, B4, and B5.

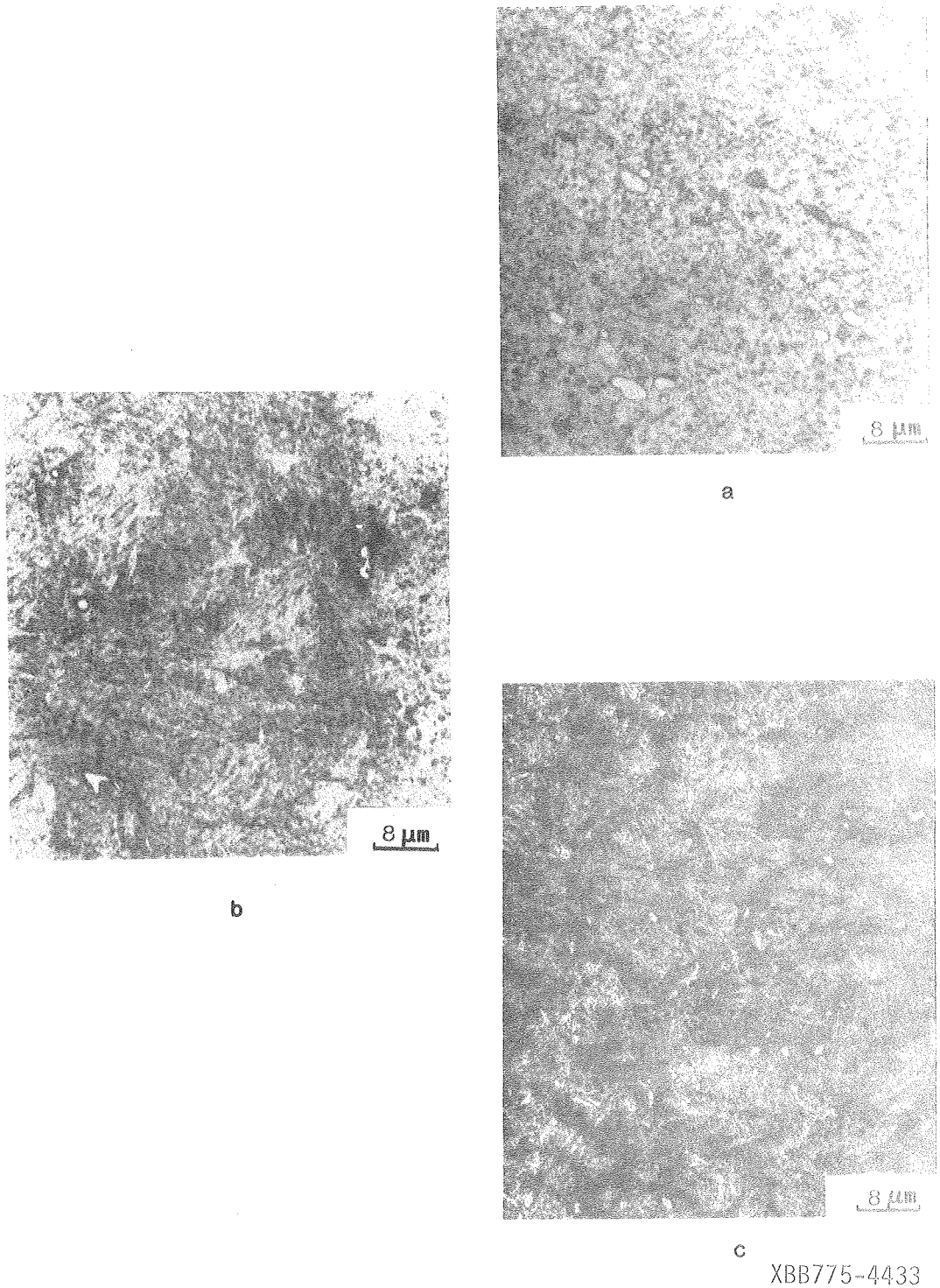

Figure 42. Optical micrographs of steels (a) B1, (b) B2, and (c) B3, austenitized at 900°C and quenched to room temperature.

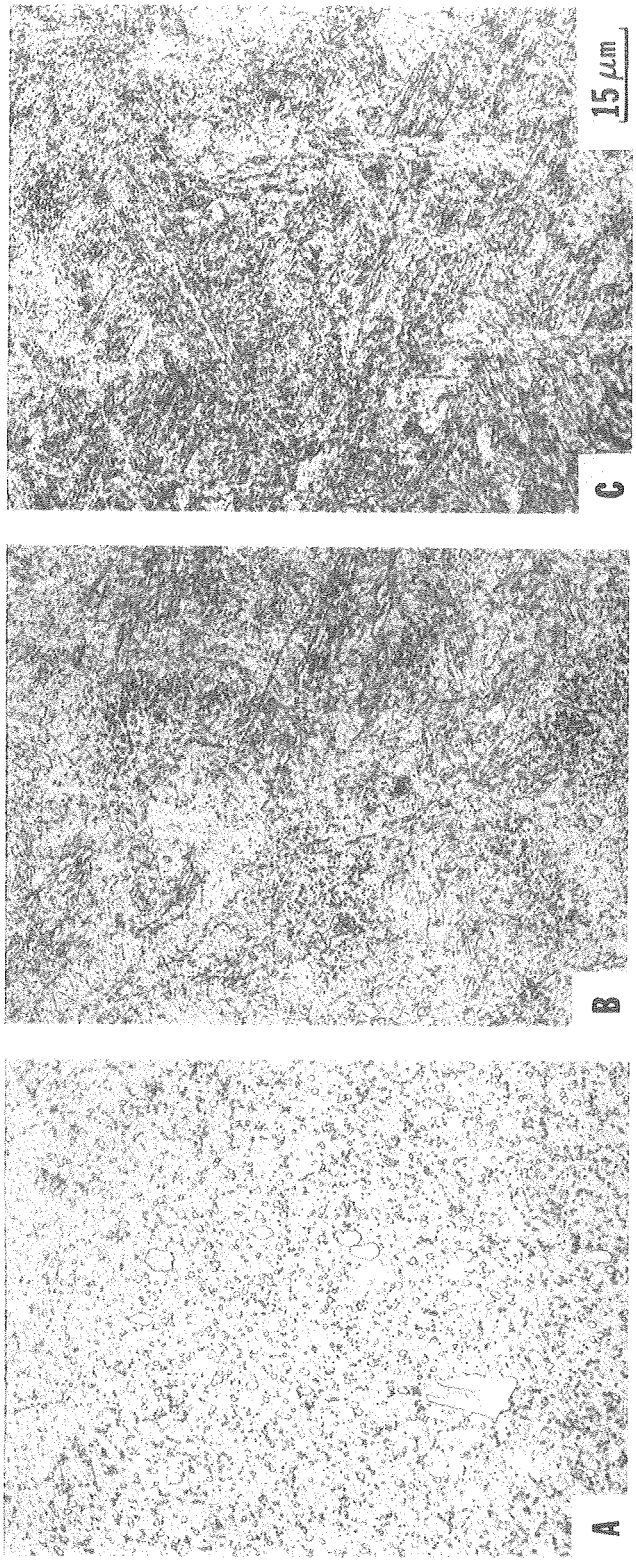

Figure 43. Optical micrographs of as-quenched steels austenitized at 1000°C (a) B1, (b) B4, and (c) B5.

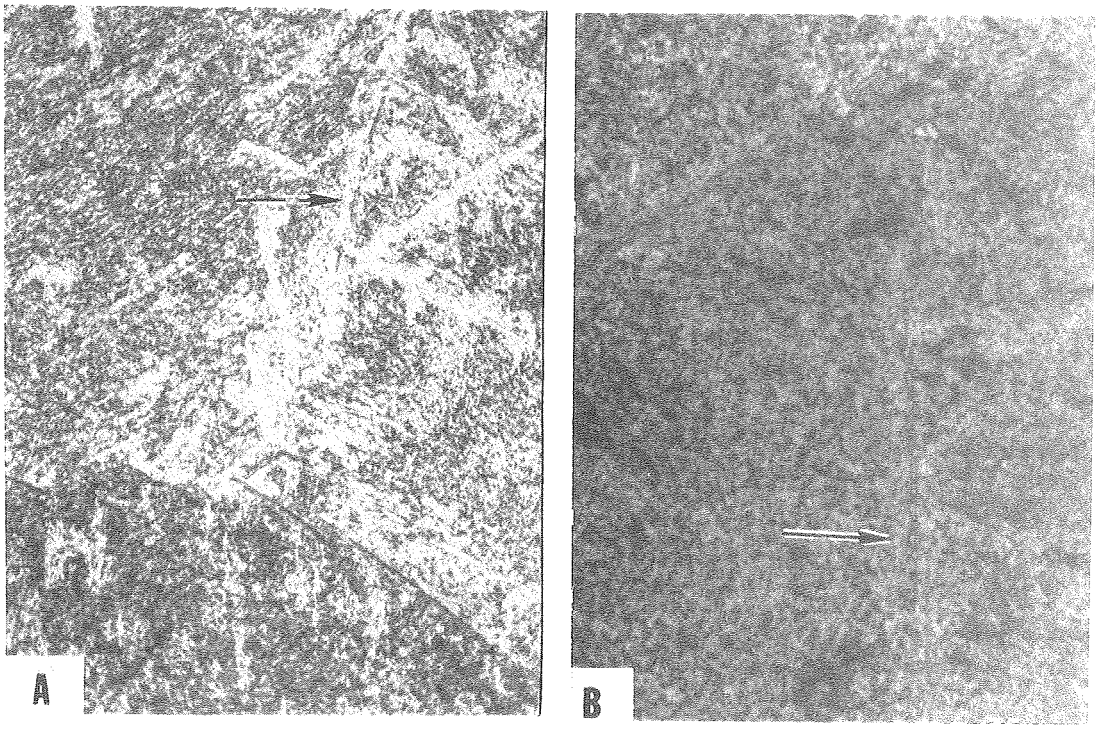

XBB777-6457

Figure 44. Optical micrographs of quenched and tempered (600°C) steels (a) B1 and (b) B4.

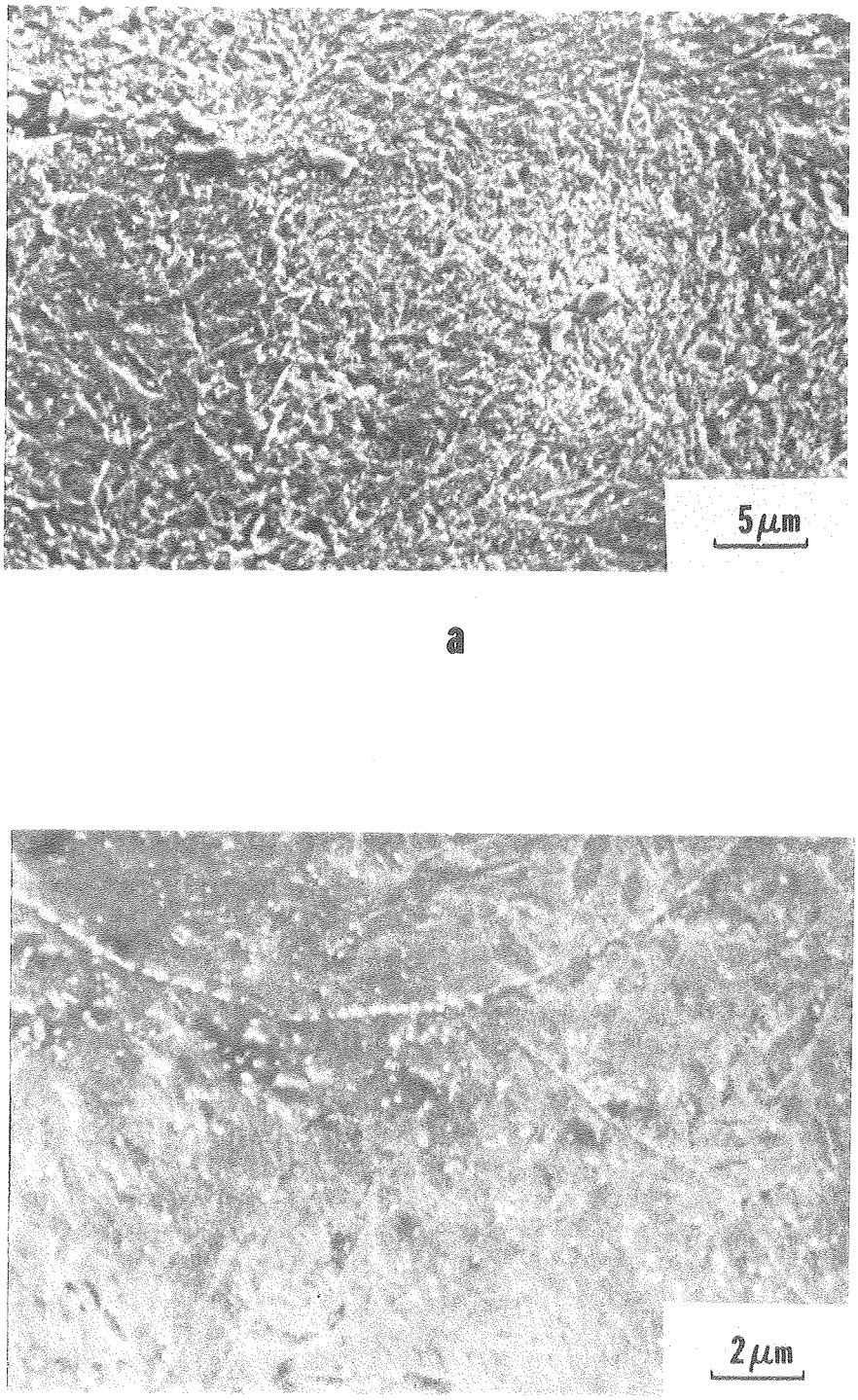

Figure 45. Scanning electron micrographs of steel B4, austenitized for 1 hour at (a) 900°C, and (b) 1000°C.

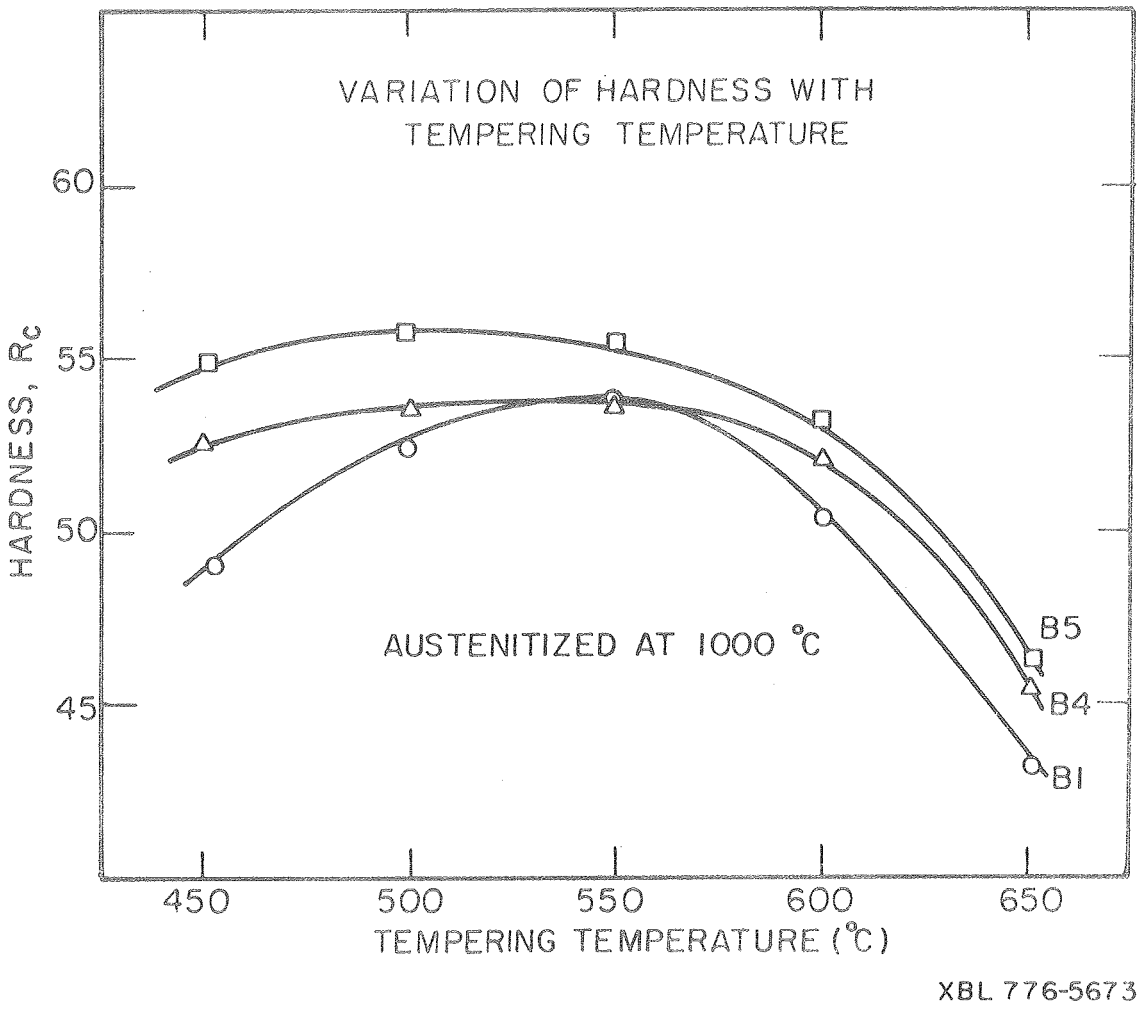

Figure 46. Plots of hardness versus tempering temperature for steels B1, B4, and B5, austenitized at 1000°C.

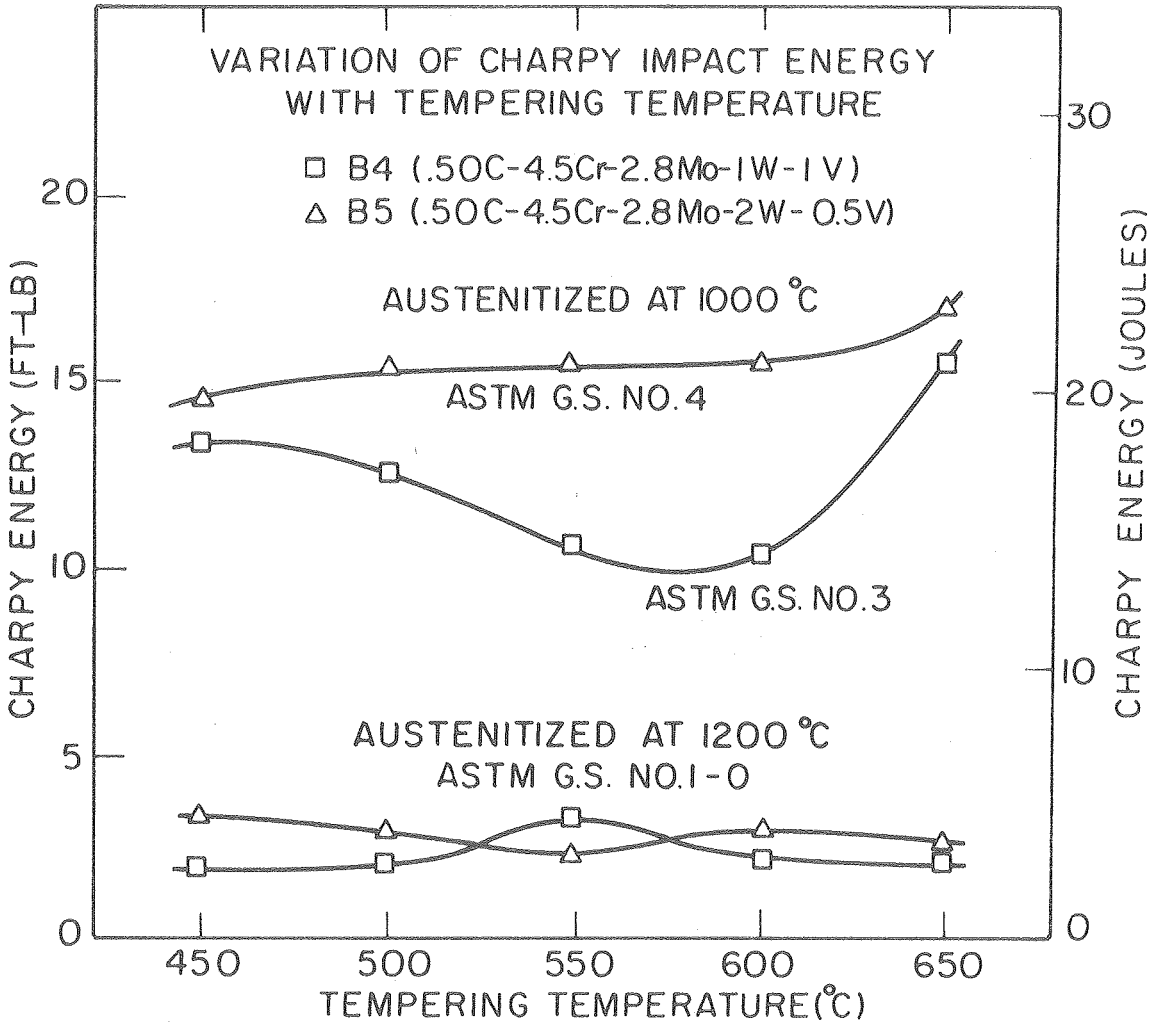

Figure 47. Plots of room temperature Charpy energy versus tempering temperature of steels B4 and B5, austenitized at 1000°C and 1200°C.

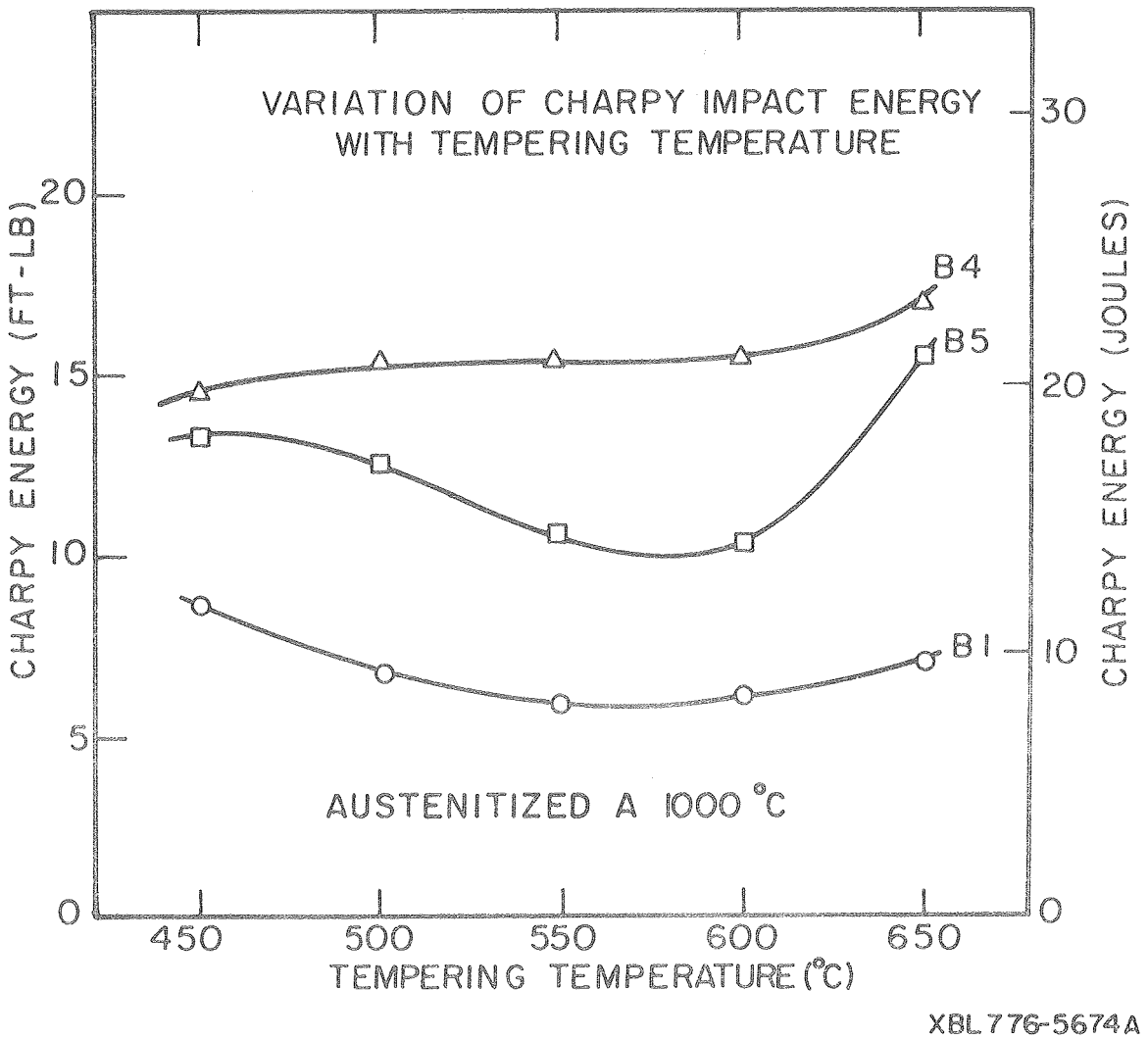

Figure 48. Plots of room temperature Charpy energy versus tempering temperature for steels B1, B4, and B5 austenitized at 1000°C.

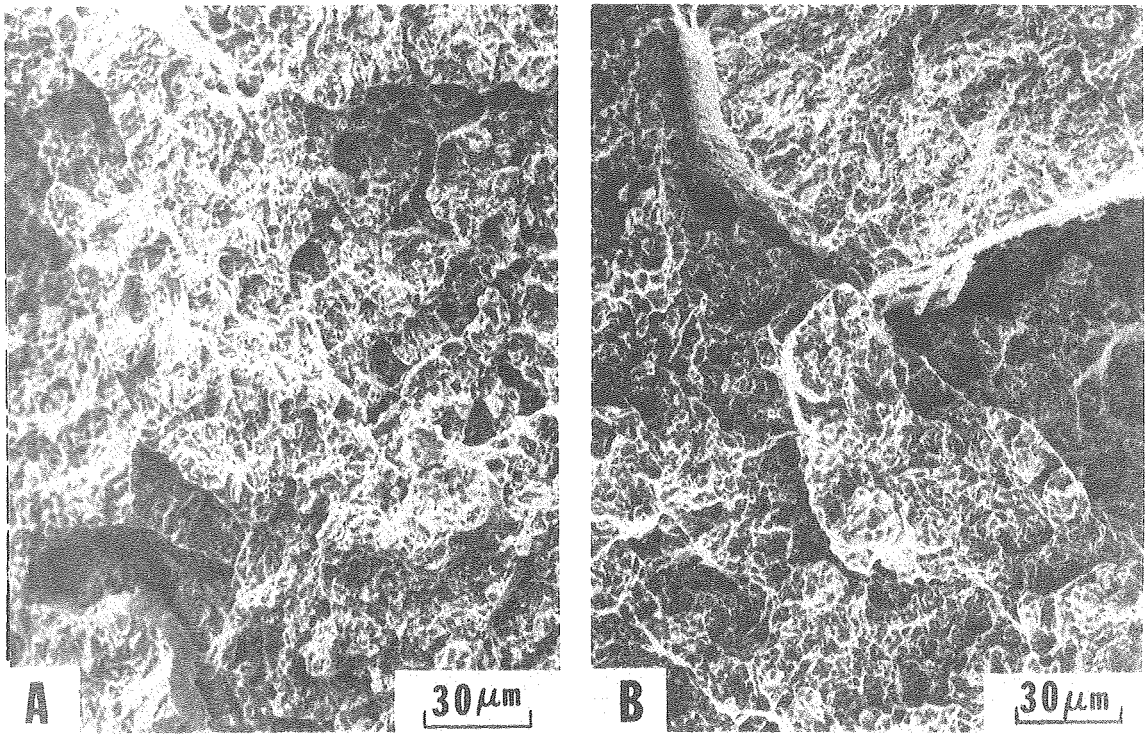

XBB777-6459

Figure 49. Scanning electron fractographs of broken Charpy specimens of quenched and tempered (600°C) steels: (a) B5, and (b) B4.

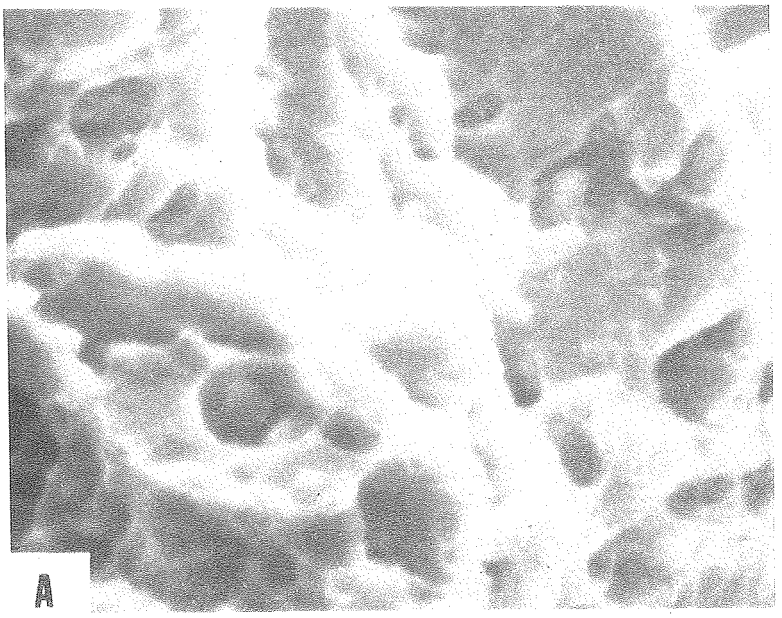

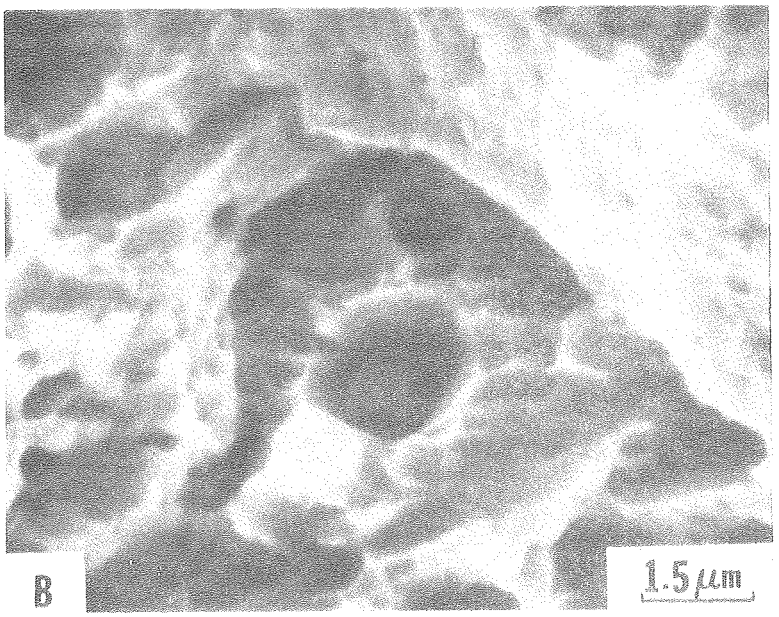

XBB776-6142

Figure 50. High magnification scanning electron fractographs of steels (a) B4, and (b) B5, showing carbides associated with dimples.

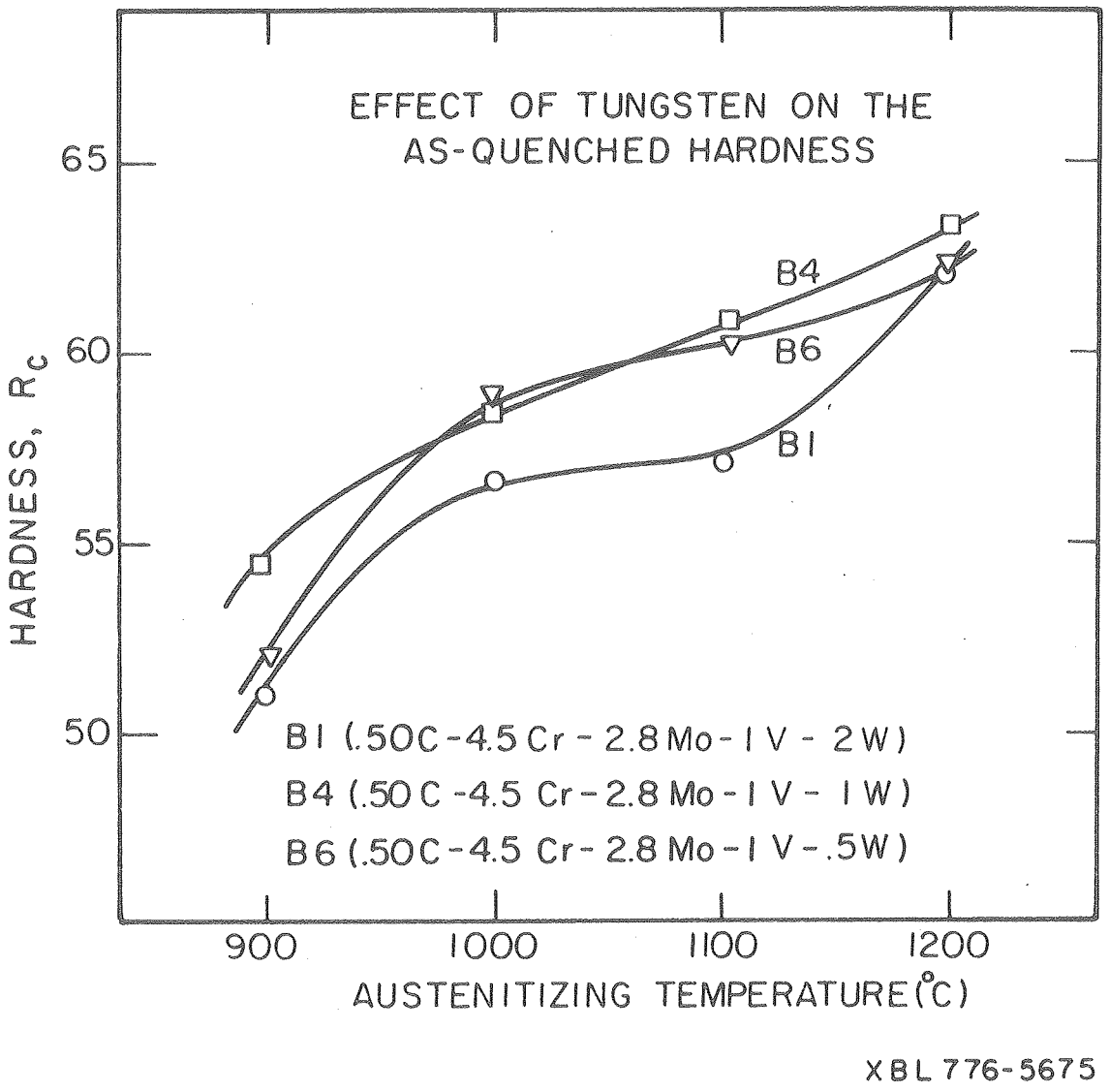

Figure 51. Plots of hardness versus austenitization temperature for as-quenched B1, B4, and B6 steels.

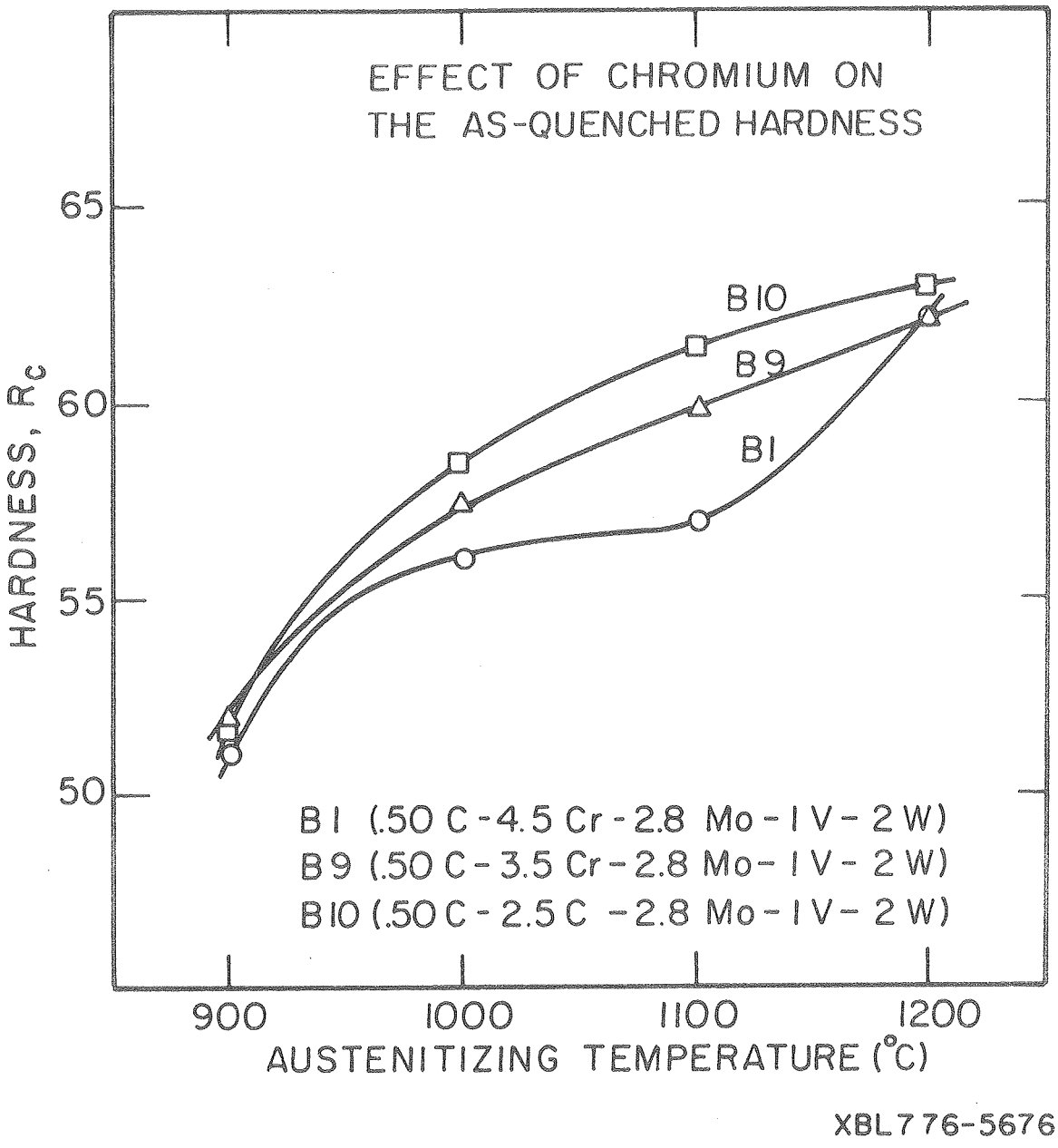

Figure 52. Plots of hardness versus austenitization temperature for as-quenched B1, B9, and B10 steels.

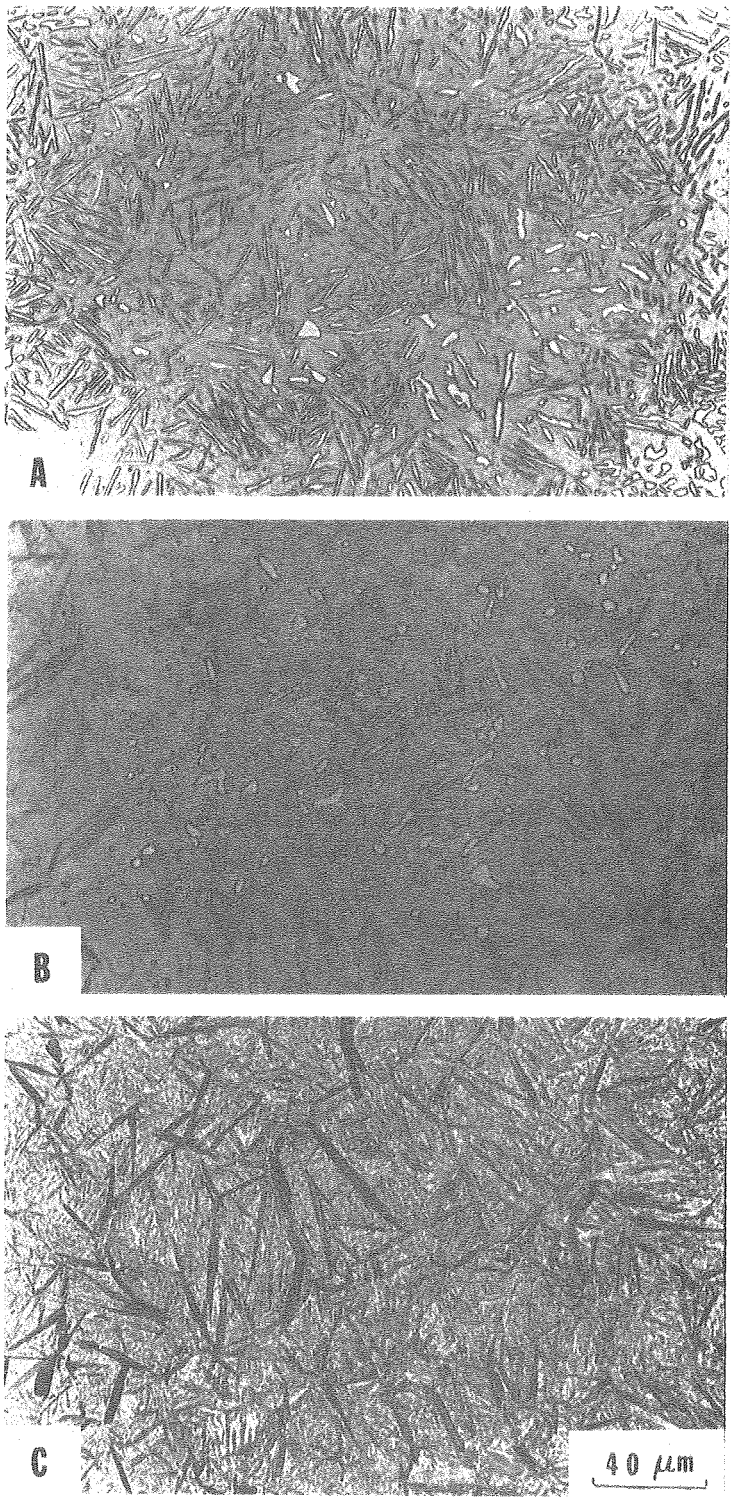

XBB770-12502

Figure 53. Optical micrographs of 4340 + 2Al + 2Si steel, austenitized at (a) 900°C, (b) 950°C, and (c) 1000°C. The white etching phase in (a) and (b) is ferrite.

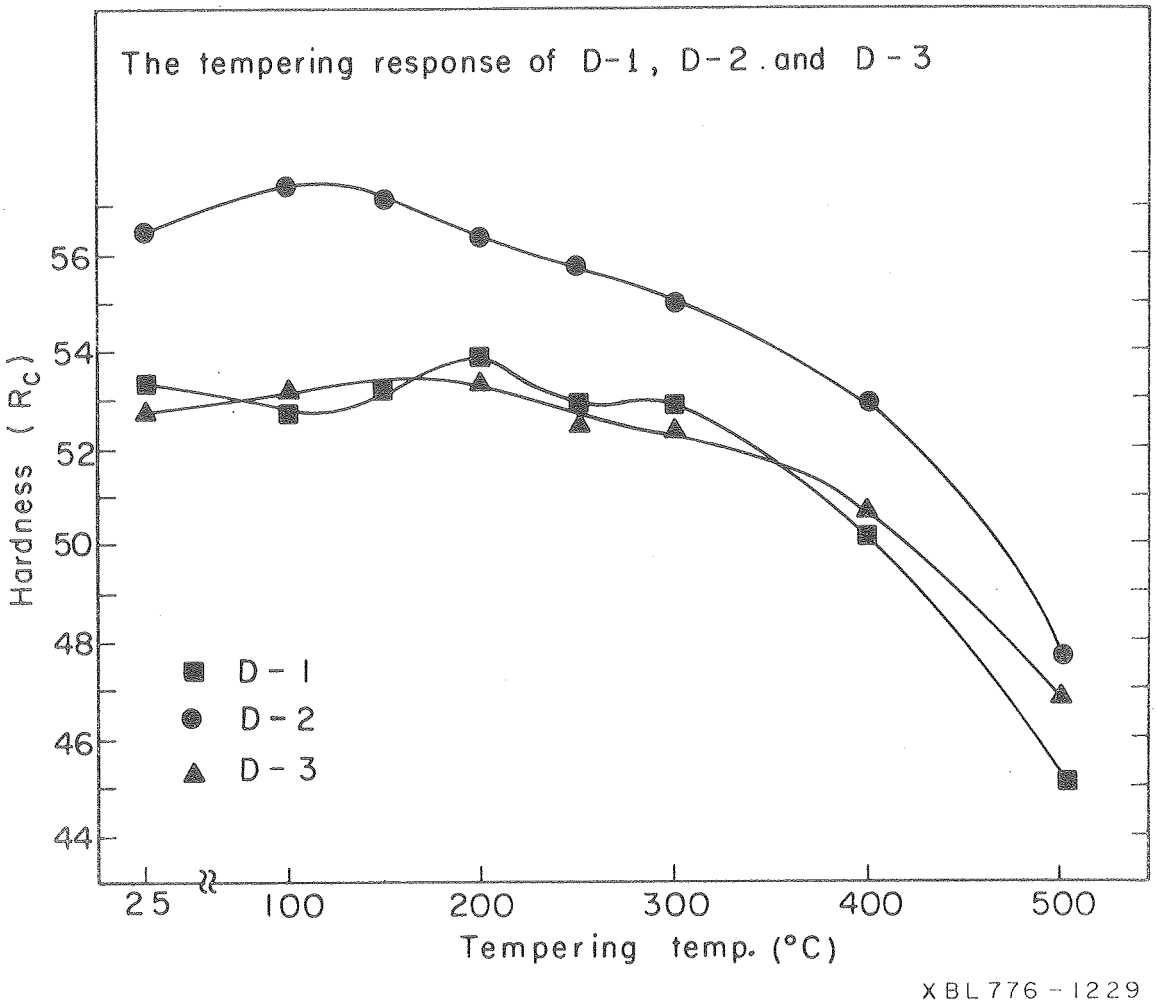

Figure 54. Plots of hardness versus tempering temperature for steels D1, D2, and D3, austenitized at 900°C.

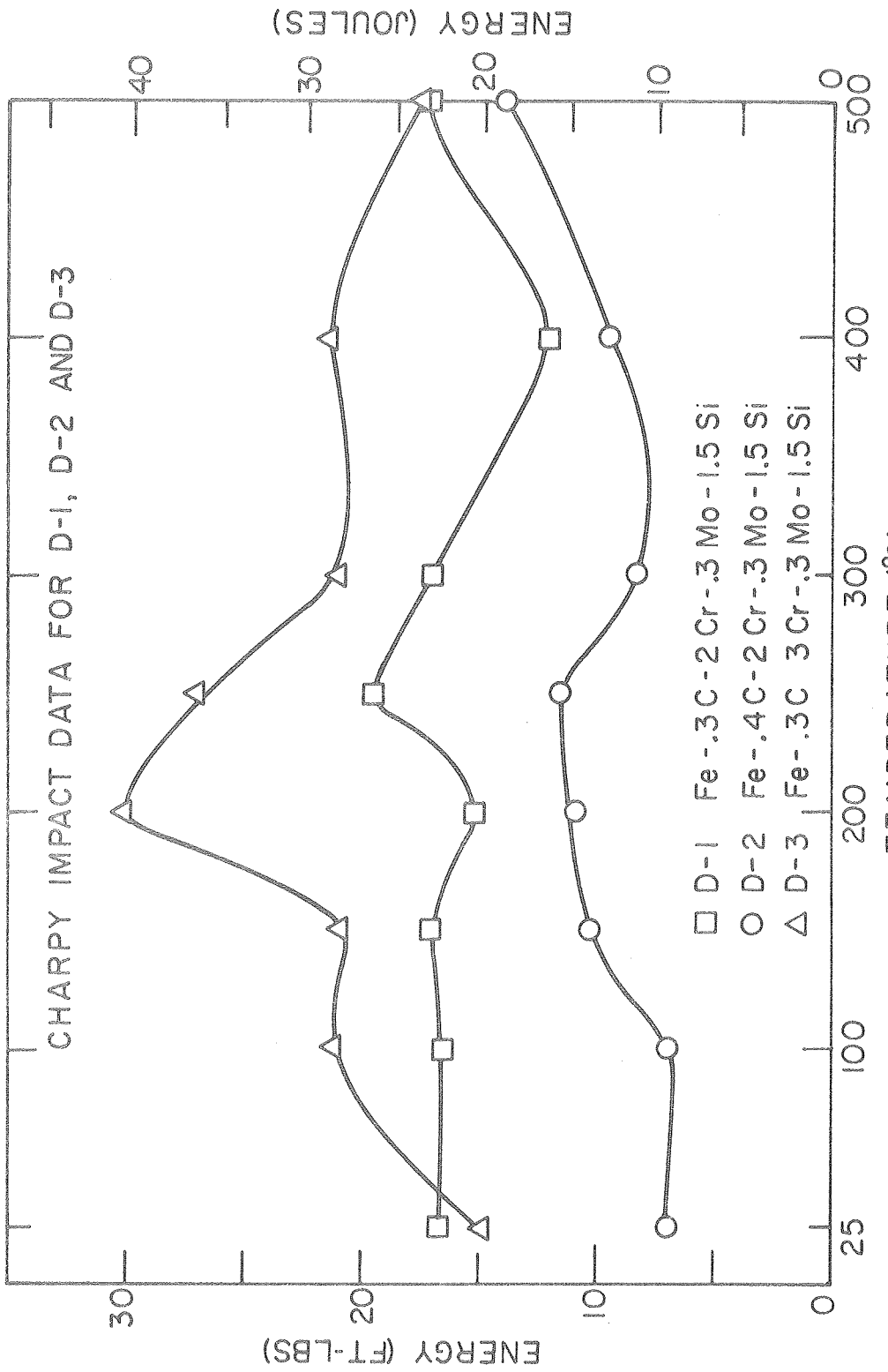

XBL 778-6018

Figure 55. Plots of room temperature Charpy energy versus tempering temperature for steels D1, D2, and D3, austenitized at 900°C.